Polariton-polariton interactions in a cavity-embedded 2D-electron gas

Luc Nguyen-The

Université Paris Diderot - Paris 7
Sorbonne Paris Cité

ED 518: Matière Condensée et Interfaces

Laboratoire Matériaux et Phénomènes Quantiques

DOCTORAT

Physique

LUC NGUYEN-THÊ

Polariton-Polariton interactions in a cavity-embedded 2D-electron gas

Interactions polariton-polariton dans un gaz d'électrons bidimensionnel en cavité

Thèse dirigée par Cristiano CIUTI

Soutenue le 25 février 2014

JURY

M.	Cristiano CIUTI	Directeur
M.	Raffaelle COLOMBELLI	Membre
M.	Carlo PIERMAROCCHI	Rapporteur
M.	Carlo SIRTORI	Président
M.	Alessandro TREDICUCCI	Rapporteur

Résumé

Les polaritons inter-sous-bandes sont des excitations issues du couplage fort entre la transition inter-sous-bande d'un puits quantique et un mode photonique d'une cavity micrométrique. Dans la limite de faible densité d'excitations, c'est-à-dire quand seule une infime fraction de la mer de Fermi est excitée, ces excitations sont bien décrites par un Hamiltonien effectif bosonique et quadratique. Cependant, quand le nombre d'excitations augmente, on s'attend à observer des écarts par rapport aux prédictions issues de cet Hamiltonien. Dans cette thèse nous adaptons la méthode des commutateurs pour bosons composites aux polaritons inter-sous-bandes afin étudier les effets conjoints de l'interaction de Coulomb et du principe d'exclusion de Pauli sur leur comportement à plus haute densité. Suivant une approche microscopique, nous calculons la valeur de l'interaction à deux corps entre polaritons et nous expliquons comment elle peut être encodée dans un Hamiltonien effectif bosonique et quartique. Finalement, en utilisant des paramètres réalistes, nous montrons que l'interaction entre polaritons inter-sous-bandes peut-être importante, et ce, particulièrement dans le THz. Ce résultat ouvre la voie à de futurs travaux en optique non linéaire à base de polaritons inter-sous-bandes. Les principaux résultats de ce travail sont publiés dans la référence [1]

Abstract

Intersubband polaritons are light-matter excitations originating from the strong coupling between an intersubband quantum well electronic transition and a microcavity photon mode. In the low density limit, *i.e.*, when only a tiny fraction of the Fermi sea is excited, these excitations are well described by a quadratic effective bosonic Hamiltonian. However, when the number of excitations in the system increases, deviations from this behavior occur. In this thesis we study how the Coulomb electron-electron interaction and the Pauli saturation of the electronic transitions affect the physics of intersubband polaritons by adapting a commutator technique for composite bosons. We develop a microscopic theory to derive the polariton-polariton interactions and explain how it can be encoded in effective quartic bosonic Hamiltonian. Using realistic set of parameters we predict that polariton-polariton interactions can be signicant, especially in the THz range. This work paves the way to promising future studies in nonlinear optics with intersubband polaritons. The main results of this work are published in Ref. [1].

Acknowledgements

Je souhaite remercier tous ceux qui ont contribué, directement ou indirectement, à ce travail de thèse.

Je remercie tout naturellement mon directeur de thèse Cristiano Ciuti qui m'a tant apporté pendant ces trois années. Merci pour ta gentillesse et ta disponibilité. Merci pour tes très nombreuses idées et les discussions intéressantes qu'elles ont engendrées.

Je suis aussi très reconnaissant aux membres du jury d'avoir accepté l'invitation et d'avoir pris le temps de lire ma thèse. Merci aux rapporteurs Carlo Piermarocchi et Alessandro Tredicucci pour être venus d'aussi loin et pour leurs remarques constructives sur le contenu du manuscrit. Merci à Raffaelle Colombelli et à Carlo Sirtori pour leurs suggestions et leur enthousiasme scientifique.

Je tiens aussi à remercier l'administration du laboratoire et l'Ecole Doctorale (ex 518) qui nous permettent de travailler dans de bonnes conditions. Merci à Anne Servouze, Jocelyne Moreau et Joëlle Mercier pour leur accueil, leur gentillesse et leur efficacité, sans oublier les carambars. Merci à Thomas Coudreau et Joëlle Taïeb pour leur disponibilité et la qualité des formations proposées.

Je voudrais aussi remercier les gens avec qui j'ai collaboré directement. Merci à Motoaki Bamba et Simone De Liberato pour m'avoir apporté leur expérience et leurs idées. Merci aux membres de l'équipe QUAD, et particulièrement à Carlo Sirtori, Angela Vasanelli, Yanko Todorov, Aymeric Delteil et Benjamin Askenzi pour les discussions sur les polaritons inter-sous-bandes (quoi d'autre ?). Et bien sûr un grand merci à Etienne Parizot, Maximilien Cazayous, Jaysen Nelayah et Sara Ducci avec qui j'ai enseigné. Ce fut un plaisir de travailler avec vous.

Je voudrais enfin remercier ceux qui ont rendu les journées et les soirées au labo agréables. Merci à Loïc pour sa présence tranquillisante, Jonathan pour l'initiation à l'escalade, Alexandre pour la touche culturelle, Alexandre (la confusion n'est pas possible) pour son *humour* unique, Philippe pour les discussions profondes, Juan pour ses goûts cinématographiques, Hélène pour avoir transformé le thésarium en

pays des bisounours, Constance pour la touche de cyber-originalité, JB pour ses jeux étranges, Siham pour sa gentillesse, Thibaud pour les recommentations sur les sries et Kelly pour le gîte et le couvert. Merci à ceux qui rejoignent tout juste le labo, Pierre, thésard des SQWAP, et mes anciens étudiants Charlotte et Romain. Je leur souhaite bonne chance pour la suite. Merci aussi à ceux qui sont déjà partis, Simon pour sa bonne humeur légendaire, Pierre pour ses talents d'imitateurs. Un merci tout particulier à David pour avoir lu ma thèse. Les contacts avec les autres thésariums sont trop rares mais non moins agréables. Merci à Benjamin, David, Chris, Julia, Sylvia et tous ceux que j'oublie pour l'ambiance générale du labo. Du côté des permanents n'oublions pas Giuliano, Idranil, Edouard, Maximilien, Yann et Marie-Aude pour l'humour et les discussions en tout genre, Maria Luisa et Maria pour le séminaire thésard.

Un grand merci à ma famille qui m'a soutenu pendant ces trois années. Merci à mes parents, ma tante Nathalie, mon cousin Alexandre et à Jean et Anaïs pour avoir assisté à ma soutenance. Merci à mon grand-père Jean pour sa curiosité pour mon travail. Et bien sûr, un très grand merci à Soizic qui m'a accompagné, soutenu, supporté et encouragé tout au long de ce travail (et même un peu entretenu sur la fin).

Contents

Introduction

Quantum electrodynamics is the study of the light-matter coupling in a regime where the quantum nature of the excitations is significant. The system under study is composed of two interacting subsytems: the electromagnetic field on the one hand, and an electronic medium (atom, semiconductor, superconductor,...) on the other hand. In the absence of a cavity, the radiative properties of an excited atom are determined by its coupling to the continuum of modes of the electromagnetic field, resulting to the relaxation to the ground state via the spontaneous emission of photons. In 1946, Purcell [2] discovered that this emission rate and, thus, the coupling can be dramatically affected by confining the system in a cavity. The fundamental idea of cavity quantum electrodynamics is, thus, to tune the light-matter coupling by carefully engineering the cavity [3].

Since then, experiments with ever growing light-matter couplings and cavity quality factors have been realized [4, 5, 6, 7, 8]. Eventually, the *strong coupling regime* was reached [9, 10, 11], when the photon lifetime in the cavity is much larger than the emission rate of the atom. In this case, a photon can be absorbed and emitted by the atom several times before it leaves the cavity, leading to a quasi-reversible energy transfer between the two subsystems. The normal modes of the system are then hybrid light-matter excitations called *dressed states*. Such systems were proposed as potential candidates for quantum information due the long coherence lifetimes and the possibility to control entanglement. Because of their simplicity, they were also used to test the fondations of quantum mechanics and explore the frontier between classical and quantum physics [12].

In condensed matter physics, the strong coupling regime has been reached in cavity embedded quantum wells [13, 14] and quantum dots [15, 16, 17] or artificial atoms based on Josephson junctions in superconducting circuits [18, 19].

In this PhD thesis manuscript, we will focus on the nonlinear interactions of cavity excitations in planar microcavities strongly coupled to doped quantum wells. If the wells are undoped, the role of the atom is played by *excitons*, *i.e.*, electron-

hole pairs bounded by the Coulomb interaction, where holes lie in the valence band and electrons in the conduction band. The normal modes of the coupled system, called *exciton polaritons*, can be seen as bosons, interacting, because of their matter part, through dipole-dipole and dipole exchange interactions [20, 21, 22]. Thanks to these interactions, spectacular nonlinear effects have been observed like parametric amplification [23] and oscillation [24], light hydrodynamics and even superfluidity [25, 26, 27, 28, 29]. Bose-Einstein condensation was also observed and, due to exciton polariton's small effective mass, it was achieved at a temperature of only a few kelvin, compared to hundreds of nanokelvin for atomic condensates. Electroluminescent [30] and lasing [31, 32] devices have also been realized, presenting remarkable performances at room-temperature. Recently, theoretical results [33, 34, 35, 36] have shown that it is possible to simulate complex bosonic systems, like out-of-equilibrium Bose-Hubbard models [37], using exciton polaritons in coupled cavities.

In 2003, the strong coupling regime was also observed in doped, instead of undoped, quantum wells in planar cavities [14]. In this case, electrons are present in at least one conduction subband of the well. An excitation is thus due to the promotion of an electron from an occupied subband to a higher and empty subband leaving a hole in the Fermi sea. In contrast to excitons, which are interband excitations, they are named *intersubband excitations* and the corresponding dressed states are *intersubband polaritons*. These excitations differ from excitons on several points, namely their energy range (from the mid infrared to the terahertz (THz) region of the spectrum) and their nature (intersubband transitions do not involve bound state). Moreover, a key difference is the possibility to control their coupling to photons. Indeed, in such systems, the light-matter coupling is collectively enhanced by the presence of the Fermi sea in the conduction subbands and scales like the square root of the density of electrons in the wells. The doping can, thus, be increased until the strong coupling regime is reached. In fact, it is possible to go even further [38] and the coupling strength can become comparable to the energy of the transition. Then, the system enters a new qualitatively different regime called *ultra-strong coupling regime*. This regime presents exciting original features. In particular, the ground state of the system is a squeezed vacuum [38] and pairs of photons can be extracted from the cavity by non-adiabatic tuning of the coupling [39], a manifestation of the dynamical Casimir effect [40]. The *in situ* fast tuning of the ligth-matter coupling has also been exploited to study the onset of the strong and ultra-strong coupling regimes [41, 42]. Benefiting from the maturity of quantum cascade structures [43], photovoltaic probes [44] and electroluminescent devices [45, 46, 47] have been re-

alised. Original structures allowing lasing without population inversion have also been proposed [48, 49]. Realizing such structures is still an active research field [50].

Intersubband polaritonics is, thus, a very rich, promising and exciting field, both from the fundamental and applied point of view. However, while much effort has been devoted so far to explore the ultra-strong coupling regime and realise devices, very little is known about the nonlinear physics of intersubband polaritons. Indeed, structures studied so far work in the *low density* limit, where only a tiny fraction of the Fermi sea is excited. The number of polaritons in the cavity is then much smaller than the number of electrons and the system is well described by a linear theory (quadratic Hamiltonian). The physics happening when the number of polaritons increases has proved to be a highly relevant one in the case of exciton polaritons, and should be adressed for intersubband polaritons too. But, at the exception of polariton bleaching under intense coherent pumping [42], little so far has been explored in the nonlinear regime. Here, we propose to fill in the gap by providing a comprehensive theory of polariton-polariton interactions and deriving an effective Hamiltonian taking them into account.

In the first chapter, we give a general presentation of the system. We introduce separately its electronic and photonic parts and describe their excitations. We then present the different coupling regimes between these excitations. When the coupling is strong enough, the normal modes of the system are hybrid light-matter excitations called intersubband polaritons. We describe such excitations in a very simple fashion and give an overview of the experimental realizations. All results presented in this chapter correspond to the linear regime, where the number of excitations is small compared to the number of electrons in the Fermi sea.

In the second chapter, we present the second-quantized Hamiltonian of the system. Because of its complexity, we introduce some simplifications, which leads us to define more precisely the notion of intersubband excitation. In particular, we define creation and annihilation operators for intersubband excitations, and we show that these excitations are almost bosonic. Based on simple physical ideas, we then derive a quadratic bosonic Hamiltonian and we show that, in the linear regime, it correctly describes our system. This approach is very convenient, since it allows to solve problems with few and simple calculations. However, this approach is limited to the linear regime.

In the third chapter, we show how to extend the previous Hamiltonian to treat the nonlinear regime in a rigorous and controlled manner. We first present the al-

gebra of the intersubband excitations. We then present a rigorous method allowing us to include many-body interactions in our models. We are then able to develop these interactions in a perturbative way, controled by the ratio of the number of polariton and the number of electrons in the system. Limiting ourselves to the first order, we obtain an effective bosonic Hamiltonian with quartic terms describing effective polariton-polariton interactions. Numerical results are given for realistic set of parameters and conclusions are drawn. Our work paves the way to the exploration and control of nonlinear dynamics due to polariton-polariton interactions in semiconductor intersubband systems and quantum cascade devices operating in the strong coupling regime.

Chapter 1

Introduction on intersubband polaritons

In this chapter, we will introduce the semiconductor heterostructures in which intersubband polaritons can be observed. Intersubband polaritons are excitations resulting from the strong coupling between an electronic transition and a photon in microcavity embedded doped quantum wells. First, we will review the physical properties of quantum wells and semiconductor microcavities separatly. We will then discuss the notion of strong coupling between their excitations. To illustrate this, we will present and solve a simplified model of the system exhibiting intersubband polaritons. Results are in agreement with the experiments in the linear regime, where the number of excitations is much smaller than the number of electrons in the quantum wells. We will finish with an overview of some recent developments in the field. All systems presented here, at the exception of the one presented in Ref. [42], are working in this linear regime.

1.1 The electronic part

1.1.1 The physical system

The matter part of the system is a semiconductor multi-quantum wells structure where materials are doped with donors so that electrons are present in the conduction band (figure 1.1). If the quantum wells are thin enough and/or the barriers are high enough, wells can have several bound states and the electronic dynamics is dramatically affected: motion along the growth axis is quantified while it remains free in the plane. The conduction band is then split into several subbands and

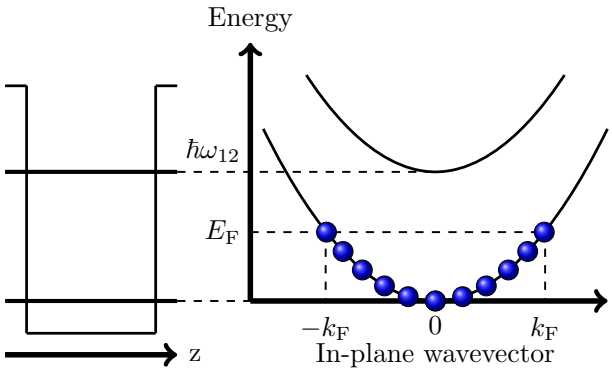

Figure 1.1: Left: energy profile of one quantum well in the z direction and its two lowest bound states. Right: Electronic dispersion of the first two conduction subbands in each well as a function of the in-plane wave vector. Because the wells are doped, electrons are present in the lowest subband even in the ground state. The Fermi energy E_F, the Fermi wave vector k_F and the energy difference between the two bound states $\hbar\omega_{12}$ are highlighted.

electrons behave as an effective two-dimensional electron gas.

Realizations of such systems can be made of an alternance of AlGaAs and GaAs layers, where the percentage of aluminum in the barriers can be adapted to tune their height. The energy between the wells' bound states can then cover an energy range from the mid infrared [46] to the THz [51]. The doping can be achieved by adding silicon atoms in the wells or the barriers. Other possibilities are InAs/AlSb or GaInAs/AlInAs heterostructures [50, 52].

In the following we will use the effective mass approximation and neglect the dependence of the mass over the energy. The conduction subbands are then parabolic and parallel and the one-electron wavefunction for the n^{th} subband is

$$\psi_{\mathbf{k},n}(\mathbf{r},z) = \frac{1}{\sqrt{S}}\,\mathrm{e}^{\mathbf{i}\mathbf{k}.\mathbf{r}}\,\chi_n(z), \tag{1.1}$$

where S is the sample area, $\mathbf{r}$ is the two-dimensional position in the plane of the wells, $\mathbf{k}$ is the two-dimensional wave vector and χ_n is the wavefunction of the n^{th} bound state of the quantum wells. The associated energy is

$$\hbar\omega_{n,k} = \hbar\omega_n + \frac{\hbar^2 k^2}{2m^*}. \tag{1.2}$$

In the previous expressions, spin indices have been omitted. Similar expressions can be derived for the valence subbands but we do not consider them here. For sake

of simplicity, we will also assume that the wells are identical, symmetric, square and infinitely deep, even if some interesting effects are predicted for non-symmetric wells [53]. Analytical expressions for χ_n and $\hbar\omega_n$ are then obtained

$$\begin{aligned} \chi_n(z) &= \sqrt{\frac{2}{L}} \sin\left(n\pi\frac{z}{L}\right), \\ \hbar\omega_n &= \frac{\hbar^2\pi^2 n^2}{2m^* L^2}, \end{aligned} \tag{1.3}$$

where L is the length of the well.

1.1.2 Ground state and excitations

We will now describe the ground state and the excitations of the system for independent electrons. For the moment, we will thus neglect the Coulomb interaction.

In the ground state, every electronic state whose energy is below the Fermi energy is filled, taking into account the spin degeneracy. Because of the doping, the Fermi energy, which lies in the gap for bare semiconductors, is shifted above the minimum of the lowest conduction subband. In the following we will assume that it is below the minimum of the second subband so that only the first subband is populated (figure 1.1).

An excitation of the system is the promotion of an electron from a state below the Fermi energy to a state above, thus creating an electron-hole pair. Even if electrons can come both from the valence subbands and the lowest conduction subband we will neglect the former case as we are interested only in the physics inside the conduction band. Electron-hole excitations can be of different types: while the hole is necessarily in the Fermi sea, the electron can be in the lowest or in a higher subband, defining respectively an intrasubband or an intersubband excitation (figure 1.2a). Note that an electron-hole pair is then indexed by two wave vectors and one subband index.

Now that we know what the excitations look like, we need to calculate the corresponding energies and dispersions. For the case of intersubband excitations we consider an electron with wave vector $\mathbf{k}$ in the Fermi sea, promoted to a state with wave vector $\mathbf{k}+\mathbf{q}$ in a higher subband ($n > 1$). The wave vector carried by this excitation is then $\mathbf{q}$ and the associated energy is

$$E_{\mathbf{q},1\to n} = \hbar\omega_{1n} + \frac{\hbar^2}{2m^*}\left(2\mathbf{k}.\mathbf{q} + q^2\right), \tag{1.4}$$

where $\omega_{1n} = \omega_n - \omega_1$. The $\mathbf{k}$ wave vector's modulus can be as high as the Fermi

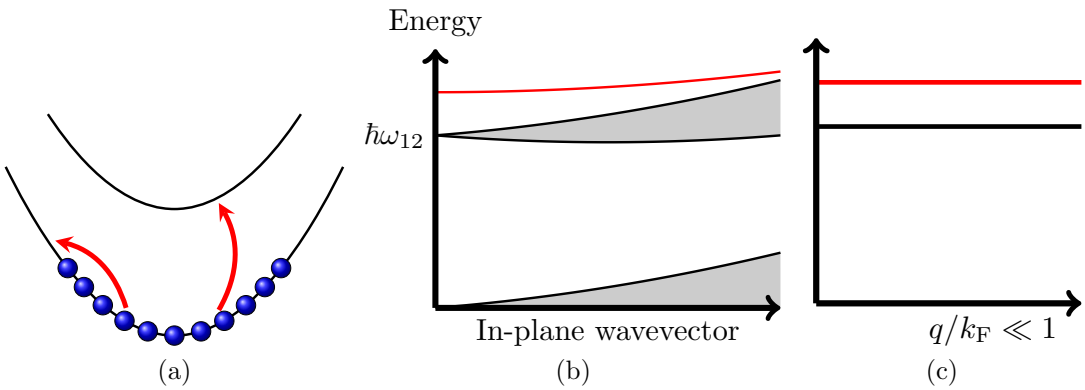

Figure 1.2: (a) The different types of excitations: intrasubband (left arrow) and intersubband excitations (right arrow). (b) Dispersions of the intrasubband excitations (lowest dispersion) and intersubband excitations (top dispersion). Red line is the dispersion of the intersubband plasmon. (c) Dispersions in the long wavelength limit. Black line: highly degenerated electron-hole continuum. Red line: intersubband plasmon.

wave vector k_F and the angle between $\mathbf{k}$ and $\mathbf{q}$ can take any value so the energy is bounded below and above by two parabola (figure 1.2b)

$$\frac{\hbar^2}{2m^*}\left(q^2 - 2k_F q\right) \leq E_{\mathbf{q},1\to n} - \hbar\omega_{1n} \leq \frac{\hbar^2}{2m^*}\left(q^2 + 2k_F q\right). \tag{1.5}$$

The case of intrasubband excitations is more complicated to describe due to Pauli blocking. Nevertheless, it is very similar in spite of the fact that the energy of the excitation cannot be negative. Equation (1.5) is still valid in this case with $\hbar\omega_{11} = 0$ only when the lower bound is positive. When it is not, the energy is bounded below by zero and above by the upper parabola (figure 1.2b).

As we shall see, only some intersubband excitations are coupled to light and for our study we can restrict ourselves to the two lowest subbands. The subband index can then be dropped and only two wave vectors are necessary to characterize an electron-hole pair. Moreover, only the limit $q \ll k_F$ (long wavelength approximation) is relevant so the dispersion is reduced to a flat line at the energy $\hbar\omega_{12}$ (figure 1.2c). From a classical point of view, such an excitation is an oscillation of the electrons along the z direction. They can thus be created by an oscillating electric field with a non-zero z component.

Until now Coulomb interactions have not been mentioned. However, electron densities can be high in our system, so many-body effects cannot be neglected.

The main effect of the Coulomb interaction is to give a collective character to the elementary excitations, namely creating the so-called intersubband plasmons. Its energy is blue-shifted with respect to the electron-hole continuum and it concentrates (almost) all the oscillator strength of the transition [51, 54, 55].

1.2 The photonic part

The light-matter coupling is a key quantity to consider when optimizing the efficiency of optical emitters and detectors, or to explore some exotic physics [12, 29, 41]. In both cases the basic rule is: the more, the better. A solution is to confine photons in a cavity, an effect known as Purcell effect [2]. Here we consider only planar microcavities (figure 1.3a), where photons are sandwiched between two mirrors made of metallic or low refractive-index dielectric layers or even a semiconductor/air interface. In the last two cases, the confinement is then ensured by total reflections at the interface.

The motion of the photons is quantified in the direction normal to the plane and photons acquire an effective two-dimensional dynamics. The modes are then indexed by an integer $j > 1$, a two-dimensional wave vector $\mathbf{q}$ and a polarization $\sigma = \mathrm{TM/TE}$ (magnetic/electric field in the plane of the cavity), and their dispersion is given by the following relation

$$\hbar\omega_{\mathrm{cav},j,\sigma}(\mathbf{q}) = \frac{\hbar c}{n}\sqrt{q^2 + {q_j}^2}. \tag{1.6}$$

Here q_j is the quantized z component of the wave vector, c is the speed of light in the vacuum and n is the refractive index of the medium enclosed in the cavity. A typical photonic dispersion of the lowest mode is plotted in figure 1.3b. In the following we will treat cavities whose lower branch lies in the mid infrared or the THz range. The typical wave vector $\mathbf{q}$ will then be of the order of 10^{-2} to $10^{-1}\,\mu\mathrm{m}^{-1}$. As a comparison, the Fermi wave vector of a two-dimensional electron gas with density $n_{\mathrm{el}} = 10^{11}\,\mathrm{cm}^{-1}$ is around $100\,\mu\mathrm{m}^{-1}$, which justifies the long wavelength approximation mentionned in the previous section.

Note that all modes have a parabolic shape for small wave vectors, with a non-zero frequency and that the linear dispersion is recovered only for high wave vectors. Each mode is twice degenerate, but the TE polarization has no electric field along the z direction, so only the TM polarization is coupled to the intersubband excitations. To further simplify the problem we will now assume that only the lowest cavity

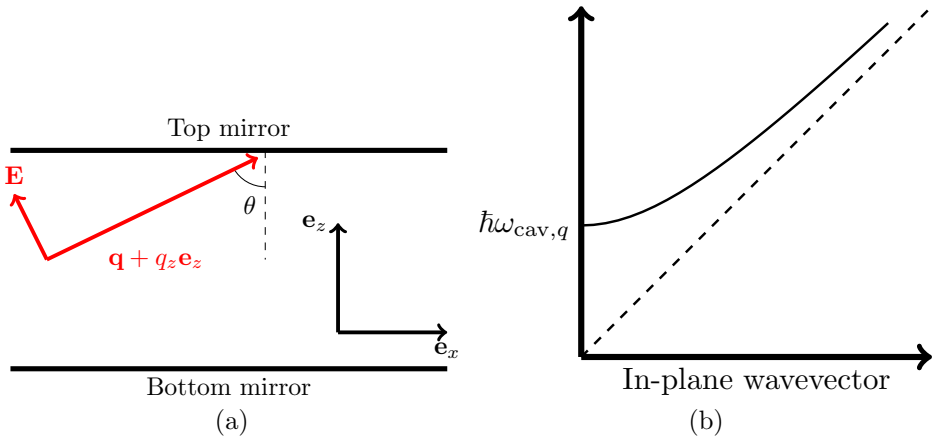

Figure 1.3: (a) Schematic of the cavity and electric field for a TM mode. In this configuration, the magnetic field is parallel to $\mathbf{e}_y$, in the plane of the cavity. (b) Solid line: dispersion of the lowest cavity mode. Dashed line: dispersion in free space.

branch can be resonant with the electronic excitations so we can drop the others. The frequency of the only remaining branch will be denoted $\omega_{\mathrm{cav},q}$ with no mention of the polarization or the mode index since it is no longer ambiguous. We are then left with one photonic mode coupled to an intersubband excitation (plasmon).

This analysis is sligthly modified for double metal cavities, where another TM mode with index $j = 0$ and linear dispersion is present. This mode is coupled to the intersubband excitations presented in the previous section and the confinement can be much better than with other types of cavities. However it is poorly coupled to the field outside the cavity making it difficult to measure. To overcome this difficulty, one can change the cavity shape to obtain a two or three-dimensional confinement (figure 1.13b). The current highest light-matter coupling has been obtained in the THz regime with such geometries [51]. But, as we focus here only on planar cavities, we will not consider this mode.

1.3 The light-matter coupling

Both parts of the system have now been introduced, but as isolated subsystems. We also saw that some of their excitations are coupled—namely the intersubband plasmon and the lowest TM mode—but without discussing the effect of this coupling on the physics of the whole system. We will now present different kinds of coupling regimes in a general fashion. We will then apply these general considerations to our

case.

1.3.1 Weak, strong and ultra-strong coupling

Consider two states, one in each subsystem. For sake of simplicity, assume that these states are resonant at the energy $\hbar\omega$. When these wo states are coupled with strength $\hbar\Omega$, the energy is transferred from one subsystem to the other with frequency Ω [56]. These oscillations are called Rabi oscillations and Ω is the vacuum Rabi frequency. The new eigenstates of the whole system then have energy $\hbar\omega \pm \hbar\Omega$. They are, thus, separated by $2\hbar\Omega$ (figure 1.4a), *i.e.*, energy levels repel each other. The more general case of non resonant excitations is given in Eq. (1.14).

Before coupling our two subsystems together, we must also consider their coupling to the environment. Because of this coupling, the energy injected into them is irreversibly transferred to the environment and lost. The system is said to be dissipative. Excited states then acquire a finite lifetime τ, corresponding to the mean time the system remains in this state before it relaxes. In the frequency domain, this translates into a finite linewidth $\gamma = 1/\tau$ (figures 1.4b and 1.4c). For the photonic part, the environment can be the electromagnetic field outside the cavity, and losses come from the finite reflectivity of the mirrors. For the electronic part, the environment can be a phononic field and losses are due to the interaction between electrons and ions of the lattice.

The dynamics of the coupled system is then the result of the interplay between reversible energy transfer between the two subsystems and energy losses in the environment. Depending on the value of the ratio γ/Ω, different regimes can be identified.

If $\hbar\Omega < \hbar\gamma$, the system is in the weak coupling regime. In average, an excitation is lost before a single Rabi oscillation has occured. It might be transferred to the other subsystem but it will not be transferred back. For example, a cavity photon can be converted into an electron-hole pair, but this pair will recombine non-radiatively. In the frequency domain, the two levels repel each other but they remain too close in energy and cannot be resolved (figure 1.4b).

If $\hbar\Omega > \hbar\gamma$, the system is in the strong coupling regime. In average, an excitation is transfered back and forth between the two subsystems before it is lost in the environment. We thus observe damped Rabi oscillations [57]. Cavity photons are absorbed and reemited several times before they leave the cavity or an electron-hole pair recombines non-radiatively. The new energy levels are well separated in energy

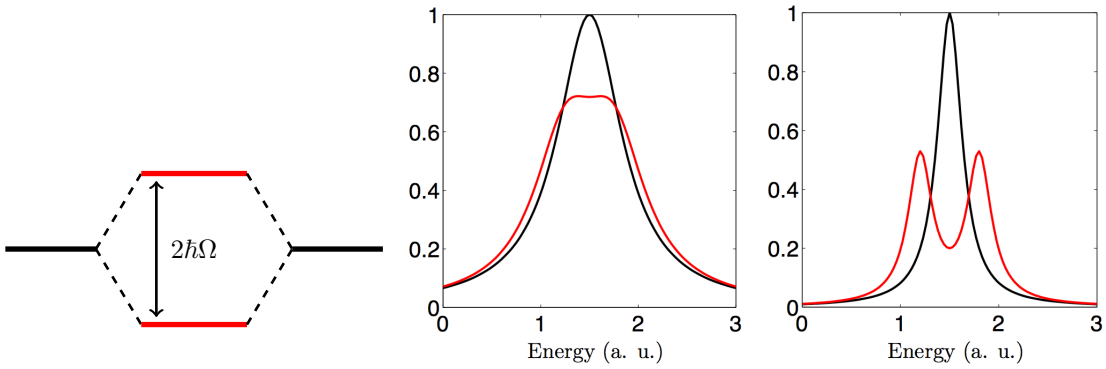

(a) (b) (c)

Figure 1.4: (a) Two coupled resonant energy levels. The new eigenstates of the system are states separeted in energy by twice the Rabi frequency. (b) Typical absorption shape for uncoupled (black) and coupled (red) two resonant levels in the weak coupling regime. (c) The same in the strong coupling regime. The Rabi splitting is now large enough to resolve the absorption peaks of the two states.

and can be resolved in frequency domain (figure 1.4c).

When the coupling increases enough to become comparable to the transition energy—in our case $\hbar\omega_{12}$—the system enters a third qualitatively different regime called ultra-strong coupling regime [38]. In this regime, the ground state is a two-mode squeezed vacuum, which contains virtual excitations. These excitations cannot be observed directly due to the energy conservation. But if the coupling is varied non-adiabatically, these virtual excitations can be turned into real entangled ones and observed [58, 41, 39, 59].

1.3.2 Intersubband polaritons

The light-matter coupling between single atoms and cavity photons is very small [60], so the strong coupling regime can be obtained only for extremely high quality cavities and atoms in vacuum [12]. In condensed matter physics, such cavities cannot be obtained. However, the strong coupling regime has been reached for atom-like structures like quantum dots [15, 16, 17] in nanocavities or Josephson junctions in supraconducting circuits [18, 19]. In our system, the coupling between a single electron and cavity photons is small, so the strong coupling regime is very unlikely to be reached. However, the situation is dramatically different when considering a large number of electrons interacting collectively with the cavity photons. If the number of electrons is large enough, the light-matter coupling between photons and

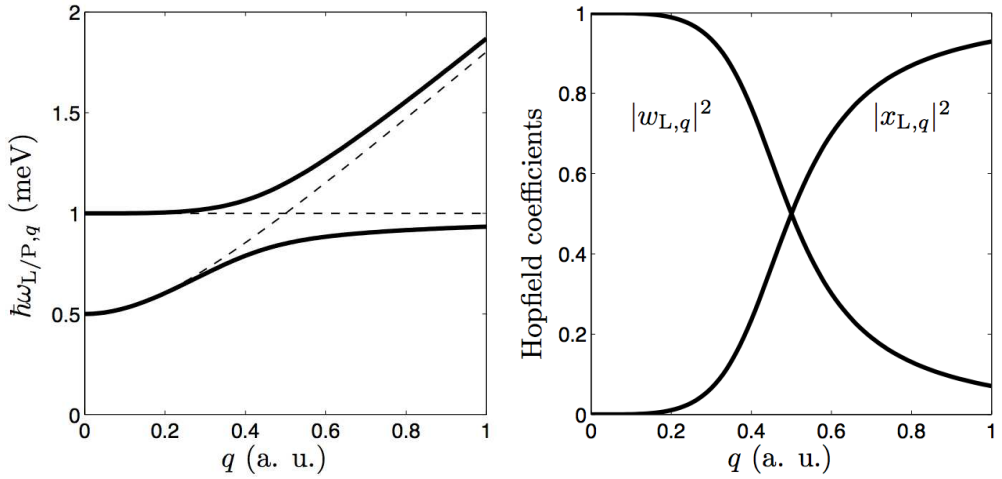

(a) (b)

Figure 1.5: Typical shape of the polaritonic dispersions (figure (a)) and Hopfield coefficients (figure (b)).

some collective excitation is enhanced and can be larger than the linewidth of the bare excitations. In our case, this large assembly of electrons is our effective two-dimensional electron gas.

To understand this last point, let's consider the following simplified model, with one quantum well and no Coulomb interaction. Moreover, we assume that only one excitation is injected in the system. Then, it can either contain a photon of wave vector $\mathbf{q}$, $|\mathrm{ph} : \mathbf{q}\rangle$, or an electron-hole pair, indexed by $\mathbf{k}$ and $\mathbf{q}$, $|\text{e-h} : \mathbf{k}, \mathbf{q}\rangle$. There are N_{el} electron-hole pair states, where N_{el} is the number of electrons the well, all at the same energy $\hbar\omega_{12}$ (because the Coulomb interaction is omitted in this simplified model) and equally coupled to the cavity field. Let's denote $\hbar\chi_q$ the coupling between a single electron-hole pair and a cavity photon. We will see in chapter 2 that it is inversely proportional to the sqare root of the surface of the cavity S, and proportional to the electric dipole of the electron-hole pairs. The Hamiltonian, restricted to the one-excitation subspace can then be written

$$H_{\mathbf{q}} = \begin{pmatrix} \hbar\omega_{\mathrm{cav},q} & \hbar\chi_q & \dots & \hbar\chi_q \\ \hbar\chi_q^* & \hbar\omega_{12} & 0 & \dots \\ \vdots & 0 & \ddots & \\ \hbar\chi_q^* & \vdots & & \hbar\omega_{12} \end{pmatrix}. \tag{1.7}$$

This problem can be greatly simplified thanks to a change of basis for the matter part,

$$\{|\text{e-h} : \mathbf{k}, \mathbf{q}\rangle\}_{\mathbf{k}} \to \{|\text{e-h} : i, \mathbf{q}\rangle\}_i, \tag{1.8}$$

where index i runs from zero to $N_{\text{el}} - 1$. State $|0, \mathbf{q}\rangle$ is defined as

$$|\text{e-h} : 0, \mathbf{q}\rangle = \frac{1}{n_{\text{QW}} N_{\text{el}}} \sum_{\mathbf{k}} |\text{e-h} : \mathbf{k}, \mathbf{q}\rangle \,, \tag{1.9}$$

while the others are obtained by an orthonormalization procedure. In this new basis the Hamiltonian is

$$\bar{H}_{\mathbf{q}} = \begin{pmatrix} \hbar\omega_{\text{cav},q} & \sqrt{N_{\text{el}}}\,\hbar\chi_q & 0 & \dots \\ \sqrt{N_{\text{el}}}\,\hbar\chi_q^* & \hbar\omega_{12} & 0 & \dots \\ 0 & 0 & \hbar\omega_{12} & \\ \vdots & \vdots & & \ddots \end{pmatrix}. \tag{1.10}$$

This matrix is almost diagonal and the interesting part, the light-matter coupling, can be studied in the smaller subspace generated by $|\text{ph} : \mathbf{q}\rangle$ and $|\text{e-h} : 0, \mathbf{q}\rangle$. State $|\text{e-h} : 0, \mathbf{q}\rangle$ is called bright excitation, while orthogonal uncoupled states are said to be dark. Then, it has the simpler form

$$\tilde{H}_{\mathbf{q}} = \begin{pmatrix} \hbar\omega_{\text{cav},q} & \hbar\Omega_q \\ \hbar\Omega_q^* & \hbar\omega_{12} \end{pmatrix}, \tag{1.11}$$

where $\hbar\Omega_q = \sqrt{N_{\text{el}}}\,\hbar\chi_q$ is the vacuum Rabi frequency. It is proportional to the areal electronic density in the quantum well and is the relevant quantity to consider when coupling the electron gas to the cavity field. It is now clear that the photon is coupled to only one collective excitation, the bright excitation, and that the coupling strength is greatly enhanced as the number of electrons increases. In other words, instead of an assembly of small dipoles, the cavity field sees a giant collective dipole. This drastic enhancement of the coupling between a collection of collectively excited oscillators and a radiation field was discovered by Dicke [61, 62, 63, 64]. Historically, these collective excitations were first introduced to explain the surprisingly high spontaneous emission rate of an assembly of molecules interacting with the same field. Even if the original treatment was a little different from the one presented above, this high spontaneous emission rate is, of course, due to the collective enhancement of the light-matter coupling. This phenomenon is known as the Dicke

superradiance. In our case, this means that, by simply increasing the electronic density in the wells, the strong coupling regime can be reached even with a cavity quality much lower than with single atom [12] or in exciton polaritons [13] experiments. Moreover, contrary to the two aforementioned cases, the coupling strength is now a tunable parameter, which opens new possibilities in cavity quantum electrodynamics [39, 41, 42].

The eigenstates of this reduced Hamiltonian are called upper and lower intersubband polaritons. They are linear superpositions of one photon and one bright excitation,

$$\begin{aligned} |\mathrm{U},\mathbf{q}\rangle &= w_{\mathrm{U},q}\,|\mathrm{ph}:\mathbf{q}\rangle + x_{\mathrm{U},q}\,|\text{e-h}:0,\mathbf{q}\rangle \\ |\mathrm{L},\mathbf{q}\rangle &= w_{\mathrm{L},q}\,|\mathrm{ph}:\mathbf{q}\rangle + x_{\mathrm{L},q}\,|\text{e-h}:0,\mathbf{q}\rangle\,, \end{aligned} \tag{1.12}$$

where $w_{\mathrm{L},q}$ and $x_{\mathrm{L},q}$ are the Hopfield coefficients [65],

$$w_{\mathrm{L},q} = -\frac{1}{\sqrt{1+\left(\frac{\omega_{\mathrm{L},q}-\omega_{\mathrm{cav},q}}{\Omega_q}\right)^2}}, \quad x_{\mathrm{L},q} = \frac{1}{\sqrt{1+\left(\frac{\Omega_q}{\omega_{\mathrm{L},q}-\omega_{\mathrm{cav},q}}\right)^2}}, \tag{1.13}$$

obeying the following relation: $w_{\mathrm{U},q} = x_{\mathrm{L},q}$ and $x_{\mathrm{U},q} = -w_{\mathrm{L},q}$. The associated energies are

$$\hbar\omega_{\mathrm{U/L},q} = \frac{\hbar\omega_{\mathrm{cav},q}+\hbar\omega_{12}}{2} \pm \frac{1}{2}\sqrt{(\hbar\omega_{\mathrm{cav},q}-\hbar\omega_{12})^2 + 4\hbar\,|\Omega_q|^2}. \tag{1.14}$$

The polaritonic dispersion, with the anticrossing typical of strong or ultra-strong coupling, is plotted in figure 2.2. The Hopfield coefficients of the lower polaritons are also given (figure 1.5b). For small wave vectors, before the resonance, the lower polaritons are almost photons, while for higher wave vectors, after the resonance, they are bare intersubband excitations. At the resonance, they are mixed light-matter states. Notice that, contrary to what is observed in zero-dimensional cavities [51], there is no polariton gap in the dispersion shown in figure 2.2. This is due to the planar geometry of the cavity and the selection rules, which impose that the Rabi frequency vanishes for small wave vectors. A quick comparison with experimental results shown in figure 1.6 shows that this simple model qualitatively describe the physics of intersubband polaritons. However, this model is limited, *e.g.*, it does not take into the Coulomb interaction. It, thus, cannot explain the plasmonic nature of intersubband excitations, nor some intersubband excitation dipole-dipole inter-

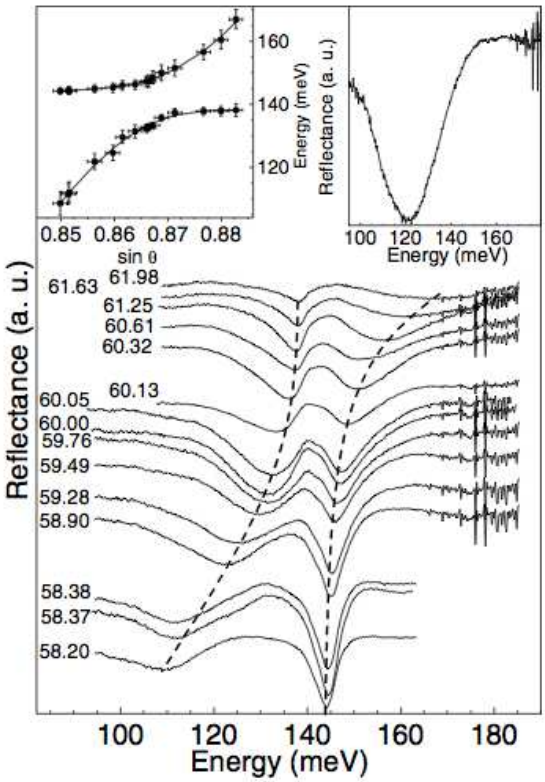

Figure 1.6: Experimental data from Ref. [14]. Reflectance for different angles of incidence for the TM polarization. Left inset: position of the peaks. Right inset: results for the TE polarization. Because it is not coupled to the electron gas, only one peak is observed corresponding the cavity mode.

action. These features will be presented in chapters 2 and 3. Moreover, this is a one-excitation model. As such, it fails to describe polariton-polarion interactions, which appeared to be extremely relevant in the case of exciton polaritons [29]. Because of this limitation, this model is limited to the linear regime, where the number of polaritons is much smaller than the number of electrons in the Fermi sea. We will explain in Chapter 3 how to treat the non linear regime.

1.3.3 Experimental realisations

We have just seen that the light-matter coupling can be much higher than could naively be expected. But is it high enough to reach the strong coupling regime?

It turns out that the answer is positive. The first observation of intersubband polaritons dates back to 2003 in the mid infrared range (140 meV) [14]. These results are plotted in figure 1.6. The linewidths of the bare intersubband bright excitation

and the cavity TM mode are respectively 5 meV and 15 meV. At the anti-crossing, they average and polariton linewidths are around 10 meV. As a comparison, the splitting at resonance, corresponding to twice the Rabi frequency, is 14 meV, which is enough to resolve the two picks.

Since then, other similar realizations have been developed and intersubband polaritons have been extensively studied.

Tuning the light-matter coupling

Some devices have been designed to test the influence of the number of electrons on the coupling [58, 66, 67] in the mid infrared. The number of electrons can be varied thanks to electrical gating, charge transfert in double quantum well structures or temperature variation. In the first case [58, 68], one of the mirror is metallic and can be used as Schottky gate as shown in figure 1.7a. By applying a gate voltage, the number of electrons in the quantum wells, and , thus, the coupling strength, can be varied (figure 1.7b). In the second case [66], the structure is very similar but the confinement of the electrons is achieved by two asymmetric coupled quantum wells (figure 1.8a). Only the largest well is doped while the thinner well transition is resonant with the cavity field. By applying a gate voltage, the well lowest subbands can be brought to resonance to populate the thin well's ground state and vary the light-matter coupling (figure 1.8b). It is *a priori* also possible to create a charge oscillation between the two wells to modulate the coupling strength at the rate of the resonant-tunneling process. Compared to the first case, much higher modulation speed can be reached, since the capacitance of the device is not a limiting factor anymore. In the third case [67], wells are doped such that the Fermi energy lies between the first and second excited subbands. Electrons involved in the light-matter coupling are in the first excited subband intead of the lowest one. Then, by increasing the temperature, electrons are promoted from the lowest to the first excited subband, thus increasing the coupling. Results are consistent with the theory.

In practice, non-adiabatic switch on and off of the light-matter coupling has been achieved [41, 69, 42]. In the first case, the system is initially undoped and is, thus, not coupled. Electrons from the valence band can then be optically injected in the lowest conduction subband thanks to an ultra-short pulse—12 fs as compared to a cavity cycle around 40 fs. Injection happens so fast that the coupling can be switched on within less than a period of the cavity (figure 1.9a), and, thanks to a THz probe,

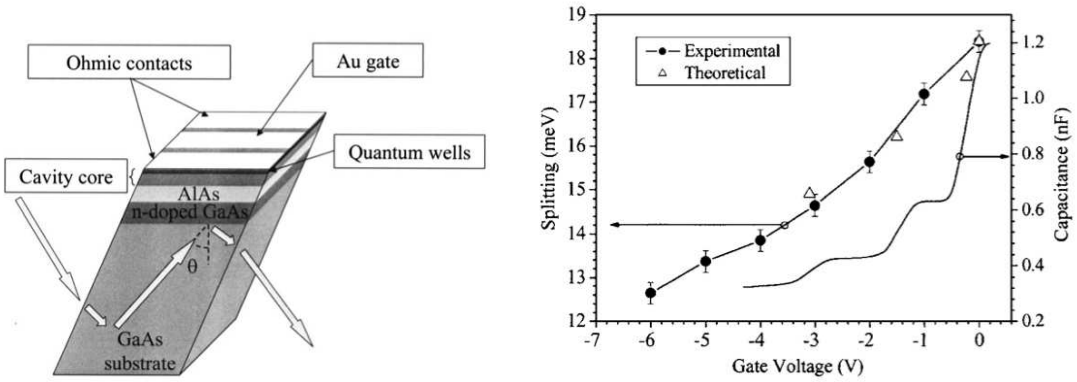

(a) (b)

Figure 1.7: (a) Schematic of a cavity with top metallic mirror. The mirror is also used as an electric contact, thus allowing to change the number of electrons in the wells. The ligth-matter coupling can then be tuned. (b) Coupling versus gate voltage. Figures taken from Ref. [58].

the system can be monitored during this short time interval. In particular, it is possible to observe the conversion of coherent photons into cavity polaritons or the evolution of the band structure in a photonic crystal. The reverse switching is also possible by optically exciting electrons from the lowest conduction subband to the first excited one thanks to a 100 fs pulse [42]. The electron gas is then depleted, thus reducing the light-matter coupling. When the intensity of the incident pulse is high enough, the system enters the weak coupling regime and polaritons are bleached (figure 1.9b). Such realisations are good candidates for the generation of entangled photons pairs from the ground state of the ultra-strongly coupled system [59].

Towards optoelectronics devices

Efforts have also been made to realize photovoltaic probes [44] and electroluminescent devices [45, 46, 47]. The heterostructure is then turned into a quantum cascade to allow electrical extraction or injection of polaritons (figure 1.10). In such systems, electrons tunnel from one well to another through tunneling minibands and are selectively extracted from or injected into upper or lower polariton states by varying the bias. The influence of the cavity has been studied, confirming its importance to reach the strong coupling regime [70]: when missing, the electroluminscent signal is the one of the bare intersubband transition (figure 1.11b); when present, its main contribution comes from the polaritonic states (figure 1.11a). The secondary

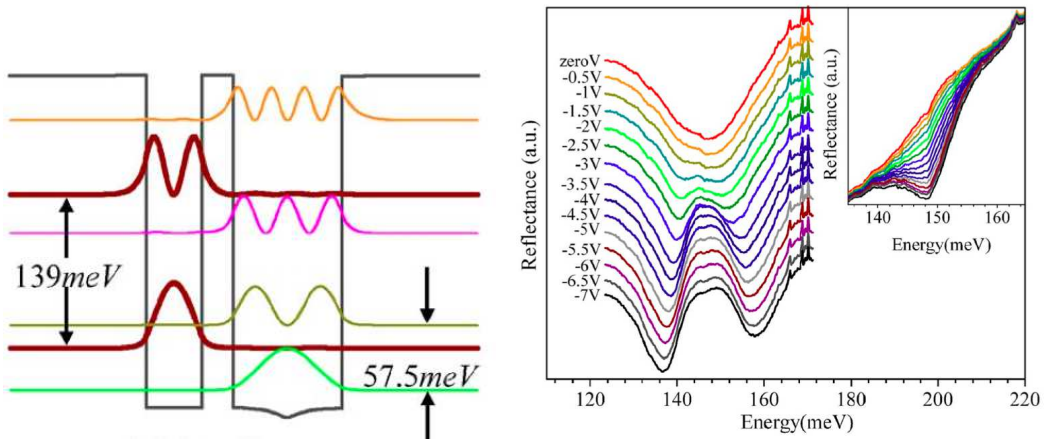

(a) (b)

Figure 1.8: (a) Band profile and energies of confined states in a double asymmetric well at zero bias. The transition occurs between the left well's two levels (thick black lines) while the electrons are in the right well's ground state (green line). By applying a bias, the two well ground states can be resonant. (b) Reflectance spectra at a given angle for different applid biases. Figures taken from Ref. [66].

feature in figure (1.11a) comes from the coupling between intersubband excitations and higher photonic modes [71, 72].

Coherent scattering of polaritons due to optical phonons was also studied [50] in such systems. Upper polaritons are electrically injected and then relax to the lower branch by emitting phonons (figure 1.12). It is then *a priori* possible to observe stimulated scattering of polaritons [48].

Increasing the light-matter coupling

Other studies focused on the ultra-strong coupling regime for THz transtions by changing the shape of the heterostructure [73, 74] or of the cavity [51, 75]. In the first case, the multi-quantum wells structure mimics a parabolic confinement along the growth direction (figure 1.13a). The transition is not blue-shifted by the Coulomb interaction even for high doping [76], making it possible to increase the Rabi frequency without increasing the transition frequency. The ultra-strong coupling regime is thus favored and a Rabi frequency of 27% of the intersubband energy was reported. In the second case, a double metal cavity is used to better confine the electromagnetic field and the TM_0 mode is used (figure 1.13b). As mentioned above, this results to the current highest ratio with a Rabi frequency of

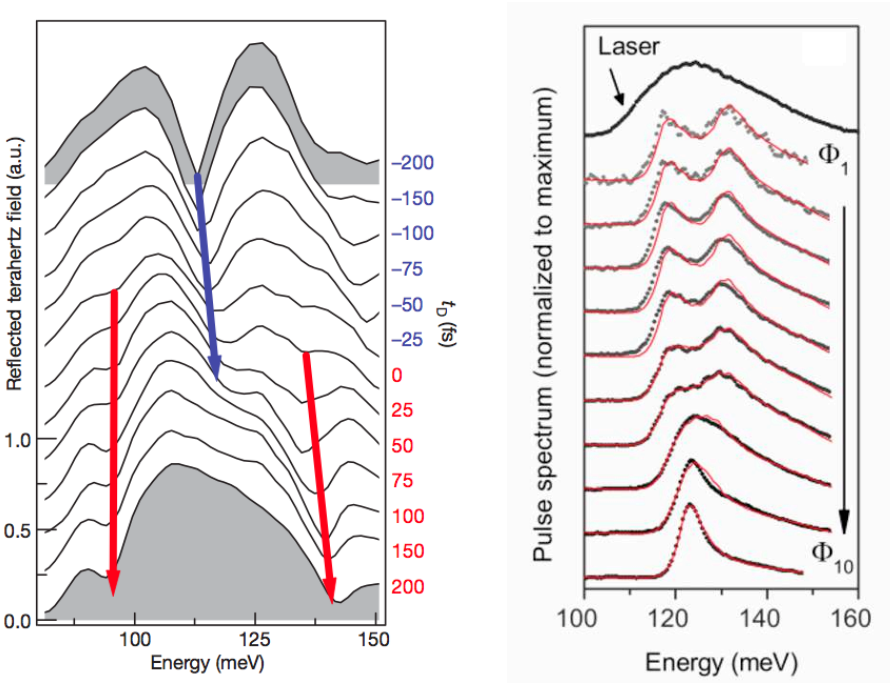

(a) (b)

Figure 1.9: Experimental results from Refs. [41] (left) and [42] (right). (a) Reflectance spectra of the cavity for different delay times t_D. A 12 fs pulse arrives at $t_D = 0$. Blue and red arrows indicate respectively positions of the bare cavity mode and of the two polaritonic branches. Switching from the weak to ultra-string coupling is abrupt: less than a cavity cycle. (b) Spectra of the 100 fs pulse after interacting with the cavity for increasing intensity (top to bottom). The incident spectra is also reported at the very top. As the intensity increases, more and more electrons are excited to higher subbands and the light-matter coupling thus decreases. At high enough intensities, polaritonic modes merge into a single bare photonic mode.

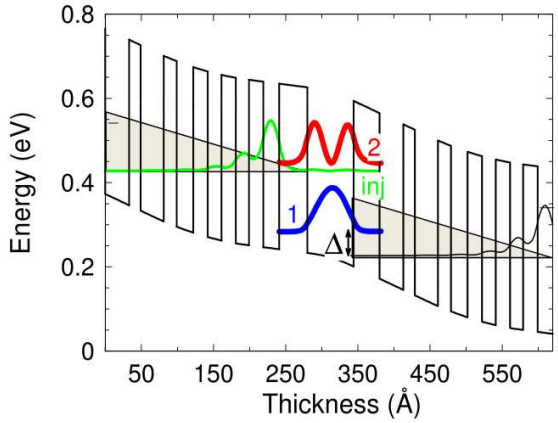

Figure 1.10: Band diagram of the quantum cascade structure reported in Ref. [70] for 6 V bias. Fundamental (1), excited (2) and injection (inj) states are also plotted. Minibands corresponds to the grey-shaded zones.

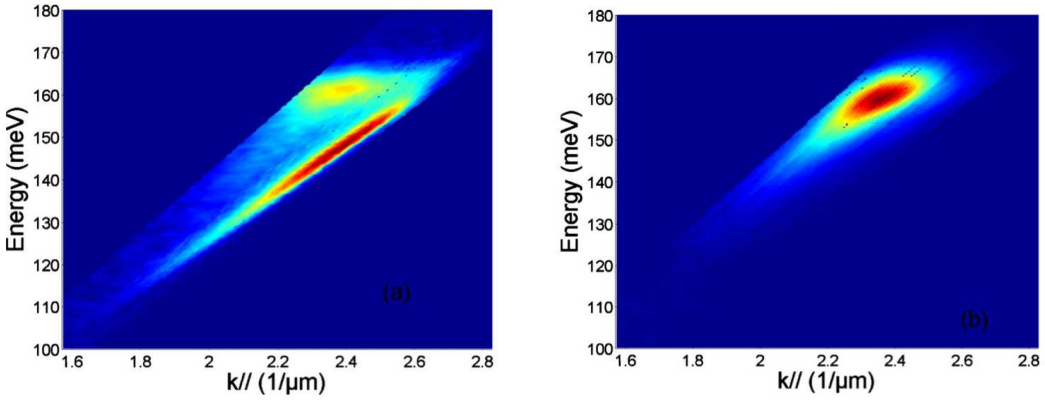

(a) (b)

Figure 1.11: Measured electroluminescence reported in Ref. [70]. (a) With the cavity. The main contribution comes from the lower polariton mode. There is also a feature at the energy of the bare transition due to coupling with higher cavity modes. (b) Without the cavity. Electroluminescence comes from the bare intersubband excitations.

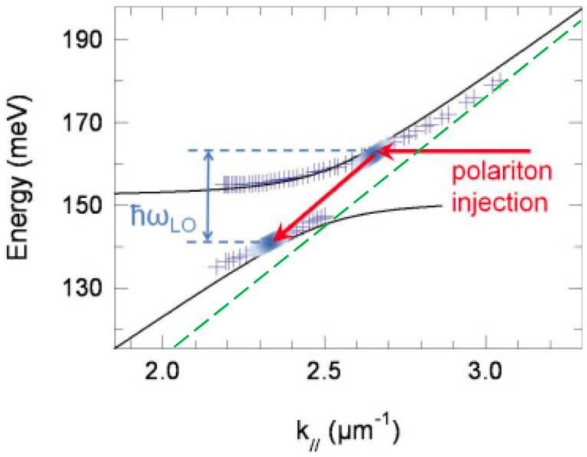

Figure 1.12: Experimental data from Ref. [50]. Electroluminescence maxima (crosses) compared with polaritonic dispersion (solid lines). Electrons are injected in upper polariton states and relax to lower polariton states by emitting a LO-phonon.

48% of the transition.

In the mid infrared, the ultra-strong coupling has been reached in highly doped quantum wells where up to four subbands are populated (figure 1.14a). Dipolar oscillators with different frequencies are phase locked by the Coulomb interaction, resulting in an intersubband plasmon concentrating all the oscillator strength. The absorption spectrum shows a narrow resonant peak, the plasmon, instead of a patch of overlaping peaks corresponding to independent incoherent oscillators (figure 1.14b). Moreover, the plasmon peak is blue-shifted with respect to the independent oscillators peaks because of the depolarization shift. Notice that the linewidth of the plasmon does not increase with temperature, making it a good candidate for room temperature operating devices. Embedded in a double metal cavity, this structure allows to reach a ratio of 33%, the highest in the mid infrared at room temperature.

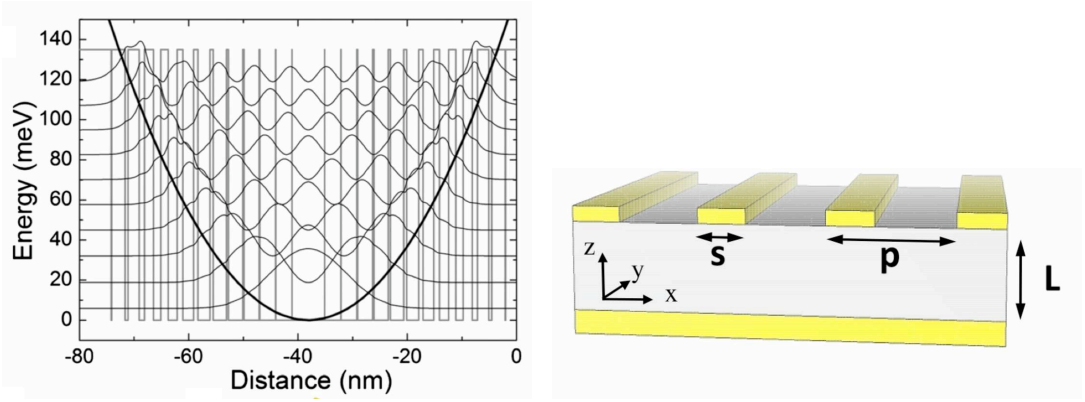

(a) (b)

Figure 1.13: (a) Band diagram of the heterostructure (gray line) with harmonic-like trapping (black line) reported in Ref. [74]. (b) Schematic of a double metal cavity. The width of the cavity can be much smaller than the wavelength of the photonic mode. The confinement of the mode is better so the light-matter coupling is higher. The coupling to the external electromagnetic field is improved thanks to the grating of the top layer. Figure taken from [77]

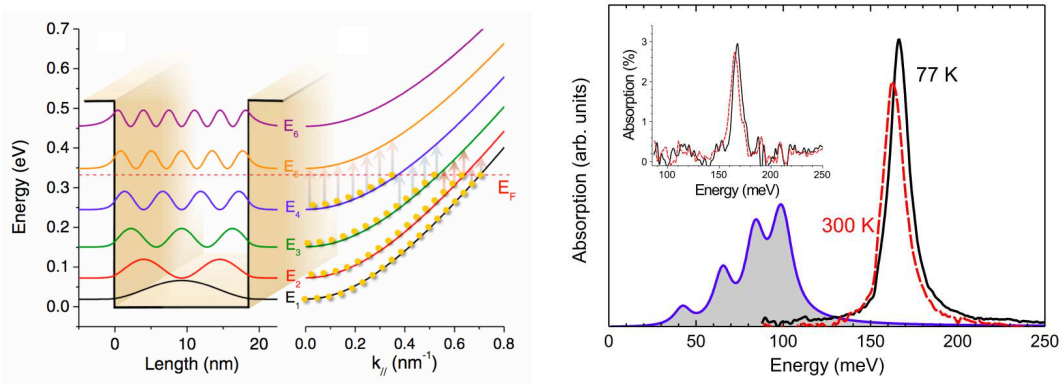

(a) (b)

Figure 1.14: (a) Schematic of the quantum well with six bound states associated subbands considered in Ref. [52]. Dashed line indicates the position of the Fermi energy, which is between the fourth and fifth subbands. (b) Experimental absorption spectrum at 77 K (black) and 300 K from Ref. [52]. Blue curve is the asborption expected from the independent electrons picture. From left to right, peaks correspond to transitions $1 \to 2$, $2 \to 3$, $3 \to 4$ and $4 \to 5$.

Chapter 2

Hamiltonian models for intersubband polaritons

In this chapter, we will present three second-quantized Hamiltonians to describe our system. We will start with the most general one, describing the electromagnetic field interacting with an assembly of electrons in the Coulomb gauge. This Hamiltonian is derived in Appendix B. Because the system consists of electron-hole excitations interacting with photons, it will combine both bosonic and pairs of fermionic operators. Moreover, because electrons interact with each other through the Coulomb interaction, it is quartic in fermionic operators. The final Hamiltonian is then too complicated to be diagonalized exactly. However, some approximations can be introduced to simplify it. Only a small subspace of the initial Hilbert space is necessary to capture the physics described in the first chapter. First, all electronic degrees of freedom outside the Fermi sea in the first subband are irrelevant for our purpose, so we remove them. We can, thus, write a second Hamiltonian whose fermionic part is written solely in terms of electrons in the second subband and holes in the Fermi sea. This Hamiltonian will be used in Chapter 3. Second, the space can be truncated to conserve only bright intersubband excitations. Moreover, these excitations introduced are almost bosonic. Based on simple physical considerations, it is then possible to write an effective bosonic Hamiltonian. Because this Hamiltonian is quadratic, it can be diagonalized exactly. It is, however, limited to the linear regime.

2.1 Fermionic Hamiltonians

2.1.1 Electron-Electron Hamiltonian

The Hamiltonian of the system can be split into five contributions,

$$H = H_{\text{Cav}} + H_{\text{Elec}} + H_{\text{I1}} + H_{\text{I2}} + H_{\text{Coul}}, \tag{2.1}$$

where H_{Cav} is the free cavity field Hamiltonian, H_{Elec} is the free quasi two-dimensional electron gas Hamiltonian, H_{I1} and H_{I2} are light-matter coupling terms and H_{Coul} is the Coulomb interaction between electrons.

Free photons and electrons

Hamiltonian H_{Cav} is obtained from the free electromagnetic field to which we add the boundary conditions corresponding to the cavity [78],

$$H_{\text{Cav}} = \sum_{\mathbf{q}} \hbar\omega_{\text{cav},q} \left(a^\dagger_{\mathbf{q}} a_{\mathbf{q}} + \frac{1}{2} \right), \tag{2.2}$$

where $a_{\mathbf{q}}$ is annihilation operator for photons satisfying

$$\left[a_{\mathbf{q}}, a^\dagger_{\mathbf{q}'} \right] = \delta_{\mathbf{q},\mathbf{q}'}. \tag{2.3}$$

Hamiltonian H_{Elec} describes the dynamics of a free electron gas subject to the confining potential of the quantum wells,

$$H_{\text{Elec}} = \sum_{n,\mathbf{k}} \left(\hbar\omega_n + \frac{\hbar^2 k^2}{2m^*} \right) c^\dagger_{n,\mathbf{k}} c_{n,\mathbf{k}}, \tag{2.4}$$

where $c_{n,\mathbf{k}}$ is the annihilation operator for an electron in the conduction subband n with wave vector $\mathbf{k}$ satisfying the fermionic anticommutation rule,

$$\left\{ c_{n,\mathbf{k}}, c^\dagger_{n',\mathbf{k}'} \right\} = \delta_{n,n'}\delta_{\mathbf{k},\mathbf{k}'}. \tag{2.5}$$

It is the kinetic energy operator of the quasi two-dimensional electron gas.

Consistently with chapter 1, we consider only the first photonic mode and the first two electronic conduction subbands. We also omit the polarization, since only the TM mode is relevant here. To simplify the notations, spin and quantum well indices are not mentioned. Electrons have the same spin and well index and there

is an implicit sum over them.

Light-matter couplings

The two ligth-matter terms $H_{\mathrm{I}1}$ and $H_{\mathrm{I}2}$ in Eq. (2.1) correspond to the absorption and emission of photons by electron-pairs, and scattering of photons on the electron gas.

Hamiltonian $H_{\mathrm{I}1}$ is given by

$$H_{\mathrm{I}1} = \sum_{\mathbf{k},\mathbf{q}} \hbar\chi_q \left(a_{\mathbf{q}} + a^\dagger_{-\mathbf{q}}\right)\left(c^\dagger_{2,\mathbf{k}+\mathbf{q}} c_{1,\mathbf{k}} + c^\dagger_{1,\mathbf{k}} c_{2,\mathbf{k}-\mathbf{q}}\right), \tag{2.6}$$

where χ_q is the coupling between a single electron and a cavity photon,

$$\hbar\chi_q = \sqrt{\frac{\hbar e^2 \sin(\theta)^2}{\epsilon_0 \epsilon_r m^{*2} S L_{\mathrm{cav}} \omega_{\mathrm{cav},q}}}\, p_{12}, \quad p_{12} = \int_0^L \mathrm{d}z\, \chi_2(z)\, p_z\, \chi_1(z). \tag{2.7}$$

This coupling is proportional to the quantum fluctuations of the field in the cavity [79]. It is then inversely proportional to the square root of the volume of the microcavity SL_{cav}. It is also proportional to the electric dipole moment of the transition, which yields the geometrical factor p_{12}, encoding selection rules of the transition. Again, the two fermionic operators act on the same quantum well and summation over the wells is implicit. This interaction is also spin conserving and sum over spins is implicit too. Hamiltonian $H_{\mathrm{I}1}$ has two different contributions. First, resonant terms describing absorption (emission) of photons by creation (recombination) of electron-hole pairs. Second, non resonant terms where two excitations can be created or annihilated simultaneously. Because they do not conserve the energy, they are negligeable in the weak and strong coupling regime. They, however, become important in the ultra-strong coupling regime where they change the nature of the ground-state [38].

Hamiltonian $H_{\mathrm{I}2}$ is given by

$$H_{\mathrm{I}2} = \sum_{\mathbf{k},\mathbf{q}} \frac{n_{\mathrm{QW}} N_{\mathrm{el}} |\hbar\chi_q|^2}{\hbar\omega_{12}} \left(a_{-\mathbf{q}'} + a^\dagger_{\mathbf{q}'}\right)\left(a_{\mathbf{q}} + a^\dagger_{-\mathbf{q}}\right). \tag{2.8}$$

A comparison with Eq. (B.20) shows that only the A^2-term from Hamiltonian $H_{\mathrm{I}2}$ has been conserved. This is justified by the fact the scattering part (see Eq. (B.20)) gives a negligeable compared to the A^2-term. Also, a coefficient was omited in the expression of the Hamiltonian. This introduces a minor correction in the case

of an infinite quantum well and is exact for a parabolic one. As for the previous light-matter term, anti-resonant terms become significant only in the ultra-strong coupling regime.

Coulomb interaction

The Coulomb interation is given by

$$H_{\text{Coul}} = \frac{1}{2} \sum_{\substack{\mathbf{k},\mathbf{k}',\mathbf{q}\neq 0 \\ \mu,\mu',\nu,\nu'}} V_q^{\mu\nu\nu'\mu'}\, c^\dagger_{\mu,\mathbf{k}+\mathbf{q}} c^\dagger_{\nu,\mathbf{k}'-\mathbf{q}} c_{\nu',\mathbf{k}'} c_{\mu',\mathbf{k}}. \tag{2.9}$$

Notice first that the sum does not contain the troublesome terms $\mathbf{q} = 0$ [80, 81]. Once again, electrons in different wells are not coupled, the interaction is spin conserving and sums over wells and spins are implicit.

The Coulomb coefficients are given by

$$\begin{aligned} V_q^{\mu\nu\nu'\mu'} &= \frac{e^2}{2\epsilon_0\epsilon_r S q}\, I_q^{\mu\nu\nu'\mu'}, \\ I_q^{\mu\nu\nu'\mu'} &= \int \mathrm{d}z\, \mathrm{d}z'\, \chi_\mu(z)\chi_\nu(z')\mathrm{e}^{-q|z-z'|}\chi_{\nu'}(z')\chi_{\mu'}(z). \end{aligned} \tag{2.10}$$

First factor in Eq. (2.10) is the Coulomb interaction for a true two-dimensional electron gas. The geometrical factor $I_q^{\mu\nu\nu'\mu'}$ is due to the spatial confinement of the electrons in the wells and introduces some selection rules: For symmetric wells, the coefficient is non zero only if the wavefunction products $\chi_\mu\chi_{\mu'}$ and $\chi_\nu\chi_{\nu'}$ have the same parity. As we limit ourselves to the first two subbands, this corresponds to cases where the sequence $\mu\nu\nu'\mu'$ contains an even number of 1 and 2 indices. Moreover, some of them are equal,

$$\begin{aligned} V_q^{1122} &= V_q^{1212} = V_q^{2121} = V_q^{2211}, \\ V_q^{1221} &= V_q^{2112}, \end{aligned} \tag{2.11}$$

leaving us with only four distinct coefficients V_q^{1111}, V_q^{2222}, V_q^{1221} and V_q^{1212}.

These four coefficients correspond to four different processes (figure 2.1), which we can divide into two categories depending on their impact on intersubband excitations. In the first three cases, electrons in subbands μ and ν interact with each other and are scattered inside the same subbands. They, thus, cannot create or annihilate intersubband excitations. We can, however, expect them to scatter pairs of intersub-

band excitations [21]. In the last case, electrons are scattered to the other subbands, thus creating or annihilating electron-hole pairs. These terms are responsible for the depolarization shift [54, 55]. In the following, we will refer to these two categories respectively as the intrasubband and intersubband Coulomb interactions. As we shall see, they have a different impact on the physics of intersubband polaritons.

For the moment, we can see that they have a very different behavior in the long-wavelength limit (figure 2.1). In the absence of screening, the intrasubband Coulomb terms diverge, like for a true two-dimensional electron gas [80, 81], while the intersubband Coulomb interaction does not.

Screened Coulomb interaction

The dense two-dimensional electron gas in the first electronic subband screens the Coulomb interaction. In order to take this into account, we will replace the bare Coulomb interaction $V_q^{\mu\nu\nu'\mu'}$ in Eq. (2.10), with its static RPA-screened version $\tilde{V}_q^{\mu\nu\nu'\mu'}$. These coefficients obey the Dyson equation [82, 83]

$$\tilde{V}_q^{\mu\nu\nu'\mu'} = V_q^{\mu\nu\nu'\mu'} + \sum_{\alpha,\beta} V_q^{\mu\beta\alpha\mu'}\, \Pi^{\alpha\beta}(\mathbf{q}, \omega = 0)\, \tilde{V}_q^{\alpha\nu\nu'\beta}, \tag{2.12}$$

where $\Pi^{\alpha\beta}(\mathrm{q}, \omega)$ is the RPA polarization function for the $\alpha \to \beta$ transition

$$\Pi^{\alpha\beta}(\mathbf{q}, \omega) = \lim_{\delta\to 0} \frac{1}{\hbar} \sum_{\mathbf{k}} \frac{f_{\alpha,\mathbf{k}+\mathbf{q}} - f_{\beta,\mathbf{k}}}{\omega_{\alpha,|\mathbf{k}+\mathbf{q}|} - \omega_{\beta,k} - \omega - \mathrm{i}\delta}, \tag{2.13}$$

where $f_{i,\mathbf{k}}$ is the occupation number in the subband i. We assume that the matter part of the unperturbed system—free electrons—is in its ground state with all electrons in the Fermi sea. The polarization function for $2 \to 2$ transition is then zero. The screened interactions, thus, take the form

$$\begin{aligned} \tilde{V}_q^{1\nu\nu1} &= \frac{V_q^{1\nu\nu1}}{1 - V_q^{1111}\Pi^{11}(\mathbf{q}, 0)}, \\ \tilde{V}_q^{2222} &= \frac{V_q^{2222} + [(V_q^{1221})^2 - V_q^{1111}V_q^{2222}]\Pi^{11}(\mathbf{q}, 0)}{1 - V_q^{1111}\Pi^{11}(\mathbf{q}, 0)}, \\ \tilde{V}_q^{1212} &= \frac{V_q^{1212}}{1 - V_q^{1212}[\Pi^{12}(\mathbf{q}, 0) + \Pi^{21}(\mathbf{q}, 0)]}, \end{aligned} \tag{2.14}$$

where $\nu = \{1, 2\}$. Screening of intrasubband and intersubband processes is, thus, different and can be encoded respectively in the dielectric functions $\epsilon(\mathbf{q})$ and $\epsilon_{12}(\mathbf{q})$,

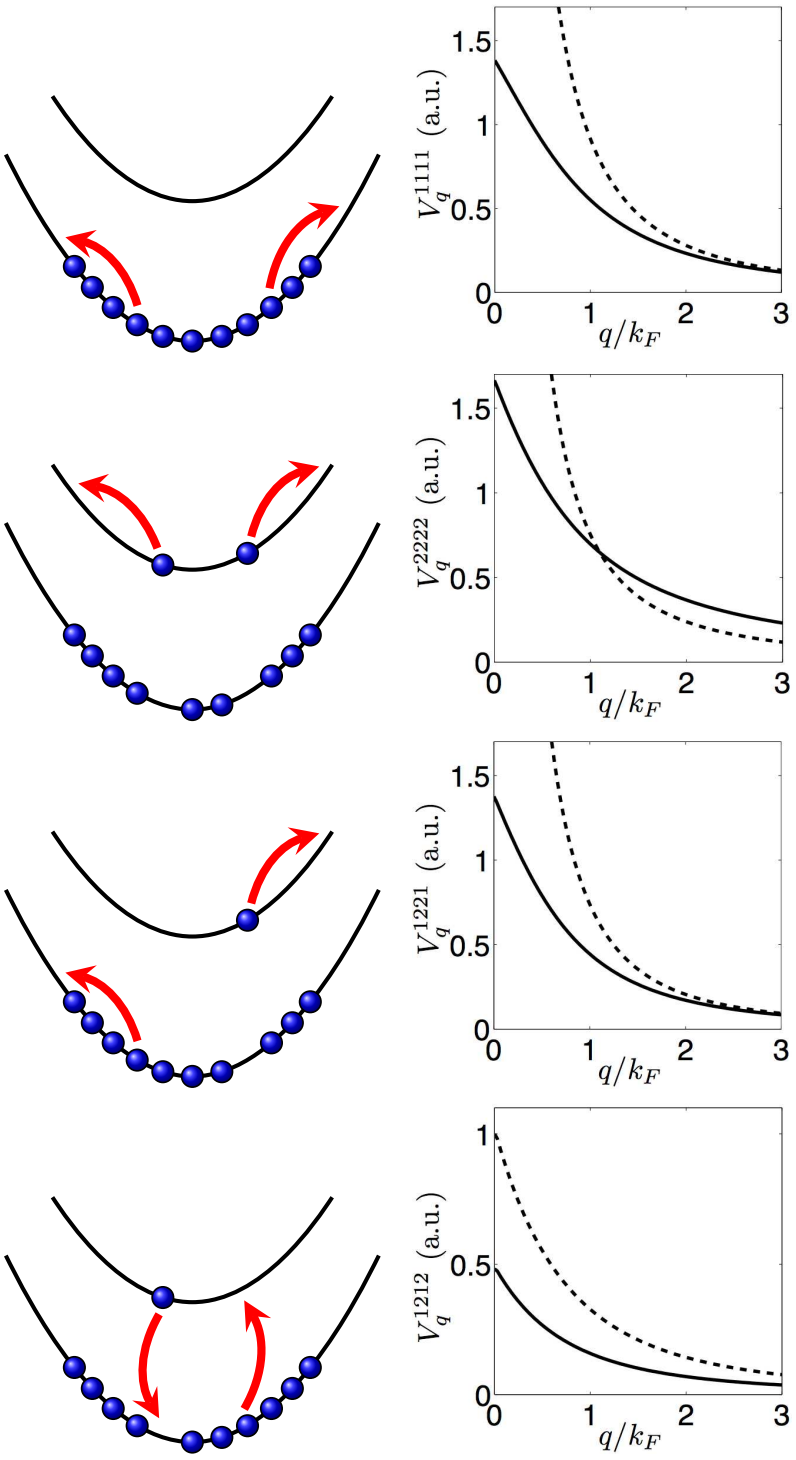

Figure 2.1: The different Coulomb processes. The left column present a schematic of the four relevant processes. The right column shows the wave vector dependency of the Coulomb coefficients in Eq. (2.10) in the THz range with $\hbar\omega_{12} = 15$ meV and electronic density in the wells $n_{\text{el}} = 3 \times 10^{11}$ cm^{-2}. Solid line: RPA-screened Coulomb interaction. Dashed line: bare Coulomb interaction.

where

$$\epsilon(\mathbf{q}) = 1 - V_q^{1111}\Pi^{11}(\mathbf{q}, 0), \tag{2.15}$$

and

$$\epsilon_{12}(\mathbf{q}) = 1 - V_q^{1212}[\Pi^{12}(\mathbf{q}, 0) + \Pi^{21}(\mathbf{q}, 0)]. \tag{2.16}$$

Notice that the dielectric function for the intrasubband processes is very similar to the one for a true two-dimensional electron gas.

We can then write the analogue of Eq. (2.10) with screening

$$\begin{aligned} \tilde{V}_q^{\mu\nu\nu\mu} &= \frac{e^2}{2\epsilon_0\epsilon_r\epsilon(\mathbf{q})Sq}\,\tilde{I}_q^{\mu\nu\nu\mu}, \\ \tilde{V}_q^{1212} &= \frac{e^2}{2\epsilon_0\epsilon_r\epsilon_{12}(\mathbf{q})Sq}\,\tilde{I}_q^{1212}. \end{aligned} \tag{2.17}$$

In Eq. (2.17), all geometric factors $I^{\mu\nu\nu'\mu'}$ remain the same except for I_q^{2222}.

As already mentioned in the first chapter, only the long-wavelength limit is relevant to study the electronic part of the system. We thus consider the $\mathbf{q} \to 0$ limit of the above expressions. The dielectric function for the intra- and intersubband Coulomb processes is [82]

$$\epsilon(q \to 0) = 1 + \frac{\kappa}{q} I_q^{1111}, \tag{2.18}$$

$$\epsilon_{12}(0) = 1 + \frac{20(k_{\mathrm{F}}L)^2\kappa L}{27\pi^4}, \tag{2.19}$$

where κ is the Thomas-Fermi wave vector

$$\kappa = \frac{m^* e^2}{2\pi\hbar^2\epsilon_0\epsilon_r}. \tag{2.20}$$

The geometrical factor I_q^{2222} is modified as follows

$$\tilde{I}_q^{2222} = I_q^{2222} + \frac{5\kappa L}{16\pi^2}. \tag{2.21}$$

For the intrasubband Coulomb processes screening removes the divergence. When the wave vector q tends to zero, the geometrical factor I_q^{1111} tends to one and the dielectric function of the true two-dimensional electron gas is found. For the in-

tersubband Coulomb process, screening only renormalizes the bare interaction (figure 2.1).

2.1.2 Simplified electron-hole Hamiltonian

We now know the different terms of the Hamiltonian but it is too complicated to be diagonalized exactly. Before going any further, we need to simplify it. To do so, we can remove some irrelevant terms, thus reducing the size of the Hilbert space. For convenience and consistence with the electron-hole pair concept, we also introduce the hole operators. This allows us to simplify the calculation of matix elements, which will the quantity of interest in chapter 3.

Ground state

As defined in the first chapter, the ground state is

$$|F\rangle = \prod_{k<k_{\mathrm{F}}} c^{\dagger}_{1,\mathbf{k}} |0\rangle \,, \tag{2.22}$$

where state $|0\rangle$ is the vacuum, with no photons nor electrons. What we call here ground state is in fact the ground state of the system with no Coulomb interaction and no light-matter coupling. This state has no photon in the cavity and a Fermi sea in each quantum well. Remember, however, that when the Coulomb interaction and the light-matter coupling are turned-on and large enough, it is not the ground state of the system anymore [38]. However, in this case, the true ground groud state can be easily expressed in terms of $|F\rangle$ [84]. State $|F\rangle$ will, thus, serve as a reference and be the starting point of all the following calculations: all excitations are created on such a state, by applying creation operators.

Truncating the Hibert space

Remember that we are interested in intersubband excitations and that these excitations are composed of a hole in the Fermi sea and an electron in the second subband. What happens in the first subband outside the Fermi is not relevant when studying such excitations, so it is tempting to conserve only terms acting in the Fermi sea. In Eqs. (2.4), (2.6), (2.8) and (2.9), we truncate all sums to $k < k_{\mathrm{F}}$ in the first subband. Doing so, we cannot describe intrasubband excitations in the first subband corresponding to the lowest continuum in figure 1.2b. We have thus removed some

unnecessary degrees of freedom.

In chapter 3, quantities of interest will be matrix elements between states containing intersubband excitations created from the ground state. In the normal ordered Hamiltonian, all $c_{1,\mathbf{k}}$ with $|\mathbf{k}| > k_\mathrm{F}$ will not contribute to such matrix elements, so it is indeed reasonable to remove them.

Electron-hole formalism

We saw that intersubband excitations are electron-hole pairs, *i.e.*, promotion of an electron from the Fermi sea to the second subband, leaving behind a hole. But for now the Hamiltonian is not expressed in terms of hole operators. It is then advantageous, and coherent with the language used so far, to introduce the hole creation and annihilation operators. In the Hamiltonian, we replace the annihilation of an electron in the Fermi sea with wave vector $\mathbf{k}$ by the creation of a hole with wave vector $-\mathbf{k}$,

$$c_{1,\mathbf{k}} \mapsto h^\dagger_{-\mathbf{k}}, \tag{2.23}$$

and we normal order the new Hamiltonian with respect to the hole operators. The ground state $|F\rangle$ now behaves like the vacuum—it is annihilated by any annihilation operator—which is convenient for the calculation of matrix elements.

The electron-hole Hamiltonian is then

$$H = H_\mathrm{Cav} + H_\mathrm{Elec} + H_\mathrm{I1} + H_\mathrm{I2} + H_\mathrm{Intra} + H_\mathrm{Depol}, \tag{2.24}$$

where H_Cav is unchanged and Coulomb Hamiltonian has been split into its intrasubband and intersubband contributions. The new expression of the kinetic energy operator is, up to a constant shift,

$$H_\mathrm{Elec} = \sum_{\mathbf{k}} \hbar\tilde{\omega}_{2,k}\, c^\dagger_{2,\mathbf{k}} c_{2,\mathbf{k}} - \sum_{|k|<k_\mathrm{F}} \hbar\tilde{\omega}_{1,k}\, h^\dagger_{-\mathbf{k}} h_{-\mathbf{k}}, \tag{2.25}$$

where $\tilde{\omega}_{1,\mathbf{k}}$ and $\tilde{\omega}_{2,\mathbf{k}}$ are hole and electron dispersions renormalized by the screened Coulomb interaction

$$\begin{aligned} \hbar\tilde{\omega}_{1,k} &= \hbar\omega_{1,k} - \sum_{|\mathbf{k}'|<k_F} \tilde{V}^{1111}_{|\mathbf{k}-\mathbf{k}'|} \\ \hbar\tilde{\omega}_{2,k} &= \hbar\omega_{2,k} - \sum_{|\mathbf{k}'|<k_F} \tilde{V}^{1212}_{|\mathbf{k}-\mathbf{k}'|}. \end{aligned} \tag{2.26}$$

These renormalizations are the same as the one obtained by diagrammatic method in the Hartree-Fock approximation [54, 55]. Hartree-Fock terms are larger for the holes than for the electrons in the second subband, so the renormalization globally blue-shifts the energy of the transition. Because of these terms, the two subbands are not parallel anymore. We, however, define an averaged intersubband transition energy $\hbar\tilde{\omega}_{12}$.

The light-matter coupling term H_{I1} is

$$H_{\mathrm{I1}} = \sum_{\mathbf{q}} \hbar\chi_q \left(a_{\mathbf{q}} + a^{\dagger}_{-\mathbf{q}}\right) \sum_{k<k_{\mathrm{F}}} \left(c^{\dagger}_{2,\mathbf{k}+\mathbf{q}} h^{\dagger}_{-\mathbf{k}} + h_{-\mathbf{k}} c_{2,\mathbf{k}-\mathbf{q}}\right), \tag{2.27}$$

while Hamiltonian H_{I2} is unchanged. In Hamiltonian H_{I1}, it is now more appearant that photons are coupled to a symmetric linear superposition of electron-hole pairs,

$$\sum_{k<k_{\mathrm{F}}} c^{\dagger}_{2,\mathbf{k}+\mathbf{q}} h^{\dagger}_{-\mathbf{k}}, \tag{2.28}$$

like the one obtained in the simplified model of the first chapter.

Coulomb terms are

$$\begin{aligned} H_{\mathrm{Intra}} \;=\; & \frac{1}{2} \sum_{\mathbf{k},\mathbf{k}',\mathbf{q}} \tilde{V}^{2222}_{q}\, c^{\dagger}_{2,\mathbf{k}+\mathbf{q}} c^{\dagger}_{2,\mathbf{k}'-\mathbf{q}} c_{2,\mathbf{k}'} c_{2,\mathbf{k}} \\ & + \frac{1}{2} \sum_{\mathbf{k},\mathbf{k}',\mathbf{q}} \tilde{V}^{1111}_{q}\, h^{\dagger}_{-\mathbf{k}-\mathbf{q}} h^{\dagger}_{-\mathbf{k}'+\mathbf{q}} h_{-\mathbf{k}'} h_{-\mathbf{k}} \\ & - \sum_{\mathbf{k},\mathbf{k}',\mathbf{q}} \tilde{V}^{1221}_{q}\, h^{\dagger}_{-\mathbf{k}-\mathbf{q}} c^{\dagger}_{2,\mathbf{k}'-\mathbf{q}} c_{2,\mathbf{k}'} h_{-\mathbf{k}}, \end{aligned} \tag{2.29}$$

and

$$\begin{aligned} H_{\mathrm{Depol}} = \frac{1}{2} \sum_{\mathbf{q}} V^{1212}_{q} \sum_{\mathbf{k},\mathbf{k}'} \Big(& 2\, c^{\dagger}_{2,\mathbf{k}+\mathbf{q}} h^{\dagger}_{-\mathbf{k}}\, h_{-\mathbf{k}'+\mathbf{q}} c_{2,\mathbf{k}'} \\ & + c^{\dagger}_{2,\mathbf{k}+\mathbf{q}} h^{\dagger}_{-\mathbf{k}}\, c^{\dagger}_{2,\mathbf{k}'-\mathbf{q}} h^{\dagger}_{-\mathbf{k}'} + h_{-\mathbf{k}+\mathbf{q}} c_{2,\mathbf{k}}\, h_{-\mathbf{k}'-\mathbf{q}} c_{2,\mathbf{k}'} \Big), \end{aligned} \tag{2.30}$$

where terms $\mathbf{q} = 0$ are removed and sums are truncated to the Fermi sea. In Hamiltonian H_{Depol}, the same electron-hole pairs superpositions as in Hamiltonian (2.27) are present. Because we will treat this part of the Coulomb interaction exactly, we do not use the screened coefficient.

2.2 Intersubband excitations and bosonic Hamiltonian

In the previous section, we wrote a simplified Hamiltonian in terms of electrons in the second subband and holes in the Fermi sea and we saw that only a particular superposition of electron-hole pairs is coupled to the electromagnetic field. We are now in good position to define more precisely the notion of intersubband excitation, so we can further simplify our Hamiltonian. As we will see, these excitations are almost bosonic, so it is possible to write an effective purely bosonic Hamiltonian to describe the system. Here, we present only the physical ideas behind this transformation and let the details for the next chapter.

2.2.1 Definition

Consider the light-matter Hamiltonian as written in Eq. (2.27). As explained above, it is clear that photons are coupled only to a symmetric linear superposition of electron-hole pairs,

$$b^\dagger_{0,\mathbf{q}} = \frac{1}{\sqrt{n_{\mathrm{QW}} N_{\mathrm{el}}}} \sum_{\mathbf{k}} \nu^*_{0,\mathbf{k}}\, c^\dagger_{2,\mathbf{k}+\mathbf{q}} h^\dagger_{-\mathbf{k}}, \tag{2.31}$$

where $\nu_{0,\mathbf{k}} = \Theta(k_{\mathrm{F}} - k)$ and Θ is the Heaviside function, $\sqrt{n_{\mathrm{QW}} N_{\mathrm{el}}}$ is a normalizing constant, and electrons and holes have opposit spins. Again, the summation is implicit over the spin and quantum well indexes. The choice of the index 0 will be explained later. Equation (2.31) defines a creation operator for a collective excitation, which we will name bright intersubband excitations. Hamiltonian H_{I1} can then be further simplified

$$H_{\mathrm{I1}} = \sum_{\mathbf{q}} \hbar\Omega_q \left(a_{\mathbf{q}} + a^\dagger_{-\mathbf{q}}\right)\left(b^\dagger_{0,\mathbf{q}} + b_{0,-\mathbf{q}}\right), \tag{2.32}$$

where $\Omega_q = \sqrt{n_{\mathrm{QW}} N_{\mathrm{el}}}\, \chi_q$ is the Rabi frequency. As explained in the simple model in the first chapter, the light-matter coupling is collectively enhanced by the presence of the electron gas in the first subband.

Intersubband excitation operators can also be directly injected in Hamiltonian H_{Depol},

$$H_{\mathrm{Depol}} = \frac{N_{\mathrm{el}}}{2} \sum_{\mathbf{q}} V^{1212}_q \left(2b^\dagger_{0,\mathbf{q}} b_{0,\mathbf{q}} + b^\dagger_{0,\mathbf{q}} b^\dagger_{0,-\mathbf{q}} + b_{0,\mathbf{q}} b_{0,-\mathbf{q}}\right). \tag{2.33}$$

The intersubband Coulomb interaction, thus, only couples bright intersubband ex-

citations with each other. Notice that it is also enhanced by the presence of the electron gas, but, contrary to the light-matter coupling, this enhancement depends only the number of electrons per quantum well. Indeed, the Coulomb interaction couples only electrons inside the same well.

Other similar excitations can be constructed by an orthonormalization procedure

$$b^\dagger_{i,\mathbf{q}} = \frac{1}{\sqrt{n_{\mathrm{QW}}N_{\mathrm{el}}}} \sum_{\mathbf{k}} \nu^*_{i,\mathbf{k}}\, c^\dagger_{2,\mathbf{k}+\mathbf{q}} c_{1,\mathbf{k}}, \tag{2.34}$$

where index i runs from 1 to $n_{\mathrm{QW}}N_{\mathrm{el}} - 1$ and the ν coefficients have support over the Fermi sea and satisfy the orthonormality relation

$$\frac{1}{n_{\mathrm{QW}}N_{\mathrm{el}}} \sum_{\mathbf{k}} \nu^*_{i,\mathbf{k}}\nu_{j,\mathbf{k}} = \delta_{i,j}. \tag{2.35}$$

However, none of these new collective excitations is coupled to the microcavity photon field. We, thus, call them dark intersubband excitations. Moreover, these dark excitations are not affected by the depolarization shift. They are, thus, not resonant with bright intersubband excitations. They correspond to the remaining electron-hole continuum shown in Figure 1.2c. We could also define spin-carrying excitations, i.e., electrons and holes have the same spin but, because the light-matter coupling is spin conserving, they are not coupled to the cavity field. Contrary to the excitons [21], the spin index is not a relevant dynamical variable for intersubband excitations.

2.2.2 Simple effective bosonic Hamiltonian

We have, thus, written in a more compact and explicit form two terms of our Hamiltonian, and we would like to do the same with the other terms. Unfortunately, the remaining terms cannot be simplified so easily. It is, however, possible to write an effective purely bosonic Hamiltonian to describe the system [85], as it was done in the case of exciton-polaritons [86, 22]. To do this, we limit ourselves to the subspace of the bright intersubband excitations and express the Hamiltonian in this subspace. This amounts, once again, to truncating the Hilbert space to relevant degrees of freedom. Moreover, intersubband excitations are almost bosonic. We now give some simple physical arguments to justify this and derive the traditional effective bosonic Hamiltonian for bright excitations [38, 49]. We postpone all calculations to chapter 3.

Bosonicity

We first explain why it is reasonable to treat intersubband excitations as bosons. The commutation rule for bright intersubband excitations is

$$\left[b_{0,\mathbf{q}}, b^{\dagger}_{0,\mathbf{q}'}\right] \approx \delta_{\mathbf{q},\mathbf{q}'}, \tag{2.36}$$

where the exact meaning of $\approx$ will be discussed in chapter 3.

We can understand this point with a simple consideration. An intersubband excitation is a collective mode containing one electron-hole pair equally spread over $n_{\mathrm{QW}}N_{\mathrm{el}}$ states, where $n_{\mathrm{QW}}N_{\mathrm{el}}$ is the number of electrons in the system. The probability for the electron or the hole to be in a given state is, thus, $1/n_{\mathrm{QW}}N_{\mathrm{el}}$. If a second intersubband excitations is injected, the probability that the two electrons or the two holes are in conflict for the same state is of the order of $1/n_{\mathrm{QW}}N_{\mathrm{el}}$. More generally, if N_{exc} intersubband excitations are present in the system, there are $N_{\mathrm{exc}}(N_{\mathrm{exc}}-1)/2$ pairs of electrons and the same number of pairs of holes, which can potentially be in conflict. The dominant Pauli blocking contribution, thus, scales like $N_{\mathrm{exc}}(N_{\mathrm{exc}}-1)/n_{\mathrm{QW}}N_{\mathrm{el}}$. This is negligeable when $N_{\mathrm{exc}}/n_{\mathrm{QW}}N_{\mathrm{el}} \ll 1$, so we expect intersubband excitations to behave like bosons in the low density regime. This simple combinatorial argument even gives the correct scaling for the correction to the bosonicity (see section 3.4).

In Hamiltonians H_{I1} and H_{Depol}, we then replace intersubband excitation operators by bosonic one

$$b^{\dagger}_{0,\mathbf{q}} \mapsto B^{\dagger}_{\mathbf{q}}, \quad \left[B_{\mathbf{q}}, B^{\dagger}_{\mathbf{q}'}\right] = \delta_{\mathbf{q},\mathbf{q}'}, \tag{2.37}$$

Because we will deal only with brigh excitations, we neglected the index in the definition of the bosonic operator $B_{\mathbf{q}}$.

Free electron gas Hamiltonian

We saw that an intersubband excitation is an electron-hole pair. To such an excitation, Hamiltonian H_{Elec} associates an energy $\hbar\tilde{\omega}_{12}$ corresponding to the energy difference between the two subbands, where we considered an averaged effect of the Hartree-Fock terms. For this assumption to be valid, the two renormalized subbands must be almost parallel. Thus, we propose a simplified expression for H_{Elec} in terms

of the bosonized bright intersubband excitations

$$H_{\text{Elec}}^{\text{B}} = \sum_{\mathbf{q}} \hbar\tilde{\omega}_{12}\, B_{\mathbf{q}}^{\dagger} B_{\mathbf{q}}. \tag{2.38}$$

We added the superscript B to insist on the fact that this Hamiltonian is bosonic. Once again, this substitution is equivalent to truncating the Hilbert space to the relevant degrees of freedom. Dark excitations, corresponding to the electron-hole continuum in figure 1.2b cannot be treated. There is also an implicit cut-off to small wave vectors.

A^2-term

To simplify the notation, we replace the bare intersubband transition energy $\hbar\omega_{12}$ by the renormalized one in the denominator in Eq. (3.18). Doing so, we only introduce a minor correction. Notice that, as the intersubband Coulomb interaction, it is collectively enhanced by the electron gas. Its contribution is then of the order of $\hbar{\Omega_q}^2/\tilde{\omega}_{12}$, which is non negligeable only in the ultra-strong coupling regime. Hamiltonian H_{I2} can, thus, be written

$$H_{\text{I2}}^{\text{B}} = \sum_{\mathbf{q}} \frac{\hbar{\Omega_q}^2}{\tilde{\omega}_{12}} \left(a_{-\mathbf{q}} + a_{\mathbf{q}}^{\dagger}\right)\left(a_{\mathbf{q}} + a_{-\mathbf{q}}^{\dagger}\right), \tag{2.39}$$

and can be omitted when the system is not in the ultra-strong coupling regime.

Coulomb interaction

The intrasubband Coulomb interaction is already expressed in terms of intersubband excitations. We, thus, only have to replace intersubband excitation operators by their bosonic counter part. To simplify the notations and to be consistent with the litterature [87], we truncate the sum in the intrasubband Coulomb interaction in Eq. (2.33) to small wave vectors. It can then be put in the simpler form

$$H_{\text{Depol}}^{\text{B}} = \frac{\hbar{\omega_{\text{P}}}^2}{4\tilde{\omega}_{12}} \sum_{\mathbf{q}} \left(2B_{\mathbf{q}}^{\dagger}B_{\mathbf{q}} + B_{\mathbf{q}}^{\dagger}B_{-\mathbf{q}}^{\dagger} + B_{\mathbf{q}}B_{-\mathbf{q}}\right), \tag{2.40}$$

where ω_{P} is the plasma frequency for an infinite quantum well,

$${\omega_{\text{P}}}^2 = \frac{e^2 n_{\text{el}}}{\epsilon_0 \epsilon_r m^* L} \frac{5\tilde{\omega}_{12}}{3\omega_{12}}. \tag{2.41}$$

This Hamiltonian is the same as in Ref. [87], up to a geometrical factor. This factor is interpreted as an image contribution to the Coulomb interaction due to the boundary conditions of the electric field on the cavity mirrors. It becomes important for double metal microcavities where the photon confinement is high. We could take it into account by considering the Coulomb interaction in a cavity instead of in free space. Since we do not consider double metal cavities, we do not consider this correction. When necessary, it can obtained from experimental results.

We saw in Eq. (2.40) that the intersubband Coulomb interaction is collectively enhanced. As a comparison, the intrasubband terms are not. We thus neglect them, as we neglected the second part of Hamiltonian $H_{\mathrm{I}2}$. However, by analogy with the excitons [88], we expect a contribution to the energy of intersubband excitations. We do not know how to compute it yet but we can include it in the definition of the energy $\hbar\tilde{\omega}_{12}$.

Bosonic Hamiltonian

Thanks to previous approximations, we can write a simple bosonic Hamiltonian to describe the system,

$$\begin{aligned}\tilde{H}^{\mathrm{B}} &= \sum_{\mathbf{q}} \hbar\omega_{\mathrm{cav},q}\, a^{\dagger}_{\mathbf{q}} a_{\mathbf{q}} + \sum_{\mathbf{q}} \frac{\hbar {\Omega_q}^2}{\tilde{\omega}_{12}} \left(a_{-\mathbf{q}} + a^{\dagger}_{\mathbf{q}}\right)\left(a_{\mathbf{q}} + a^{\dagger}_{-\mathbf{q}}\right) \\ &\quad + \sum_{\mathbf{q}} \hbar\tilde{\omega}_{12}\, B^{\dagger}_{\mathbf{q}} B_{\mathbf{q}} + \frac{\hbar {\omega_{\mathrm{P}}}^2}{4\tilde{\omega}_{12}} \sum_{\mathbf{q}} \left(2B^{\dagger}_{\mathbf{q}} B_{\mathbf{q}} + B^{\dagger}_{\mathbf{q}} B^{\dagger}_{-\mathbf{q}} + B_{\mathbf{q}} B_{-\mathbf{q}}\right) \\ &\quad + \sum_{\mathbf{q}} \hbar\Omega_q \left(a_{\mathbf{q}} + a^{\dagger}_{-\mathbf{q}}\right)\left(B^{\dagger}_{\mathbf{q}} + B_{-\mathbf{q}}\right). \end{aligned} \tag{2.42}$$

This Hamiltonian is quadratic and can, thus, be diagonalized by an Hopfield-Bogoliubov transformation [65]. It is very similar to the one obtained in Ref. [87].

2.2.3 Bogoliubov transformation

To find the energies of the eigenmodes of the Hamiltonian in Eq. (2.42), we write the evolution equations verified by intersubband excitation and photon operators,

$$\mathrm{i}\frac{\mathrm{d}}{\mathrm{d}t}\begin{pmatrix} a_{\mathbf{q}} \\ B_{\mathbf{q}} \\ a^{\dagger}_{-\mathbf{q}} \\ B^{\dagger}_{-\mathbf{q}} \end{pmatrix} = \mathcal{L}\begin{pmatrix} a_{\mathbf{q}} \\ B_{\mathbf{q}} \\ a^{\dagger}_{-\mathbf{q}} \\ B^{\dagger}_{-\mathbf{q}} \end{pmatrix}, \tag{2.43}$$

where $\mathcal{L}$ is the Bogoliubov matrix,

$$\mathcal{L} = \begin{pmatrix} \omega_{\mathrm{cav},q} + 2\frac{{\Omega_q}^2}{\tilde{\omega}_{12}} & \Omega_q & 2\frac{{\Omega_q}^2}{\tilde{\omega}_{12}} & \Omega_q \\ \Omega_q & \tilde{\omega}_{12} + \frac{{\omega_\mathrm{P}}^2}{2\tilde{\omega}_{12}} & \Omega_q & \frac{{\omega_\mathrm{P}}^2}{2\tilde{\omega}_{12}} \\ -2\frac{{\Omega_q}^2}{\tilde{\omega}_{12}} & \Omega_q & -\omega_{\mathrm{cav},q} - 2\frac{{\Omega_q}^2}{\tilde{\omega}_{12}} & \Omega_q \\ \Omega_q & -\frac{{\omega_\mathrm{P}}^2}{2\tilde{\omega}_{12}} & \Omega_q & -\tilde{\omega}_{12} - \frac{{\omega_\mathrm{P}}^2}{2\tilde{\omega}_{12}} \end{pmatrix}. \tag{2.44}$$

Eigenvalues of $\mathcal{L}$ are $\{\pm\omega_{\mathrm{L},q}, \pm\omega_{\mathrm{U},q}\}$, where subscripts L and U refer, respectively, to lower and upper polaritons and eigenmodes of the system are linear superpositions of intersubband excitations and photons,

$$p_{j,\mathbf{q}} = w_{j,q} a_{\mathbf{q}} + x_{j,q} B_{\mathbf{q}} + y_{j,q} a^\dagger_{-\mathbf{q}} + z_{j,q} B^\dagger_{-\mathbf{q}}, \tag{2.45}$$

where $j \in \{\mathrm{L}, \mathrm{U}\}$, and are bosonic,

$$\left[p_{i,\mathbf{q}}, p^\dagger_{j,\mathbf{q}'}\right] = \delta_{i,j}\delta_{\mathbf{q},\mathbf{q}'}. \tag{2.46}$$

A complete solution of the problem in the ultra-strong coupling regime, including a discussion on the nature of the new ground state of the system, can be found in Ref. [38].

Notice that if we neglect antiresonant terms in the bosonic Hamiltonian $\tilde{H}^{\mathrm{B}}$, Eqs. (2.43) and (2.44) are simplified,

$$\mathrm{i}\frac{\mathrm{d}}{\mathrm{d}t}\begin{pmatrix} a_{\mathbf{q}} \\ B_{\mathbf{q}} \end{pmatrix} = \mathcal{L}' \begin{pmatrix} a_{\mathbf{q}} \\ B_{\mathbf{q}} \end{pmatrix}, \quad \mathcal{L}' = \begin{pmatrix} \omega_{\mathrm{cav},q} + 2\frac{{\Omega_q}^2}{\tilde{\omega}_{12}} & \Omega_q \\ \Omega_q & \tilde{\omega}_{12} + \frac{{\omega_\mathrm{P}}^2}{2\tilde{\omega}_{12}} \end{pmatrix}. \tag{2.47}$$

Notice that $\mathcal{L}'$ is, up to a change of the photon and intersubband transition energy, the same matrix as in Eq. (1.11). In this approximation, polariton dispersions and expressions are then given by Eqs. (1.12), (1.13) and (1.14). There is, thus, a strong similarity between our one-excitation model from chapter 1 and Hamiltonian (2.42). This point will be discussed in chapter 3 and emphasizes the relevance of the simple model presented in chapter 1. Of course, we should not make this assumption if we want to invistigate the caracteristic features of the ultra-strong coupling regime, namely the squeezed ground state [38] or dynamical Casimir effects [39]. However, polaritonic dispersions obtained from Eq. (2.47) are qualitatively correct and quantitatively close to the exact values.

In figure 2.2, we plot the polariton dispersion with (solid lines) and without (dashed lines) the antiresonant terms for in the mid infrared (left) and in the THZ

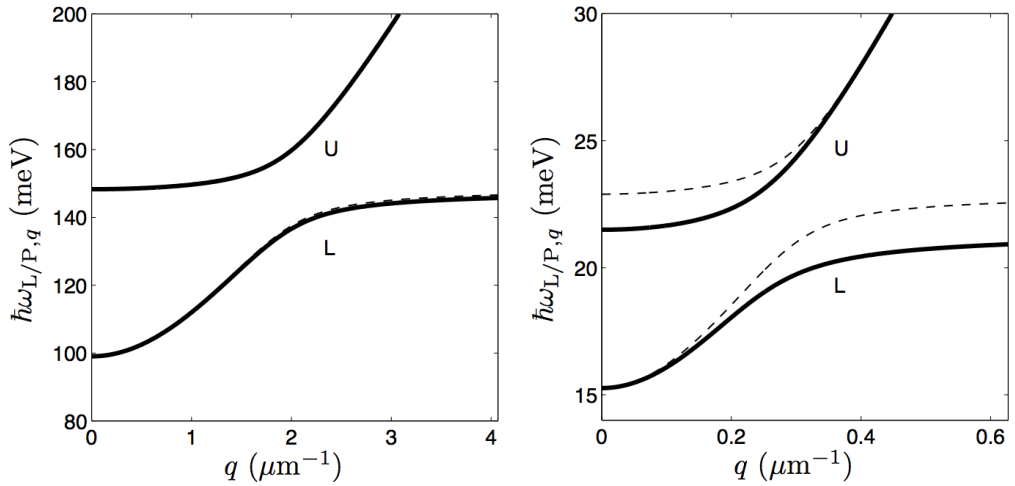

(a) (b)

Figure 2.2: Polaritonic dispersions in the mid infrared (figure (a)) and the THZ (figure (b)). Solid lines: Dispersions obtained from Eq. (2.44). Dashed lines: Dispersions obtained by neglecting the antiresonant terms. The bare intersubband transition energies are 140 meV and 15 meV for the mid infrared and THz range, respectively, and the electron densities are $n_{\mathrm{el}} = 10^{12}$ cm^{-2} and $n_{\mathrm{el}} = 3 \times 10^{11}$ cm^{-2}.

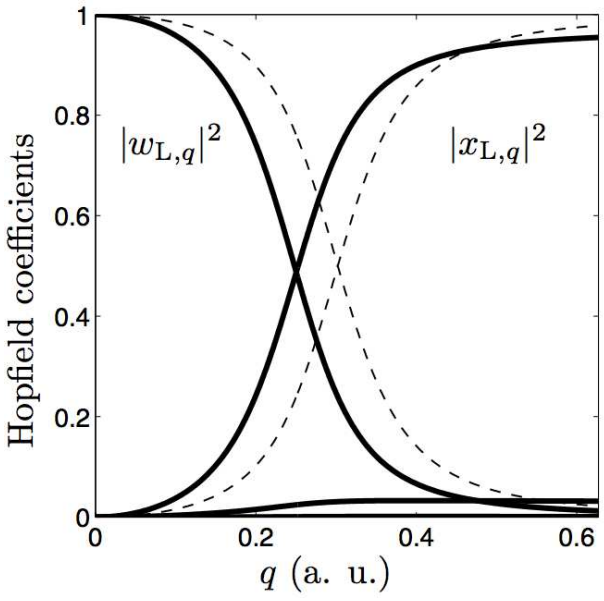

Figure 2.3: Hopfield coefficients of the lower polaritonic mode in the THz regime, from $q = 0$ (left) to higher wave vectors (right). Solid line: Obtained from Eq. (2.44). Dashed line: Obtained from Eq. (2.47) with no antiresonant terms. Hopfield coefficients $y_{\mathrm{L},q}$ and $z_{\mathrm{L},q}$ are very close to zero and are negligeable compared to $w_{\mathrm{L},q}$ and $x_{\mathrm{L},q}$ even at resonance.

(right) range with bare intersubband transition 140 meV and 15 meV and electron densities in the wells $n_{\mathrm{el}} = 10^{12}$ cm^{-2} and $n_{\mathrm{el}} = 3 \times 10^{11}$ cm^{-2} respectively. The renormalized energy $\hbar\tilde{\omega}_{12}$ was considered to be the bare one $\hbar\omega_{12}$ because we did not show how to compute the electron-hole Coulomb intrasubband contribution yet. The Rabi frequencies at resonance are around 10% of the intersubband transition energy. As explained in the section 1.3, because the Rabi frequency vanishes for $q = 0$, the polariton gap [73, 51] is missing. The discrepancy between the exact and approximated dispersions are due to the fact that the plasma frequency is overestimated in the absence of the antiresonant terms: $\tilde{\omega}_{12} + \omega_{\mathrm{P}}^2/2\tilde{\omega}_{12}$ instead of $\sqrt{\tilde{\omega}_{12}^2 + \omega_{\mathrm{P}}^2}$. This is visible in the THz range (figure 2.2b), which translates the resonance to higher wave vectors, and negligeable in the mid infrared range (figure 2.2a). Moreover, Hopfield coefficients $y_{j,q}$ and $z_{j,q}$ remain small compared to $w_{j,q}$ and $x_{j,q}$ (see Ref. [38] and figure 2.3), so the nature of the polaritons is not dramatically altered. This approximation is, thus, good enough to obtain valuable information about intersubband polaritons and we will use it in the next chapters.

The agreement with experimental results [14, 51, 89] justifies the assumptions we made. However, these results correspond to probing experiments where the number of excitations injected in the system remains low. At the exception of polariton bleaching [42], nothing is known about the physics of intersubband polaritons at higher densities of excitations. Is the Hamiltonian in Eq. (2.42) still valid to investigate this regime? It is very unlikely. First, when the number of excitations increases, the number of available electrons in the Fermi sea decreases. Pauli blocking becomes important and intersubband excitations are less and less bosonic. The transformation defined in Eq. (2.37) is less and less relevant, so deviations from Hamiltonian (2.42) are expected. Second, terms we have neglected in H_{I2} (see Eq. (B.20)) and H_{Intra} can have non negligeable contributions. They both scatter holes in the Fermi sea or electrons in the second subband, so they should become relevant when the number of electrons and holes increases. For these two reasons, nonlinear effects are expected as the number of excitations in the system increases. However, the Hamiltonian in Eq. (2.42) is quadratic and is, thus, limited to the linear regime.

In the next chapter, we will show how to keep advantage of the bosonic framework while taking nonlinear effects into account.

Chapter 3

Polariton-polariton interactions

In chapter 2, we presented the most general Hamiltonian of the system, which cannot be diagonalized exactly. Then, some approximations were made, the key one being the introduction of bosonized intersubband excitations. We were then able to derive an effective bosonic Hamiltonian, to diagonalize it, and we obtained results in agreement with the experiments in the linear regime, *i.e.*, when the number of intersubband excitations is much smaller than the number of electrons in the Fermi sea. Because it is only quadratic in the bosonic operators, this effective Hamiltonian fails to describe polariton-polariton interactions and is, thus, limited to this linear regime. In this chapter, starting from the electron-hole Hamiltonian derived in section 2.1, we will develop a rigorous method to calculate the polariton-polariton interactions. Our method consists in computing matrix elements in the subspace generated by bright intersubband excitations and then forcing the initial and effective Hamiltonians to have the same matrix elements. We will then be able to add quartic terms to our effective Hamiltonian and to describe the nonlinear physics of intersubband polaritons. In addition, it gives a rigorous justification to the derivation of the quadratic Hamiltonian in section 2.2.

First, we will describe the composite boson approach to the case of intersubband excitations. This method, initially developed to describe excitons [90] and generalized to any fermion pairs [91, 92], yields all the commutation relations needed to compute the fermionic Hamiltonian's matrix elements. Then, we will compute matrix elements and properly normalize them [93]. Here, we limit ourselves to states with one or two excitations but the method can be generalized to any arbitrary number of them. We will show that, thanks to this method, we are able to derive a refined version of Hamiltonian (2.42) More important, we will be able to include quartic

terms to study nonlinear effects. These nonlinearities have two origins—fermion exchange between intersubband excitations and fermions pair interaction—which are two manifestations of the non-bosonicity of intersubband excitations. We will also see that, even if we limited ourselves to matrix elements between states with one or two excitations, we are able to describe the physics of the system to first order in the dimensionless parameter $N_{\text{exc}}/n_{\text{QW}}N_{\text{el}}$ when N_{exc} is grower than two. In other words, we will determine a controled perturbative expansion in the Coulomb interaction and the non-bosonicity.

3.1 Intersubband excitations commutator formalism

The dynamics of the system is determined by the set of all commutators. In this section, we thus derive commutation rules for the intersubband excitation operators [94, 92]. Matrix elements will be treated in section 3.2. To this end, we recall the general definition of these operators given in Eq. (2.34)

$$b^\dagger_{i,\mathbf{q}} = \frac{1}{\sqrt{n_{\text{QW}}N_{\text{el}}}} \sum_{k<k_F} \nu^*_{i,\mathbf{k}}\, c^\dagger_{2,\mathbf{k}+\mathbf{q}} h^\dagger_{-\mathbf{k}}, \tag{3.1}$$

where $\nu_{0,\mathbf{k}} = \Theta(k_{\text{F}}-k)$ and the other $\nu_{i,\mathbf{k}}$ satisfy orthogonality relations in Eq. (2.35). This expression defines a change of basis from electron-hole pairs to intersubband excitations, which can be inverted thanks to the following relation

$$c^\dagger_{2,\mathbf{k}+\mathbf{q}} h^\dagger_{-\mathbf{k}} = \frac{1}{\sqrt{n_{\text{QW}}N_{\text{el}}}} \sum_{n} \nu_{n,\mathbf{k}}\, b^\dagger_{n,\mathbf{q}}, \tag{3.2}$$

where the sum runs over all modes $n \in \{0, 1, \ldots, n_{\text{QW}}N_{\text{el}} - 1\}$, 0 being the only bright mode.

3.1.1 Non-bosonicity and Pauli blocking term

In chapter 2, we treated intersubband excitations as bosons and said that this approximation holds only in the diluted regime. To make this statement clear, we compute their commutator,

$$\left[b_{m,\mathbf{q}''}, b^\dagger_{i,\mathbf{q}}\right] = \delta_{m\mathbf{q}'',i\mathbf{q}} - D_{m\mathbf{q}'',i\mathbf{q}}, \tag{3.3}$$

where

$$D_{m\mathbf{q}'',i\mathbf{q}} = D^{(1)}_{m\mathbf{q}'',i\mathbf{q}} + D^{(2)}_{m\mathbf{q}'',i\mathbf{q}}, \tag{3.4}$$

$$D^{(1)}_{m\mathbf{q}'',i\mathbf{q}} = \frac{1}{n_{\mathrm{QW}}N_{\mathrm{el}}}\sum_{\mathbf{k}} \nu_{m,\mathbf{k}}\nu^{*}_{i,\mathbf{k}+\mathbf{q}''-\mathbf{q}}\, h^{\dagger}_{-\mathbf{k}-\mathbf{q}''+\mathbf{q}} h_{-\mathbf{k}}, \tag{3.5}$$

$$D^{(2)}_{m\mathbf{q}'',i\mathbf{q}} = \frac{1}{n_{\mathrm{QW}}N_{\mathrm{el}}}\sum_{\mathbf{k}} \nu_{m,\mathbf{k}}\nu^{*}_{i,\mathbf{k}}\, c^{\dagger}_{2,\mathbf{k}+\mathbf{q}} c_{2,\mathbf{k}+\mathbf{q}''}. \tag{3.6}$$

The first part of the commutator is the Kroenecker function, reminiscent of the bosonic behavior of intersubband excitations. The second part is the deviation from bosonicity and consists of two operators, involving, respectively, holes in the Fermi sea and electrons in the second subband. They annihilate the ground state $|F\rangle$ but can become significant if the number of excitations in the system is important. Indeed, if $|\phi\rangle$ is a state with N_{exc} intersubband excitations, the mean value of the commutator is

$$\langle\phi|\left[b_{m,\mathbf{q}''}, b^{\dagger}_{i,\mathbf{q}}\right]|\phi\rangle = \delta_{m\mathbf{q}'',i\mathbf{q}} + \mathcal{O}\left(\frac{N_{\mathrm{exc}}}{n_{\mathrm{QW}}N_{\mathrm{el}}}\right), \tag{3.7}$$

which makes it clear that, at low density of excitations $N_{\mathrm{exc}} \ll n_{\mathrm{QW}}N_{\mathrm{el}}$, the commutator is bosonic.

Notice that Eq. (3.3) has not a closed form: the commutator of two intersubband operators does not depend only on intersubband excitation operators. Nevertheless, by commuting this result with another intersubband creation operator, we can close the relation,

$$\left[D^{(1)}_{m\mathbf{q}'',i\mathbf{q}}, b^{\dagger}_{j,\mathbf{q}'}\right] = \frac{1}{n_{\mathrm{QW}}N_{\mathrm{el}}}\sum_{n} \lambda^{n,j}_{m,i}(\mathbf{q}''-\mathbf{q})\, b^{\dagger}_{n,\mathbf{q}+\mathbf{q}'-\mathbf{q}''}, \tag{3.8}$$

$$\left[D^{(2)}_{m\mathbf{q}'',i\mathbf{q}}, b^{\dagger}_{j,\mathbf{q}'}\right] = \frac{1}{n_{\mathrm{QW}}N_{\mathrm{el}}}\sum_{n} \lambda^{m,j}_{n,i}(\mathbf{q}''-\mathbf{q}')\, b^{\dagger}_{n,\mathbf{q}+\mathbf{q}'-\mathbf{q}''}, \tag{3.9}$$

where

$$\lambda^{n,j}_{m,i}(\mathbf{q}''-\mathbf{q}) = \frac{1}{n_{\mathrm{QW}}N_{\mathrm{el}}}\sum_{\mathbf{k}} \nu_{m,\mathbf{k}}\nu^{*}_{i,\mathbf{k}+\mathbf{q}''-\mathbf{q}}\nu_{n,\mathbf{k}+\mathbf{q}''-\mathbf{q}}\nu^{*}_{j,\mathbf{k}} \tag{3.10}$$

is called Pauli blocking term. It is an effective scattering [95] induced by the indiscernability principle and the fermionic nature of the elementary parts of intersubband excitations—electrons and holes. For this reason, it was also called Pauli scattering in the case of the excitons [92]. Indeed, $\lambda^{n,j}_{m,i}(\mathbf{q})$ looks like the amplitude of a pair interaction process where i and j are the initial modes and m and n the

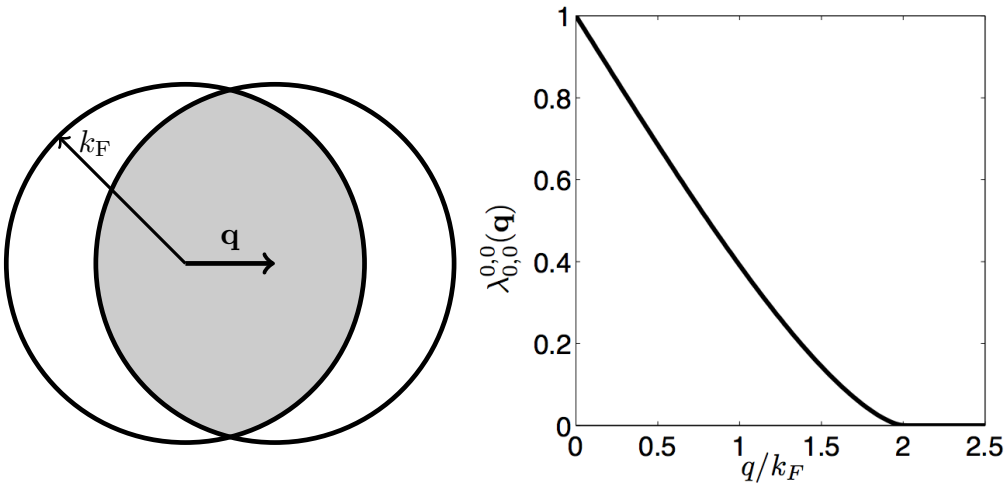

(a) (b)

Figure 3.1: (a) The Pauli blocking term $\lambda^{0,0}_{0,0}(\mathbf{q})$ for bright intersubband excitations in Eq. (3.10) is a four bright excitations overlap. It is the area of the gray-shaded surface. If q is larger than $2k_{\mathrm{F}}$, then the two Fermi seas do not overlap and Pauli blocking term vanishes. (b) Pauli coefficient $\lambda^{0,0}_{0,0}(\mathbf{q})$ dependence over the wave vector q normalized to the Fermi wave vector.

final ones (figure 3.2). This process corresponds to an exchange of fermions between two intersubband excitations. A wave vector $\mathbf{q}$ is exchanged during the process, while global momentum conservation is ensured. This coefficient is, thus, the four excitations overlap. It is plotted in figure 3.1. It manifests itself when there are at least two holes and two electrons in the system and is due to the fact that, in this situation, there are two ways of pairing them to construct intersubband excitations. Similarly, if there are N_{exc} electrons and holes in the system, there are $N_{\mathrm{exc}}(N_{\mathrm{exc}}-1)/2$ ways of pairing them. This effective scattering, thus, scales with the number of excitations as any pair interaction. In figure 3.2, we give a graphical representation of such a process using Shiva diagrams [96]. Here, we will not use these diagrams for computational reasons, but only as visualization tool. We will, thus, not explain how to use them.

Now that we know the commutations rules for intersubband excitations, we can apply them to compute commutators between H_{I1} or H_{Depol} and intersubband excitation operators. The case H_{Elec}, H_{I2} and H_{Intra} will be treated in the next sections.

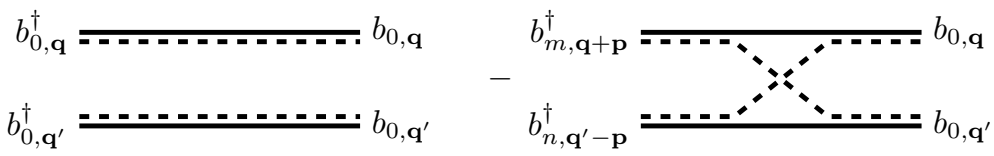

Figure 3.2: Graphical representation of Eqs. (3.3), (3.8) and (3.9) with a special class of Feynman diagrams (Shiva diagram [96]). Solid lines correspond to electrons and dashed lines to holes. These lines are grouped by pairs because intersubband excitations are electron-hole pairs. Left: Term corresponding to the bosonic part of intersubband excitations. A similar term should be added for symmetry reasons. Right: Term coming from the indiscernability principle. There are two ways of pairing two electrons and two holes, which describes an exchange of fermions between two excitations.

3.1.2 Free electron gas

To see how this Hamiltonian acts on intersubband excitations, we commute it with an intersubband excitation [94],

$$\left[H_{\text{Elec}}, b^\dagger_{i,\mathbf{q}}\right] = \frac{1}{\sqrt{n_{\text{QW}} N_{\text{el}}}} \sum_{\mathbf{k}} \left(\hbar\tilde{\omega}_{2,|\mathbf{k}+\mathbf{q}|} - \hbar\tilde{\omega}_{1,k}\right) \nu^*_{i,\mathbf{k}}\, c^\dagger_{2,\mathbf{k}+\mathbf{q}} h^\dagger_{-\mathbf{k}}. \tag{3.11}$$

If we now assume that the (renormalized) subbands are parallels and that intersubband excitations' wave vectors are small compared to the Fermi wave vector k_{F}, that is

$$\tilde{\omega}_{2,|\mathbf{k}+\mathbf{q}|} \approx \tilde{\omega}_{2,k} \approx \tilde{\omega}_{1,k} + \tilde{\omega}_{12}, \tag{3.12}$$

previous expression can be simplified into

$$\left[H_{\text{Elec}}, b^\dagger_{0,\mathbf{q}}\right] = \hbar\tilde{\omega}_{12}\, b^\dagger_{0,\mathbf{q}}. \tag{3.13}$$

Here, $\hbar\tilde{\omega}_{12}$ is the energy of the transition, renormalized by Hartree-Fock terms. Notice that this commutator is the same as the one obtained from Hamiltonian $\tilde{H}^{\text{B}}$ with bosonized intersubband excitations.

Validity of Eq. (3.13)

To obtain this Hamiltonian, we made two crucial approximations. There validity is well established and has been succesfully tested in many experiments [67, 89, 44, 46, 41, 50]. However, they oblige us to neglect a certain number of phenomena, like the interplay between non parabolicity and Coulomb interaction [97], or the scattering

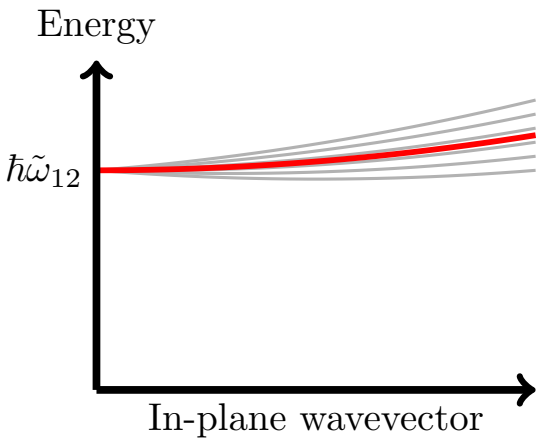

Figure 3.3: Dispersions of intersubband excitations for H_{Elec} only, without approximation Eq. (3.12). Conduction subbands are parallel but we do not neglect photonic wave vectors anymore. A comparison with Fig. 1.2b shows that the electron-hole continuum is composed of the dark modes. In the presence of the Coulomb interaction, the bright mode is blue-shifted (depolarization shift), and we recover Fig. 1.2b

toward electron-hole pairs at large wavevectors, that is known to be an important factor in the thermalization and dynamics of exciton polaritons [98, 99]. We may, thus, wonder how the previous commutator is affected when we do not make those approximations. Here, we present only the case of parallel subbands and we take into account their parabolicity. The case of non parallel subbands can be treated in a very similar way.

We consider the case of parallel parabolic subbands but we do not neglect the intersubband excitation's wave vector compared to the Fermi wave vector anymore. Instead, in Eq. (3.12), we develop the energy of the second subband and inject it in Eq. (3.11)

$$\left[H_{\text{Elec}}, b^\dagger_{i,\mathbf{q}}\right] = \frac{1}{\sqrt{n_{\text{QW}} N_{\text{el}}}} \sum_{n,\mathbf{k}} \left(\hbar\tilde{\omega}_{12} + \alpha \mathbf{k}.\mathbf{q} + \beta q^2\right) \nu^*_{i,\mathbf{k}}\, c^\dagger_{2,\mathbf{k}+\mathbf{q}} h^\dagger_{-\mathbf{k}}, \tag{3.14}$$

where $\alpha = 2\beta = \hbar^2/m^*$. As in the previous case, we then replace the electron-hole pair by its expression in terms of intersubband excitations to obtain

$$\left[H_{\text{Elec}}, b^\dagger_{i,\mathbf{q}}\right] = \hbar\tilde{\omega}_{12,i,q}\, b^\dagger_{i,\mathbf{q}} + \sum_{n\neq 0} \gamma_{i,n,q}\, b^\dagger_{n,\mathbf{q}}, \tag{3.15}$$

where

$$\hbar\tilde{\omega}_{12,i,q} = \tilde{\omega}_{12} + \beta q^2 + \alpha\,\mathbf{q}.\left(\sum_{\mathbf{k}} \mathbf{k}\,\frac{|\nu_{i,\mathbf{k}}|^2}{n_{\mathrm{QW}}N_{\mathrm{el}}}\right), \tag{3.16}$$

$$\gamma_{i,n,q} = \alpha\,\mathbf{q}.\left(\sum_{\mathbf{k}} \mathbf{k}\,\frac{\nu^*_{0,\mathbf{k}}\nu_{n,\mathbf{k}}}{n_{\mathrm{QW}}N_{\mathrm{el}}}\right), \tag{3.17}$$

are deviation operators. As in the previous case, we obtain a quasi continuum with modes couples with each other. But now the broadness of the continuum is zero for $\mathbf{q} = 0$ and it increases linearly with q, as well as the couplings. Also, the dispersion is not flat anymore but parabolic (figure 3.3). What we are describing is in fact the general dispersion of the electron-hole continuum presented in figure 1.2b.

Notice that the bright intersubband excitations acquired a finite lifetime even in the absence of any relaxation process. It is of course not possible to compute all energies and couplings. Instead, we can complete the commutator for a bright mode given in Eq. (3.13) by adding a phenomenological coupling to dark modes and/or the parabolic dispersion.

3.1.3 Photon scattering

In this section we consider the whole Hamiltonian H_{I2} in Eq. (B.20),

$$\begin{aligned} H_{\mathrm{I2}} = &\sum_{\mathbf{k},\mathbf{q}} \frac{|\hbar\Omega_q|^2}{\hbar\omega_{12}} \left(a_{-\mathbf{q}} + a^\dagger_{\mathbf{q}}\right)\left(a_{\mathbf{q}} + a^\dagger_{-\mathbf{q}}\right) \\ &+ \sum_{\mathbf{k},\mathbf{q},\mathbf{q}'} \frac{\hbar\chi_q\,\hbar\chi^*_{q'}}{\hbar\omega_{12}} \left(c^\dagger_{2,\mathbf{k}+\mathbf{q}-\mathbf{q}'}c_{2,\mathbf{k}} - h^\dagger_{-\mathbf{k}-\mathbf{q}-\mathbf{q}'}h_{-\mathbf{k}}\right)\left(a_{-\mathbf{q}'} + a^\dagger_{\mathbf{q}'}\right)\left(a_{\mathbf{q}} + a^\dagger_{-\mathbf{q}}\right), \end{aligned} \tag{3.18}$$

instead of the simplified A^2-term in Eq. (2.8). The first line has no matter part and, thus, commutes with any intersubband operator. The second line, however, contains hole-hole and electron-electron pairs of operators, just as deviation operators in Eqs. (3.5) and (3.6), and should, *a priori*, scatter intersubband excitations. Using Eqs. (3.1), (3.2) and (3.18), we obtain

$$\begin{aligned} \left[H_{\mathrm{I2}}, b^\dagger_{i,\mathbf{q}}\right] = \sum_{\mathbf{q}'\neq\mathbf{q}''} \frac{\hbar\chi_{q'}\,\hbar\chi_{q''}}{\hbar\tilde{\omega}_{12}} &\left(b^\dagger_{i,\mathbf{q}+\mathbf{q}''-\mathbf{q}'} - \sum_m \sigma_{i,m}(\mathbf{q}''-\mathbf{q}')\,b^\dagger_{m,\mathbf{q}+\mathbf{q}''-\mathbf{q}'}\right) \\ &\times \left(a_{-\mathbf{q}''} + a^\dagger_{\mathbf{q}''}\right)\left(a_{\mathbf{q}'} + a^\dagger_{-\mathbf{q}'}\right), \end{aligned} \tag{3.19}$$

where

$$\sigma_{i,m}(\mathbf{q}) = \frac{1}{n_{\mathrm{QW}} N_{\mathrm{el}}} \sum_{\mathbf{k}} \nu^*_{i,\mathbf{k}+\mathbf{q}} \nu_{m,\mathbf{k}}, \tag{3.20}$$

is the overlap between the initial and final modes' wavefunctions. As expected, intersubband excitations are scattered by this Hamiltonian. However, in the long wavelength limit, the overlap coefficient reduces to a simple scalar product between orthogonal modes and vanishes for $i \neq m$. The commutator then vanishes too,

$$\left[H_{\mathrm{I2}}, b^\dagger_{i,\mathbf{q}}\right] = 0, \tag{3.21}$$

so, for small wave vectors, Hamiltonian H_{I2} cannot scatter intersubband excitations. It can scatter both holes and electrons but these effects compensate each other. Therefore, the second part of Eq. (3.18) is irrelevant for our purpose and the more traditional A^2-term (first part of Eq. (3.18)) should be used.

3.1.4 Intrasubband Coulomb interaction

By analogy with excitons, we would expect the Coulomb correlation to lower the energy of the electron-hole pair [88] and to scatter pairs of intersubband excitations [21].

We start by calculating its commutator with an intersubband excitation creation operator

$$\left[H_{\mathrm{Intra}}, b^\dagger_{i,\mathbf{q}}\right] = -\sum_j \gamma_{i,j}\, b^\dagger_{j,\mathbf{q}} + V_{i,\mathbf{q}}, \tag{3.22}$$

where

$$\gamma_{i,j} = \sum_{\mathbf{q}} \tilde{V}^{1221}_q \sigma_{i,j}(\mathbf{q}), \tag{3.23}$$

and $V_{i,\mathbf{q}}$ is called the creation potential operator [92],

$$\begin{aligned} V_{i,\mathbf{q}} = &\sum_{\mathbf{Q},m} \left(\tilde{V}^{2222}_Q \delta_{m,i} - \tilde{V}^{1221}_Q \sigma_{i,m}(\mathbf{Q})\right) \times b^\dagger_{m,\mathbf{q}+\mathbf{Q}} \sum_{\mathbf{k}} c^\dagger_{2,\mathbf{k}-\mathbf{Q}} c_{2,\mathbf{k}} \\ &+ \sum_{\mathbf{Q},m} \left(\tilde{V}^{1111}_Q \sigma_{i,m}(\mathbf{Q}) - \tilde{V}^{1221}_Q \delta_{m,i}\right) \times b^\dagger_{m,\mathbf{q}+\mathbf{Q}} \sum_{\mathbf{k}} h^\dagger_{-\mathbf{k}+\mathbf{Q}} h_{\mathbf{k}}. \end{aligned} \tag{3.24}$$

The coefficient $\gamma_{i,j}$ for $i \neq j$ is a coupling between different modes. In particu-

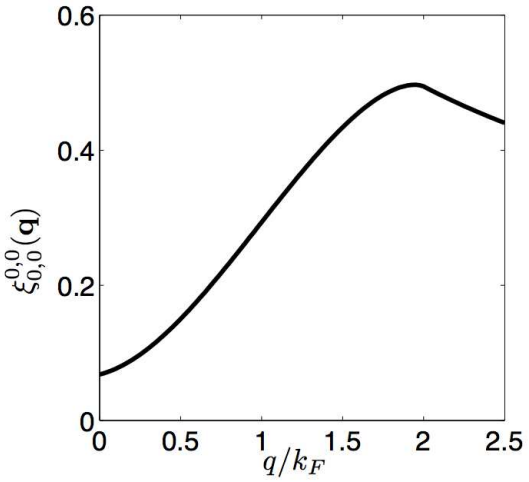

Figure 3.4: Direct interaction coefficient for bright modes only. Notice that it does not vanishes for small wave vectors.

lar, the intrasubband Coulomb interaction couples bright excitations with all dark modes. Since we cannot compute all these terms, we incorporate them in a phenomenological coupling, like we did to treat realistic electron-hole dispersions. For $i = j$, coefficient $\gamma_{i,i}$ is a renormalization of the intersubband transition energy due to the electron-hole interaction [54, 100, 55]. This is the analog of the binding of a conduction electron with a valence hole in the case of excitons. There is, however, an important difference between intersubband excitations and excitons on this point. Excitons are bound states [88] while intersubband excitations are not and can be defined even in the absence of the intrasubband Coulomb interaction [38]. As explained in section 2.2, the term $i = j = 0$ is included in the definition of the energy of a bright intersubband excitation $\hbar\tilde{\omega}_{12}$,

$$\hbar\tilde{\omega}_{12} \leftarrow \hbar\tilde{\omega}_{12} - \gamma_{0,0}. \tag{3.25}$$

Like the deviation operators in Eqs. (3.5) and (3.6), the creation potential operator contains hole-hole and electron-electron pairs of operators. Relation (3.22) is, thus, not closed. We, thus, commute the creation potential with an intersubband operator as we did for deviation operators,

$$\left[V_{i,\mathbf{q}}, b^{\dagger}_{j,\mathbf{q}'}\right] = \frac{1}{n_{\mathrm{QW}} N_{\mathrm{el}}} \frac{e^2 n_{\mathrm{el}}}{2\epsilon_0 \epsilon_r} \sum_{m,n,\mathbf{Q}} \frac{\xi^{n,j}_{m,i}(\mathbf{Q})}{Q\epsilon(\mathbf{Q})}\, b^{\dagger}_{m,\mathbf{q}+\mathbf{Q}} b^{\dagger}_{n,\mathbf{q}'-\mathbf{Q}}, \tag{3.26}$$

where the term $\mathbf{Q} = 0$ has to be removed, n_{el} is electronic density in each quantum

well and

$$\begin{aligned}\xi^{n,j}_{m,i}(\mathbf{Q}) &= \delta_{m,i}\delta_{n,j}\tilde{I}^{2222}_{Q} + \sigma_{i,m}(\mathbf{Q})\,\sigma^{*}_{j,n}(\mathbf{Q})I^{1111}_{Q} \\ &\quad -\delta_{m,i}\,\sigma^{*}_{n,j}(\mathbf{Q})I^{1221}_{Q} - \delta_{n,j}\,\sigma_{i,m}(\mathbf{Q})I^{1221}_{Q},\end{aligned} \tag{3.27}$$

is called direct scattering. This is an electrical dipole interaction: Intrasubband Coulomb interaction induces a pair interaction between intersubband excitations. This interaction is the combination of the non-bosonicity—intersubband excitations are pairs of fermions, not bosons—and a pair interaction between these fermions. It is plotted in figure 3.4. The singularity for $q = k_{\mathrm{F}}$ is due to the fact that coefficient $\sigma_{0,0}(\mathbf{0})$ vanishies at this point. Since the screening has not the same effect for all intrasubband Coulomb processes, the direct scattering does not vanish in the long wavelength limit, contrary to excitons [21, 92].

To sum this up, the intrasubband Coulomb interaction has three effects. First, it renormalized the energies of the intersubband excitations. For bright excitations, this contribution is encoded in the coefficient $\gamma_{0,0}$. Second, it mixes bright and dark modes. Third, it yields a dipole-dipole interaction between intersubband excitations.

3.2 Matrix elements

In this section, we compute matrix elements of the Hamiltonian of the system between states with one or two excitations—photons and bright intersubband excitations. As we do not deal exclusively with bosons, special care should be taken with the normalization of these states. We, thus, first compute scalar products of one- and two-excitation states. To compute these two quantities, we commute operators that annihilate the ground state all the way to the right. From Eq. (3.21), we can see that matrix elements of Hamiltonian H_{I2} between states containing at least one intersubband excitation are all zero. We can, thus, discard its fermionic part. Also, we do not need to compute matrix elements involving only photonic operators because Hamiltonian H_{Cav} and the photonic part of H_{I2} are already known. Hamiltonians H_{I1} and H_{Depol} are already expressed in terms of intersubband excitation operators but, because of the normalization subtleties treated below, we have to compute their matrix elements anyway.

3.2.1 Scalar products and normalization

The states we are considering are constructed by successive application of creation operators and, thus, have to be normalized. When excitations are bosonic, the normalizing constant can be easily computed thanks to the bosonic commutation rule. In the case of photons, *e.g.*, we obtain

$$\langle F|\, a_{\mathbf{q}}^{N_{\text{exc}}}\, a_{\mathbf{q}'}^{\dagger\, N_{\text{exc}}}\, |F\rangle = \delta_{\mathbf{q},\mathbf{q}'}\, N_{\text{exc}}!. \tag{3.28}$$

In the case of intersubband excitations the calculation is trickier: The first contribution of Eq. (3.3) is bosonic, so we expect the term $N_{\text{exc}}!$ to be present, but the deviation from the bosonicity should bring a significant correction when $N_{\text{exc}} \gg 1$. In the following, we will need the normalizing constant for N_{exc} equals to one and two so we focus on these two cases. We will also present the computation for large N_{exc} in some simple cases. Even if we need matrix elements for bright excitations only, we will present the computation of these scalar products for any kind of intersubband excitations.

One-excitation states

To compute scalar products between states with one intersubband excitation, we only need the commutator from Eq. (3.3). We commute the annihilation operator to the right and, because $b_{m,\mathbf{q}}$ and $D_{m\mathbf{q},i\mathbf{q}'}$ annihilate the ground state $|F\rangle$, we obtain

$$\langle F|\, b''_{m,\mathbf{q}}\, b^{\dagger}_{i,\mathbf{q}}\, |F\rangle = \delta_{m\mathbf{q}'',i\mathbf{q}}. \tag{3.29}$$

This result is the same as for elementary bosons, so one-intersubband-excitation states form an orthonormal basis.

Two-excitation states

We now apply the same method to compute two-excitation scalar products. We first commute the annihilation operators all the way to the right,

$$\begin{aligned}\langle F|\, b_{n,\mathbf{q}'''} b_{m,\mathbf{q}''}\, b^{\dagger}_{i,\mathbf{q}} b^{\dagger}_{j,\mathbf{q}'}\, |F\rangle = \delta_{m\mathbf{q}'',i\mathbf{q}}\delta_{n\mathbf{q}''',j\mathbf{q}'} + \delta_{m\mathbf{q}'',j\mathbf{q}'}\delta_{n\mathbf{q}''',i\mathbf{q}} \\ - \langle F|\, b_{n,\mathbf{q}'''}\, D_{m\mathbf{q}'',i\mathbf{q}}\, b^{\dagger}_{j,\mathbf{q}'}\, |F\rangle\,,\end{aligned} \tag{3.30}$$

where we again used the fact that $b_{m,\mathbf{q}}$ and $D_{m\mathbf{q},i\mathbf{q}'}$ annihilate $|F\rangle$. The first two terms yield the symmetric result expected for elementary bosons, while the third one is the correction due to the deviation from bosonicity. The non-bosonicity, thus, starts to play a role when there are at least two excitations in the system. We now commute $D_{m\mathbf{q},i\mathbf{q}'}$ to the right to make it act on $|F\rangle$ and annihilate it. From Eqs. (3.8) and (3.9), we obtain

$$\langle F|\, b_{n,\mathbf{q}'''} b''_{m,\mathbf{q}}\, b^\dagger_{i,\mathbf{q}} b^\dagger_{j,\mathbf{q}'}\, |F\rangle = \delta_{m\mathbf{q}'',i\mathbf{q}}\delta_{n\mathbf{q}'',j\mathbf{q}'} + \delta_{m\mathbf{q}'',j\mathbf{q}'}\delta_{n\mathbf{q}''',i\mathbf{q}} - \delta_{\mathbf{q}''+\mathbf{q}''',\mathbf{q}+\mathbf{q}'} \times \frac{1}{n_{\mathrm{QW}}N_{\mathrm{el}}}\left(\lambda^{n,j}_{m,i}(\mathbf{q}''-\mathbf{q}) + \lambda^{m,j}_{n,i}(\mathbf{q}''-\mathbf{q}')\right). \quad (3.31)$$

The Pauli blocking term is a slow varying function on the scale of optical wavevectors, so we consider the long wavelength limit of the previous equation,

$$\langle F|\, b_{n,\mathbf{q}'''} b_{m,\mathbf{q}''}\, b^\dagger_{i,\mathbf{q}} b^\dagger_{j,\mathbf{q}'}\, |F\rangle = \delta_{m\mathbf{q}'',i\mathbf{q}}\delta_{n\mathbf{q}''',j\mathbf{q}'} + \delta_{m\mathbf{q}'',j\mathbf{q}'}\delta_{n\mathbf{q}''',i\mathbf{q}} - \delta_{\mathbf{q}''+\mathbf{q}''',\mathbf{q}+\mathbf{q}'}\,\frac{2}{n_{\mathrm{QW}}N_{\mathrm{el}}}\lambda^{n,j}_{m,i}(\mathbf{0}). \quad (3.32)$$

Therefore, there is a correction of the order of $1/n_{\mathrm{QW}}N_{\mathrm{el}}$ on the scalar product due to the fermionic statistics of the elementary constituents of the intersubband excitations. This correction might seem irrelevant since states will be normalized anyway. However, it appears that, due to this correction, states with pairs of intersubband excitations with the same total momentum are no longer orthogonal. The family $\{b^\dagger_{i,\mathbf{q}} b^\dagger_{j,\mathbf{q}'}\,|F\rangle\}$ is not orthogonal. It is also overcomplete in the two-excitation space. To see this, we write the product of two creation operators in terms of electron and holes using Eq. (3.1) and pair the fermions in a different way,

$$\begin{aligned} b^\dagger_{i,\mathbf{q}} b^\dagger_{j,\mathbf{q}'} &= \frac{1}{n_{\mathrm{QW}}N_{\mathrm{el}}}\sum_{\mathbf{k},\mathbf{k}'}\nu^*_{i,\mathbf{k}}\nu^*_{j,\mathbf{k}'}\, c^\dagger_{2,\mathbf{k}+\mathbf{q}} h^\dagger_{-\mathbf{k}}\, c^\dagger_{2,\mathbf{k}'+\mathbf{q}'} h^\dagger_{-\mathbf{k}'}, \\ &= -\frac{1}{n_{\mathrm{QW}}N_{\mathrm{el}}}\sum_{\mathbf{k},\mathbf{k}'}\nu^*_{i,\mathbf{k}}\nu^*_{j,\mathbf{k}'}\, c^\dagger_{2,\mathbf{k}'+\mathbf{q}'} h^\dagger_{-\mathbf{k}}\, c^\dagger_{2,\mathbf{k}+\mathbf{q}} h^\dagger_{-\mathbf{k}'}. \end{aligned} \quad (3.33)$$

We then use Eq. (3.2) and the total momentum conservation to express the result in terms of intersubband excitations,

$$b^\dagger_{i,\mathbf{q}} b^\dagger_{j,\mathbf{q}'} = -\frac{1}{n_{\mathrm{QW}}N_{\mathrm{el}}}\sum_{m,n,\mathbf{q}'',\mathbf{q}'''}\lambda^{n,j}_{m,i}(\mathbf{q}''-\mathbf{q})\, b^\dagger_{m,\mathbf{q}''} b^\dagger_{n,\mathbf{q}'''}. \quad (3.34)$$

Any two-excitation state is coupled through Pauli blocking term to all other two-excitation states with same global momentum. In particular, it can be expressed in terms of all the others,

$$b^\dagger_{i,\mathbf{q}} b^\dagger_{j,\mathbf{q}'} = -\frac{n_{\mathrm{QW}} N_{\mathrm{el}}}{1 + n_{\mathrm{QW}} N_{\mathrm{el}}} \sum_{\substack{m,n,\mathbf{q}'',\mathbf{q}''' \\ \neq i,j,\mathbf{q},\mathbf{q}'}} \lambda^{n,j}_{m,i}(\mathbf{q}'' - \mathbf{q}')\, b^\dagger_{m,\mathbf{q}''} b^\dagger_{n,\mathbf{q}'''}. \tag{3.35}$$

As explained in section 3.1, this comes from the fact that there are two ways of pairing two electrons and two holes.

Since the non-orthogonality and the overcompleteness of the two- and, more generally, many-excitation states, there is no exact mapping between intersubband excitations and bosons [101]. It is, however, still possible to derive some effective bosonic Hamiltonian capable of reproducing the dynamics of the system in the long wavelength limit and at low density of excitations [102].

Many-excitation states

We now compute the analog of Eq. (3.28) for intersubband excitations. The method we used to treat the two-excitation case can be generalized to any situation but the computation is cumbersome for arbitrary states. We therefore limit ourselves to cases where all excitations are in the same mode, or in a limited number of them, for which simple rules can be derived [93, 96]. The scalar product reads

$$\langle F |\, b^{N_{\mathrm{exc}}}_{i,\mathbf{q}}\, b^{\dagger\, N_{\mathrm{exc}}}_{i,\mathbf{q}}\, |F\rangle = N_{\mathrm{exc}}!\, \mathcal{F}_{N_{\mathrm{exc}}}, \tag{3.36}$$

where $\mathcal{F}_{N_{\mathrm{exc}}}$ is the deviation from bosonicity contribution. This scalar product is computed through a recursive procedure: We commute the rightmost annihilation operator all the way to the right until it annihilates the ground state $|F\rangle$. Doing so, we leave behind N_{exc} deviation operators $D_{m\mathbf{q},m\mathbf{q}}$, which we commute to the right too. We finally obtain

$$\begin{aligned}\langle F |\, b^{N_{\mathrm{exc}}}_{i,\mathbf{q}}\, b^{\dagger\, N_{\mathrm{exc}}}_{i,\mathbf{q}}\, |F\rangle = N_{\mathrm{exc}}\, \langle F |\, b^{N_{\mathrm{exc}}-1}_{i,\mathbf{q}}\, b^{\dagger\, N_{\mathrm{exc}}-1}_{i,\mathbf{q}}\, |F\rangle - \frac{N_{\mathrm{exc}}(N_{\mathrm{exc}}-1)}{2} \\ \times \sum_n 2\frac{\lambda^{m,i}_{i,i}(\mathbf{0})}{n_{\mathrm{QW}} N_{\mathrm{el}}}\, \langle F |\, b^{N_{\mathrm{exc}}-1}_{i,\mathbf{q}}\, b^\dagger_{m,\mathbf{q}} b^{\dagger\, N_{\mathrm{exc}}-2}_{i,\mathbf{q}}\, |F\rangle\,.\end{aligned} \tag{3.37}$$

First term is linear in the number of excitations because there are N_{exc} ways to associate an annihilation operator to a creation one. Similarly, there are $N_{\mathrm{exc}}(N_{\mathrm{exc}} -$

1)/2 ways to associate a pair of creation operators to an annihilation one, each of these associations yielding a linear superposition of creation operators weighted by the appropriate Pauli blocking term. Using Eqs. (3.10) and (3.36), we obtain a recursive relation for $\mathcal{F}_{N_{\rm exc}}$,

$$\frac{\mathcal{F}_{N_{\rm exc}}}{\mathcal{F}_{N_{\rm exc}-1}} = 1 - \frac{N_{\rm exc}-1}{n_{\rm QW}N_{\rm el}}, \tag{3.38}$$

with the initial condition is $\mathcal{F}_0 = 1$. The $\mathcal{F}_{N_{\rm exc}}$ factor, thus, decreases extremely fast. However, at low density of excitations, *i.e.*, $N_{\rm exc}/n_{\rm QW}N_{\rm el} \ll 1$, it can be approximated by

$$\mathcal{F}_{N_{\rm exc}} \approx 1 - \frac{N_{\rm exc}(N_{\rm exc}-1)}{2\, n_{\rm QW}N_{\rm el}}. \tag{3.39}$$

Notice that, for $N_{\rm exc} = n_{\rm QW}N_{\rm el} + 1$, the recursion relatio vanishes $\mathcal{F}_{n_{\rm QW}N_{\rm el}+1} = 0$. This is due to the fact that only $n_{\rm QW}N_{\rm el}$ intersubband excitations can be created from the Fermi sea.

We can apply the same procedure to states where two modes are macroscopically populated,

$$\langle F|\, b_{j,\mathbf{q}'}^{N_2} b_{i,\mathbf{q}}^{N_1+1}\, b_{i,\mathbf{q}}^{\dagger\, N_1+1} b_{j,\mathbf{q}'}^{\dagger\, N_2}\, |F\rangle = N_2!(N_1+1)!\mathcal{F}_{N_1+1,N_2}, \tag{3.40}$$

where $N_1 + N_2 = N_{\rm exc}$. To compute the normalization factor, we commute an annihilation operator acting on mode $(i,\mathbf{q})$ to the right. There are N_1 ways to associate it with a creation operator acting on the same mode, each weighted by 1, and N_2 ways to associate it with a creation operator acting on the other mode, each weighted by $\delta_{i\mathbf{q},j\mathbf{q}'} = 0$. There are also $N_1(N_1+1)/2$ possible associations with a pair of creation operators acting on the same mode $(i,\mathbf{q})$, $N_2(N_1+1)$ with a pair acting on different modes and $N_2(N_2-1)/2$ with a pair acting on $(j,\mathbf{q}')$. Using Eq. (3.10), we finally obtain,

$$\frac{\mathcal{F}_{N_1+1,N_2}}{\mathcal{F}_{N_1,N_2}} \approx 1 - \frac{N_1+2N_2}{n_{\rm QW}N_{\rm el}}, \tag{3.41}$$

where we kept only dominant terms. Equation (3.41) can be generalized to any number of populated modes.

Analogously, the many-excitation states $\{b_{i,\mathbf{q}}^{\dagger} b_{j,\mathbf{q}'}^{\dagger} \ldots |F\rangle\}$ are not orthogonal and form an overcomplete family.

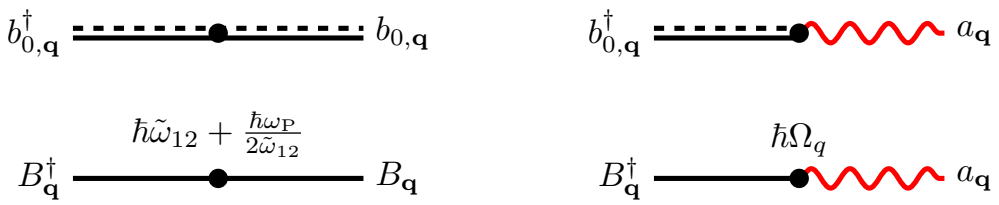

Figure 3.5: Top: Graphical representation of Eqs. 3.42 and (3.43) with Shiva diagrams. Bottom: Equivalent process for bosonized excitations. Because there is only one intersubband excitation, Pauli blocking term is irrelevant and only the bosonic part contributes. The link between Shiva diagrams and traditional Feynman diagrams for bosons is, thus, straightforward.

3.2.2 One-excitation subspace

We have just seen that the one-excitation states form an orthonormal basis, so we do not have to worry about their normalization. The two relevant matrix elements are

$$\langle F|\, b_{0,\mathbf{q}''}\, H\, b^\dagger_{0,\mathbf{q}}\, |F\rangle = \delta_{\mathbf{q},\mathbf{q}''}\left(\hbar\tilde{\omega}_{12} + \frac{\hbar\omega_\mathrm{P}{}^2}{2\tilde{\omega}_{12}}\right), \tag{3.42}$$

$$\langle F|\, b_{0,\mathbf{q}''}\, H\, a^\dagger_{\mathbf{q}}\, |F\rangle = \delta_{\mathbf{q},\mathbf{q}''}\,\hbar\Omega_q. \tag{3.43}$$

Equation (3.42) shows that the energy of a bright intersubband excitation has three contributions: The first one is the energy of a free electron-hole pair modified by the Hartree-Fock renormalization and the excitonic effect. The second one is the depolarization shift due the intersubband Coulomb interaction and the collective nature of intersubband excitations. As expected, Eq. (3.43) shows that the only contribution to the light-matter coupling is Hamiltonian H_{I1} and that this coupling is the Rabi frequency. These processes are represented in figure 3.5, as well as their bosonic counterpart (see section 3.3).

3.2.3 Antiresonant terms

Hamiltonians H_{I1} and H_{Depol} have antiresonant terms coupling the ground state to two-excitation states. We, thus, consider states of the form $b^\dagger_{0,\mathbf{q}'}a^\dagger_{\mathbf{q}'''}\,|F\rangle$ and $b^\dagger_{0,\mathbf{q}'}b^\dagger_{0,\mathbf{q}'''}\,|F\rangle$.

The first one is coupled to the ground state by Hamiltonian H_{I1},

$$\langle F|\, a_{\mathbf{q}'''}b_{0,\mathbf{q}''}\, H\, |F\rangle = \delta_{\mathbf{q}''+\mathbf{q}''',0}\,\hbar\Omega_q, \tag{3.44}$$

which, again, yields the Rabi frequency. The calculation involves only scalar products in the one-excitation subspace and can be performed as if all excitations were bosonic.

The second one is coupled to the ground state by Hamiltonian H_{Depol} and reduces to a sum of two-excitation scalar products. Because the sum runs over the whole Fermi sea, instead of being limited to small wave vectors , we need to consider the general expression of the intersubband Coulomb interaction and the scalar product,

$$\begin{aligned}\langle F|\, b_{0,\mathbf{q}'''}b_{0,\mathbf{q}''}\, H\,|F\rangle &= \frac{N_{\mathrm{el}}}{2}\sum_{\mathbf{q}} V_q^{1212}\ \langle F|\, b_{0,\mathbf{q}'''}b_{0,\mathbf{q}''}\, b^{\dagger}_{0,\mathbf{q}}b^{\dagger}_{0,-\mathbf{q}}\,|F\rangle \qquad (3.45)\\ &= \delta_{\mathbf{q}''+\mathbf{q}''',0}\, N_{\mathrm{el}}\Big(V_{q''}^{1212} - \frac{1}{2n_{\mathrm{QW}}N_{\mathrm{el}}} \qquad (3.46)\\ &\quad \times\sum_{\mathbf{q}} V_q^{1212}\left(\lambda_{0,0}^{0,0}(\mathbf{q}''-\mathbf{q}) + \lambda_{0,0}^{0,0}(\mathbf{q}''+\mathbf{q})\right)\Big).\end{aligned}$$

The two states are, thus, coupled through the creation of pairs of virtual bright intersubband excitations carrying arbitrary wave vectors $\mathbf{q}$. Wave vectors $\mathbf{q}''$ and $\mathbf{q}'''$, however, are carried by real intersubband excitations so we can neglect them when compared to $\mathbf{q}$. The matrix element, thus, reads

$$\langle F|\, b_{0,\mathbf{q}'''}b_{0,\mathbf{q}''}\, H\,|F\rangle = \delta_{\mathbf{q}''+\mathbf{q}''',0}\,\frac{\hbar{\omega_{\mathrm{P}}}^2}{2\tilde{\omega}_{12}}\,(1-\zeta)\,, \qquad (3.47)$$

where

$$\frac{\hbar{\omega_{\mathrm{P}}}^2}{2\tilde{\omega}_{12}}\,\zeta = \frac{1}{n_{\mathrm{QW}}N_{\mathrm{el}}}\sum_{\mathbf{q}} N_{\mathrm{el}}V_q^{1212}\lambda_{0,0}^{0,0}(\mathbf{q}). \qquad (3.48)$$

As such, it is not normalized, so we have to divide it by $\sqrt{1-2/n_{\mathrm{QW}}N_{\mathrm{el}}}$ according to Eq. (3.32).

3.2.4 Two-excitation subspace

In section 3.1, we have seen that pair interactions come from the Pauli (non-bosonicity) and direct (intrasubband Coulomb interaction) scatterings defined in Eqs. (3.10) and (3.27). From Eqs. (3.8), (3.9) and (3.26), we can see that these contribution are of the order of $1/n_{\mathrm{QW}}N_{\mathrm{el}}$. More generally, it can be shown that n-body interactions scale like $(1/n_{\mathrm{QW}}N_{\mathrm{el}})^{n-1}$ [92]. Because two-excitation matrix elements can only describe the one- and two-body physics, we have to truncate all our results to first order in $1/n_{\mathrm{QW}}N_{\mathrm{el}}$. Higher order terms are irrelevant and should

be discarded. Therefore, we are computing the first two terms of a perturbation series in the non-bosonicity and the intrasubband Coulomb interaction.

Orthonormalization trick

We have also seen that states $b^\dagger_{0,\mathbf{q}} b^\dagger_{0,\mathbf{q}'} |F\rangle$ form a non-orthogonal overcomplete family and, because of this mathematical subtlety, we cannot compute matrix elements in a standard way. To understand this point, let's call the ket the initial state, and the bra the final state. If they are overlapping, their matrix element contains information about transition rates from the initial state to the final one and to itself too. To remove this self-coupling, a solution is to orthonormalize our basis but this is untractable. It is also not necessary and can be replaced by a much simpler procedure. Because matrix elements involve only two states, only the final state has to be orthonalized with respect to the initial one,

$$\langle F| b_{0,\mathbf{q}'-\mathbf{p}} b_{0,\mathbf{q}+\mathbf{p}} \mapsto \langle F| b_{0,\mathbf{q}'-\mathbf{p}} b_{0,\mathbf{q}+\mathbf{p}} P_\perp, \tag{3.49}$$

where $P_\perp$ is the orthogonal projector with respect to $b^\dagger_{0,\mathbf{q}} b^\dagger_{0,\mathbf{q}'} |F\rangle$. If the initial and final states are the same, *i.e.*, $\mathbf{p} = 0$ or $\mathbf{p} = \mathbf{q}' - \mathbf{q}$, there is nothing to change and $P_\perp$ is replaced by the identity operator. This partial orthogonalization, together with a normalization, has to be performed for each matrix element, so we can compute relevant physical quantities without looking for the real orthonormal basis of the two-excitation subspace. To simplify the notation, we define the normalizing constant for states with two bright intersubband excitations,

$$N_{\mathbf{q},\mathbf{q}'} = \langle F| b_{0,\mathbf{q}'} b_{0,\mathbf{q}} b^\dagger_{0,\mathbf{q}} b^\dagger_{0,\mathbf{q}'} |F\rangle = 1 + \delta_{\mathbf{q},\mathbf{q}'} - \frac{2}{n_{\mathrm{QW}} N_{\mathrm{el}}}. \tag{3.50}$$

Because the scalar product between $b^\dagger_{0,\mathbf{q}} b^\dagger_{0,\mathbf{q}'} |F\rangle$ and $b^\dagger_{0,\mathbf{q}+\mathbf{p}} b^\dagger_{0,\mathbf{q}'-\mathbf{p}} |F\rangle$ is of the order of $1/n_{\mathrm{QW}} N_{\mathrm{el}}$, the normalizing constant $N_{\mathbf{q}+\mathbf{p},\mathbf{q}'-\mathbf{p}}$ is not affected by the orthogonalization procedure to first order in $1/n_{\mathrm{QW}} N_{\mathrm{el}}$.

Different types of matrix elements

We have to consider two kinds of two-excitation states, namely with (i) two bright intersubband excitations or (ii) one bright intersubband excitation plus one photon. Notice that the latter already constitute an orthonormal family and are orthogonal to the former. The orthonormalization trick from the previous paragraph is, thus,

not necessary to compute matrix elements involving them. Combining these two kinds of states, we obtain three matrix elements. First, there is a photon in both he initial and final states. The matrix elements involve only states of the second form and, as mentioned above, the orthonormalization trick is not needed. Second, a photon is absorbed (emitted) and a bright excitation is created (annihilated). These matrix elements involves states of both the first and second form. Again, we do not need to orthonormalize the states. Third, there is no photon in both the initial and final states. Corresponding matrix elements involves only states of the first, which must be orthonormalized. These three kinds of matrix elements are computed below.

1. A photon is present in both the initial and final states. It is just the sum of the one-excitation matrix elements, so it brings no additional information about the system and can be obtained from Eqs. (2.2) and (3.42),

$$\langle F|\, b_{0,\mathbf{q}'-\mathbf{p}} a_{\mathbf{q}+\mathbf{p}}\, H\, a^\dagger_{\mathbf{q}} b^\dagger_{0,\mathbf{q}'}\, |F\rangle = \delta_{\mathbf{p},0} \left(\hbar\omega_{\mathrm{cav},q} + \hbar\tilde{\omega}_{12} + \frac{\hbar{\omega_{\mathrm{P}}}^2}{2\tilde{\omega}_{12}} \right). \tag{3.51}$$

2. A photon is absorbed (emitted) and a bright excitation is created (annihilated) while there is already a bright intersubband excitation in the system. Only Hamiltonian $H_{\mathrm{I}1}$ contributes and, from Eqs. (2.32) and (3.32), we obtain

$$\langle F|\, b_{0,\mathbf{q}'-\mathbf{p}} b_{0,\mathbf{q}+\mathbf{p}}\, H\, a^\dagger_{\mathbf{q}} b^\dagger_{0,\mathbf{q}'}\, |F\rangle = \hbar\Omega_q \left(\delta_{\mathbf{p},0} + \delta_{\mathbf{p},\mathbf{q}'-\mathbf{q}} - \frac{2}{n_{\mathrm{QW}} N_{\mathrm{el}}} \right). \tag{3.52}$$

Normalizing the state with two bright intersubband excitations according to Eq. (3.50), we obtain, to first order in $1/n_{\mathrm{QW}}N_{\mathrm{el}}$,

$$\begin{aligned} \frac{\langle F|\, b_{0,\mathbf{q}'-\mathbf{p}} b_{0,\mathbf{q}+\mathbf{p}}\, H\, a^\dagger_{\mathbf{q}} b^\dagger_{0,\mathbf{q}'}\, |F\rangle}{\sqrt{N_{\mathbf{q}+\mathbf{p},\mathbf{q}'-\mathbf{p}}}} &= \hbar\Omega_q \\ \times \begin{cases} \sqrt{2}\left(1 - \frac{1}{2n_{\mathrm{QW}}N_{\mathrm{el}}}\right) & \text{if } \mathbf{q} = \mathbf{q}',\ \mathbf{p} = \mathbf{0}, \\ 1 - \frac{1}{n_{\mathrm{QW}}N_{\mathrm{el}}} & \text{if } \mathbf{q} \neq \mathbf{q}',\ \mathbf{p} = \mathbf{0} \text{ or } \mathbf{p} = \mathbf{q}' - \mathbf{q}, \\ -\frac{2}{n_{\mathrm{QW}}N_{\mathrm{el}}} & \text{if } \mathbf{q} \neq \mathbf{q}',\ \mathbf{p} \neq \mathbf{0} \text{ and } \mathbf{p} \neq \mathbf{q}' - \mathbf{q}. \end{cases} \end{aligned} \tag{3.53}$$

In the first two cases in Eq. (3.53), we recognize the stimulated emission factor $\sqrt{n+1}$ where $n \in \{0, 1\}$ is the number of bright intersubband excitations in the mode absorbing the photon. This confirms that these excitations are approximately bosonic. The other coefficient is the bosonicity factor [48],

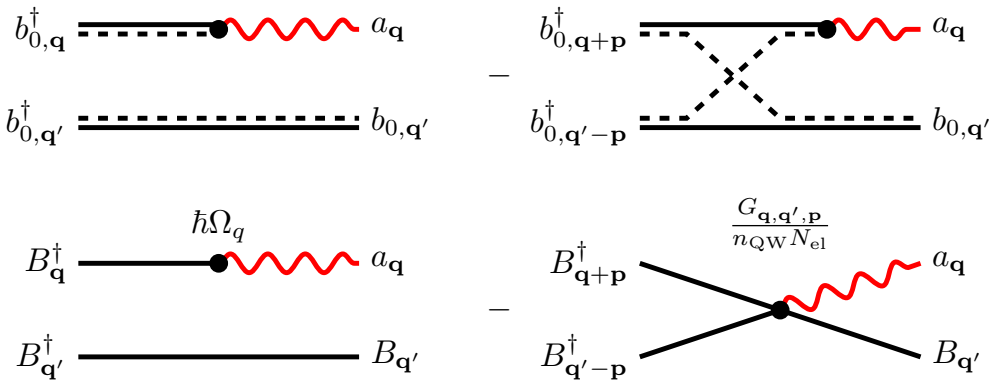

Figure 3.6: Graphical representation of Eq. (3.53) with Shiva diagrams (top panel) and its bosonic counterpart (bottom panel). The combination of Pauli blocking term and photon absorption induces an effective two-body interaction between bosonized excitations. Coefficient $G_{\mathbf{q},\mathbf{q}',\mathbf{p}}$ in bottom panel is given in Eq. (3.70).

truncated to first order in $1/n_{\mathrm{QW}}N_{\mathrm{el}}$, due to the Pauli blocking term. It describes the saturation of the light-matter coupling triggered by the Pauli exclusion principle.

Terms of the order of $1/n_{\mathrm{QW}}N_{\mathrm{el}}$ cannot be obtained from the one-excitation matrix elements only, so we interpret them as an effective two-body interaction between photons and intersubband excitations. This interaction is the combination of photon absorption/emission and the Pauli blocking term: Once the photon is absorbed, the resulting intersubband excitations pair is scattered to any other two-excitation state with the same global momentum (figure 3.6). This results, for example, in the saturation of the Rabi frequency as shown in section 3.4.

3. No photon is present in the initial nor in the final states. To compute these matrix elements, we need the general expression of the matrix elements before

any orthonormalization procedure,

$$\begin{aligned}\langle F|\, b_{0,\mathbf{q}'-\mathbf{p}} b_{0,\mathbf{q}+\mathbf{p}}\, H\, b^\dagger_{0,\mathbf{q}} b^\dagger_{0,\mathbf{q}'}\,|F\rangle = 2\hbar\tilde{\omega}_{12}\left(\delta_{\mathbf{p},0}+\delta_{\mathbf{p},\mathbf{q}'-\mathbf{q}}-\frac{2}{n_{\mathrm{QW}}N_{\mathrm{el}}}\right)\\ +\frac{\hbar{\omega_{\mathrm{P}}}^2}{\tilde{\omega}_{12}}\left(\delta_{\mathbf{p},0}+\delta_{\mathbf{p},\mathbf{q}'-\mathbf{q}}-\frac{4-2\zeta}{n_{\mathrm{QW}}N_{\mathrm{el}}}\right)\\ +\frac{1}{n_{\mathrm{QW}}N_{\mathrm{el}}}\frac{e^2 n_{\mathrm{el}}}{2\epsilon_0\epsilon_r\kappa}\left(\xi^{0,0}_{0,0}(\mathbf{p})+\xi^{0,0}_{0,0}(\mathbf{q}'-\mathbf{q}-\mathbf{p})\right)\\ -\frac{1}{n_{\mathrm{QW}}N_{\mathrm{el}}}\frac{e^2}{2\epsilon_0\epsilon_r}\sqrt{\frac{n_{\mathrm{el}}}{2\pi}}\left(x(\mathbf{p})+x(\mathbf{q}'-\mathbf{q}-\mathbf{p})\right). \quad (3.54)\end{aligned}$$

To obtain this expression, we used the long wavelength limit of the electron gas dielectric function $q\epsilon(q)\to\kappa$. Because of the absence of the $\mathbf{q}=0$ term in the Coulomb interaction in Eq. (2.9), the direct scattering in the third line is set to zero if its argument is the null vector. Otherwise, we consider its long wavelength limit, which we denote $\xi^{0,0}_{0,0}(\mathbf{0}^+)$. The coefficient $x(\mathbf{p})$ in the fourth line is the exchange Coulomb interaction,

$$x(\mathbf{p})=\frac{1}{n_{\mathrm{QW}}N_{\mathrm{el}}}\sum_{m,n,\mathbf{Q}\neq 0}\frac{k_{\mathrm{F}}}{Q\epsilon(\mathbf{Q})}\,\lambda^{0,n}_{0,m}(\mathbf{Q}-\mathbf{p})\xi^{n,0}_{m,0}(-\mathbf{Q}), \quad (3.55)$$

and results from the interplay between the intrasubband Coulomb interaction and the non-bosonicity: two intersubband excitations exchange their fermions before interacting via the direct interaction. Since it is a slow varying function of $\mathbf{p}$, we replace it by its long wavelength limit $x=x(\mathbf{0})$.

We then apply the orthogonalization trick. If the initial and final states are the same, we just replace the orthogonal projector $P_\perp$ by the identity in Eq. (3.49) and it remains unchanged. If the final state is different from the initial state, its orthogonalized version is

$$\begin{aligned}\langle F|\, b_{0,\mathbf{q}'-\mathbf{p}} b_{0,\mathbf{q}+\mathbf{p}}\, P_\perp = \langle F|\, b_{0,\mathbf{q}'-\mathbf{p}} b_{0,\mathbf{q}+\mathbf{p}} -\\ \frac{\langle F|\, b_{0,\mathbf{q}'-\mathbf{p}} b_{0,\mathbf{q}+\mathbf{p}}\, b^\dagger_{0,\mathbf{q}} b^\dagger_{0,\mathbf{q}'}\,|F\rangle}{N_{\mathbf{q},\mathbf{q}'}}\,\langle F|\, b_{0,\mathbf{q}'} b_{0,\mathbf{q}}, \quad (3.56)\end{aligned}$$

and, as stated above, its norm is unchanged to first order in $1/n_{\mathrm{QW}}N_{\mathrm{el}}$. After the proper normalization of both the initial and final states according to

Eq. (3.50), the matrix elements are given by

$$\frac{\langle F|\, b_{0,\mathbf{q}}^2\, H\, b_{0,\mathbf{q}}^{\dagger\,2}\,|F\rangle}{N_{\mathbf{q},\mathbf{q}}} = 2\left(\hbar\tilde{\omega}_{12} + \frac{\hbar{\omega_{\mathrm{P}}}^2}{2\tilde{\omega}_{12}}\right) - \frac{1}{n_{\mathrm{QW}}N_{\mathrm{el}}}\left(\frac{\hbar{\omega_{\mathrm{P}}}^2}{\tilde{\omega}_{12}}(1-\zeta) + \frac{e^2}{2\epsilon_0\epsilon_r}\sqrt{\frac{n_{\mathrm{el}}}{2\pi}}\,x\right), \quad (3.57)$$

and

$$\frac{\langle F|\, b_{0,\mathbf{q}'}b_{0,\mathbf{q}}\, H\, b_{0,\mathbf{q}}^{\dagger}b_{0,\mathbf{q}'}^{\dagger}\,|F\rangle}{N_{\mathbf{q},\mathbf{q}'}} = 2\left(\hbar\tilde{\omega}_{12} + \frac{\hbar{\omega_{\mathrm{P}}}^2}{2\tilde{\omega}_{12}}\right) - \frac{2}{n_{\mathrm{QW}}N_{\mathrm{el}}}\left(\frac{\hbar{\omega_{\mathrm{P}}}^2}{\tilde{\omega}_{12}}(1-\zeta) - \frac{e^2 n_{\mathrm{el}}}{4\epsilon_0\epsilon_r\kappa}\,\xi_{0,0}^{0,0}(\mathbf{0}^+) + \frac{e^2}{2\epsilon_0\epsilon_r}\sqrt{\frac{n_{\mathrm{el}}}{2\pi}}\,x\right), \quad (3.58)$$

if the initial and final states are the same. If they are different, the matrix element is

$$\frac{\langle F|\, b_{0,\mathbf{q}-\mathbf{p}'}b_{0,\mathbf{q}+\mathbf{p}}\, P_\perp\, H\, b_{0,\mathbf{q}}^{\dagger}b_{0,\mathbf{q}'}^{\dagger}\,|F\rangle}{\sqrt{N_{\mathbf{q}+\mathbf{p},\mathbf{q}'-\mathbf{p}}N_{\mathbf{q},\mathbf{q}'}}} = -\frac{2}{n_{\mathrm{QW}}N_{\mathrm{el}}}\left(\frac{\hbar{\omega_{\mathrm{P}}}^2}{\tilde{\omega}_{12}}(1-\zeta) - \frac{e^2 n_{\mathrm{el}}}{2\epsilon_0\epsilon_r\kappa}\,\xi_{0,0}^{0,0}(\mathbf{0}^+) + \frac{e^2}{2\epsilon_0\epsilon_r}\sqrt{\frac{n_{\mathrm{el}}}{2\pi}}\,x\right). \quad (3.59)$$

From Eq. (3.42), we can see that the first part in Eqs. (3.57) and (3.58) is the energy of two independent bright intersubband excitations. The other terms yield a correction, which is interpreted as an effective two-body interaction. This interaction has three contributions. The first one is the interplay between the Pauli blocking term and plasmonic effects. Like what was observed in Eq. (3.53), this is a saturation term. The second one, if present, is the direct intrasubband Coulomb interaction, *i.e.*, a dipole-dipole interaction. The third one is the exchange Coulomb interaction between dipoles. A graphical interpretation of these terms is given in figure 3.7.

Equations (3.53) and (3.59) show that these effective two-body interactions can scatter pairs of excitations, which makes our system a potential candidate for parametric amplification [24].

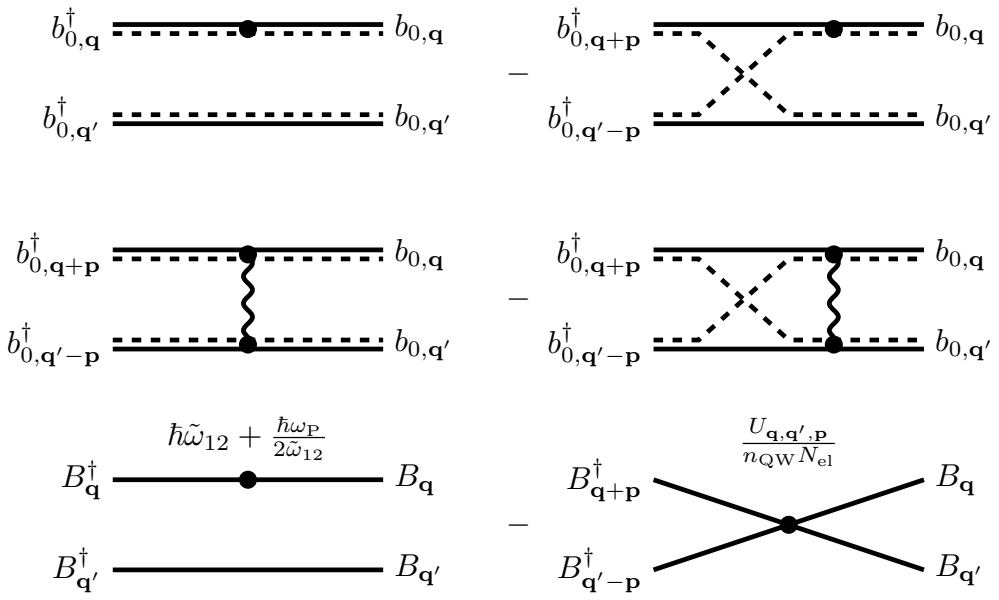

Figure 3.7: Graphical representations of Eqs. (3.57) to (3.59) and their bosonic counterparts. Top panel: one-body interaction affecting one intersubband excitations (left) while another is not affected. The two excitations can also exchange their fermions (right). Middle panel: Coulomb interaction between two intersubband excitations. On the left, direct Coulomb interaction given in Eq. (3.27), *i.e.*, dipole-dipole interaction. On the right combination of the direct Coulomb interaction with Pauli blocking term, namely the exchange Coulomb interaction. Bottom panel: in the bosonic framework, there is a one body contribution and an effective two-body interaction. Coefficient $U_{\mathbf{q},\mathbf{q}',\mathbf{p}}$ is given in Eq. (3.68).

Figure 3.8: Graphical representation of a process involving three intersubband excitations (left). A first pair interact through direct Coulomb interaction. A second pair then exchange their holes. Because the diagram is connected, this interaction cannot be separated into one- and two-body effective interactions. It is, thus, an effective three-body interaction between bosonized excitations (right). Because it involves two $1/n_{\mathrm{QW}}N_{\mathrm{el}}$ contributions, it is of order $(1/n_{\mathrm{QW}}N_{\mathrm{el}})^2$. This can be generalized to higher order process, provided the graph is connected.

3.2.5 Generalization to higher numbers of excitations

It is of course possible, even if tedious, to generalize the above calculations (figure 3.8). To identify n-body interaction between intersubband excitations and photons, we have to compute all matrix elements containing up to n excitations. Doing so, the overcompleteness and non-orthogonality of the families of vectors must be carefully taken into account. Finally, all results are truncated to the $(n-1)$-th order in $1/n_{\mathrm{QW}}N_{\mathrm{el}}$.

The highest order theoretically achievable is $n = n_{\mathrm{QW}}N_{\mathrm{el}}$. This is indeed the maximum number of intersubband excitations which can be injected in the system. However, there is no reason to push the calculation so far. Indeed, the concept of almost bosonic intersubband excitation developed here loses its meaning when the number of excitations is high. We, thus, have to limit ourselves to low number of excitations $N_{\mathrm{exc}} \ll n_{\mathrm{QW}}N_{\mathrm{el}}$. Moreover, to study a situation where there are N_{exc} excitations, where $1 \ll N_{\mathrm{exc}} \ll n_{\mathrm{QW}}N_{\mathrm{el}}$, we do not need to compute N_{exc}-excitation matrix elements. We will see in Sec. 3.4 that one- and two-body effective interactions are enough to correctly decribe the physics of the system in this limit.

3.3 Effective bosonic Hamiltonian

In this section, we construct an effective bosonic Hamiltonian capable of reproducing the physics of intersubband polaritons. We explain our method and give some numerical results.

3.3.1 Method

In section 3.2, we have computed matrix elements of the Hamiltonian between states with one excitation (Eqs. (3.42) and (3.43)), two excitations (Eqs. (3.53) and (3.57) to (3.59)) as well as anti-resonant terms (Eqs. (3.44) and (3.47)). In the case of two-excitation matrix elements, we have seen that our results, truncated to first order in $1/n_{\mathrm{QW}}N_{\mathrm{el}}$, contain the two-body physics of the system.

We now show how to construct an effective bosonic Hamiltonian capable of reproducing the dynamics of the system. Such an Hamiltonian must have a quadratic and a quartic part to respectively encode the one- and two-body interactions. Its general form is

$$H^{\mathrm{B}} = H_{\mathrm{Photon}} + H^{\mathrm{B}}_{\mathrm{ISB}} + H^{\mathrm{B}}_{\mathrm{lm}}, \tag{3.60}$$

where superscript B indicates that intersubband excitations have been bosonized. Hamiltonian H_{Photon} is the photonic part of the Hamiltonian, coming from H_{Cav} and H_{I2},

$$H_{\text{Photon}} = \sum_{\mathbf{q}} \hbar\omega_{\text{cav},q}\, a^\dagger_{\mathbf{q}} a_{\mathbf{q}} + \sum_{\mathbf{q}} \frac{\hbar{\Omega_q}^2}{\tilde{\omega}_{12}} \left(a_{-\mathbf{q}} + a^\dagger_{\mathbf{q}}\right)\left(a_{\mathbf{q}} + a^\dagger_{-\mathbf{q}}\right). \tag{3.61}$$

It has already been fully determined in chapter 2 and appendix B. Hamiltonian $H^{\text{B}}_{\text{ISB}}$ and H^{B}_{lm} are, respectively, the bosonized matter part of the system,

$$\begin{aligned} H^{\text{B}}_{\text{ISB}} &= \sum_{\mathbf{q}} K_q\, B^\dagger_{\mathbf{q}} B_{\mathbf{q}} + \sum_{\mathbf{q}} Q_q\, B_{\mathbf{q}} B_{-\mathbf{q}} + \text{H.c.} \\ &\quad -\frac{1}{2}\frac{1}{n_{\text{QW}} N_{\text{el}}} \sum_{\mathbf{q},\mathbf{q}',\mathbf{p}} U_{\mathbf{q},\mathbf{q}',\mathbf{p}}\, B^\dagger_{\mathbf{q}+\mathbf{p}} B^\dagger_{\mathbf{q}'-\mathbf{p}} B_{\mathbf{q}'} B_{\mathbf{q}}, \end{aligned} \tag{3.62}$$

and its coupling to photons,

$$\begin{aligned} H^{\text{B}}_{\text{lm}} &= \sum_{\mathbf{q}} \hbar\tilde{\Omega}_q\, a_{\mathbf{q}} B^\dagger_{\mathbf{q}} + \hbar\bar{\Omega}_q\, a^\dagger_{-\mathbf{q}} B^\dagger_{\mathbf{q}} + \text{H.c.} \\ &\quad -\frac{1}{n_{\text{QW}} N_{\text{el}}} \sum_{\mathbf{q},\mathbf{q}',\mathbf{p}} G_{\mathbf{q},\mathbf{q}',\mathbf{p}}\, B^\dagger_{\mathbf{q}+\mathbf{p}} B^\dagger_{\mathbf{q}'-\mathbf{p}} B_{\mathbf{q}'} a_{\mathbf{q}} + \text{H.c.} \end{aligned} \tag{3.63}$$

We are only interested in the dynamics of bright excitations, so we omitted the corresponding index. As explained in chapter 2, the spin of the electrons is conserved during the absorption or emission of photons. Bright intersubband excitations are, thus, electron-hole pairs with opposite spins. Also, we consider here only TM polarization of the cavity field, so the spin and polarization indices are irrelevant and we omitted them. This implies that there is no spin/polarization dependence of the polariton-polariton interaction in the intersubband case, as one could expect from a naive comparison with excitons [21, 103, 104, 105].

Coefficients of Hamiltonian H^{B} can be found by imposing that it has the same matrix elements than H^{B} in the one- and two-excitation subspaces,

$$\frac{\langle G|\, T_{\mathbf{q}'-\mathbf{p}} T_{\mathbf{q}+\mathbf{p}}\, H^{\text{B}}\, T^\dagger_{\mathbf{q}} T^\dagger_{\mathbf{q}'}\, |G\rangle}{\sqrt{N^{\text{B}}_{\mathbf{q}+\mathbf{p},\mathbf{q}'-\mathbf{p}} N^{\text{B}}_{\mathbf{q},\mathbf{q}'}}} = \frac{\langle F|\, t_{\mathbf{q}'-\mathbf{p}} t_{\mathbf{q}+\mathbf{p}}\, H\, t^\dagger_{\mathbf{q}} t^\dagger_{\mathbf{q}'}\, |F\rangle}{\sqrt{N_{\mathbf{q}+\mathbf{p},\mathbf{q}'-\mathbf{p}} N_{\mathbf{q},\mathbf{q}'}}}, \tag{3.64}$$

where $t_{\mathbf{q}} \in \{\mathbb{I}, a_{\mathbf{q}}, b_{0,\mathbf{q}}\}$, $T_{\mathbf{q}} \in \{\mathbb{I}, a_{\mathbf{q}}, B_{\mathbf{q}}\}$. The normalizing constant $N_{\mathbf{q},\mathbf{q}'}$ is defined in Eq. (3.50) for two-excitation states and is, otherwise, equal to one and $N^{\text{B}}_{\mathbf{q},\mathbf{q}'}$ is

its bosonic counter part.

Quadratic part

The quadratic part of the Hamiltonian is obtained by comparison with fermionic one-excitation matrix elements and antiresonant terms, which yields

$$K_q = \hbar\tilde{\omega}_{12} + \frac{\hbar{\omega_\mathrm{P}}^2}{2\tilde{\omega}_{12}}, \tag{3.65}$$

$$Q_q = \frac{\hbar{\omega_\mathrm{P}}^2}{4\tilde{\omega}_{12}}\left(1-\zeta\right), \tag{3.66}$$

$$\tilde{\Omega}_q = \bar{\Omega}_q = \Omega_q. \tag{3.67}$$

In the expression of coefficient Q_q, the effect of the normalization in Eq. (3.47) is negligeable. The quadratic part of Hamiltonian H^B is very similar to $\tilde{H}^\mathrm{B}$ in Eq. (2.42). The only difference is the renormalization of the antiresonant terms in the intersubband Coulomb interaction and we will see that they only have a limited effect on the physics of intersubband excitations and polaritons (figure 3.11). Moreover, if we neglect the antiresonant terms, the two Hamiltonians are the same. In addition, we now know how to calculate the contribution of the electron-hole attraction to the energy $\hbar\tilde{\omega}_{12}$ thanks to Eq. (3.23). We, thus, confirmed the relevance of our method to find quadratic effective Hamiltonians and describe the system in the linear regime. This also explains the similitude between $\tilde{H}^\mathrm{B}$ and the simple model in section 1.3: The latter is precisely a simplified one-excitation model.

Quartic part

The quartic part of Hamiltonian H^B is obtained from the fermionic two-excitation matrix elements. The purely matter part coefficient is

$$U_{\mathbf{q},\mathbf{q}',\mathbf{p}} = \frac{\hbar{\omega_\mathrm{P}}^2}{\tilde{\omega}_{12}}(1-\zeta) - f_{\mathbf{q}'-\mathbf{q},\mathbf{p}}\,\frac{e^2 n_\mathrm{el}}{2\epsilon_0\epsilon_r\kappa}\,\xi^{0,0}_{0,0}(\mathbf{0}^+) + \frac{e^2}{2\epsilon_0\epsilon_r}\sqrt{\frac{n_\mathrm{el}}{2\pi}}\,x, \tag{3.68}$$

where

$$f_{\mathbf{q}'-\mathbf{q},\mathbf{p}} = \begin{cases} 0 & \text{if } \mathbf{p}=\mathbf{0} \text{ and } \mathbf{q}'-\mathbf{q}-\mathbf{p}=\mathbf{0}, \\ 1/2 & \text{if } \mathbf{p}=\mathbf{0} \text{ xor } \mathbf{q}'-\mathbf{q}-\mathbf{p}=\mathbf{0}, \\ 1 & \text{else.} \end{cases} \tag{3.69}$$

Coefficient $U_{\mathbf{q},\mathbf{q}',\mathbf{p}}$ encodes all sources of intersubband excitations pair interaction described in section 3.2, *i.e.*, combination of the Pauli blocking term and the in-

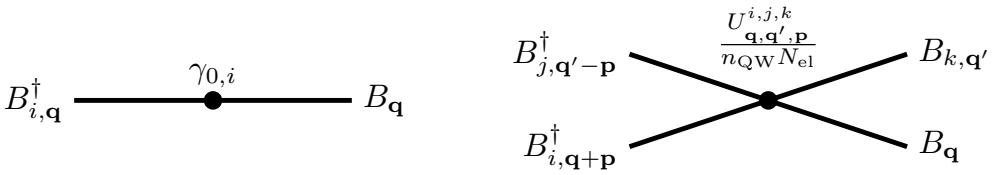

Figure 3.9: Non resonant interaction between bright and dark intersubband excitations given in Eqs. (3.72) and (3.73).

tersubband Coulomb interaction, and direct and exchange intrasubband Coulomb interaction between intersubband excitations' fermionic constituents. The quartic light-matter coupling coefficient is

$$G_{\mathbf{q},\mathbf{q}',\mathbf{p}} = g_{\mathbf{q}'-\mathbf{q},\mathbf{p}}\,\hbar\Omega_q, \tag{3.70}$$

where

$$g_{\mathbf{q}'-\mathbf{q},\mathbf{p}} = \begin{cases} 1/2 & \text{if } \mathbf{p}=\mathbf{0} \text{ or } \mathbf{p}=\mathbf{q}'-\mathbf{q}, \\ 1 & \text{else.} \end{cases} \tag{3.71}$$

It encodes the interplay between the Pauli blocking term and the light-matter coupling. To compute these coefficients, we assumed that they were invariant under the exchange of $\mathbf{q}$ and $\mathbf{q}'$ and change of $\mathbf{p}$ into $\mathbf{q}'-\mathbf{q}-\mathbf{p}$.

Notice that $U_{\mathbf{q},\mathbf{q}',\mathbf{p}}$ and $G_{\mathbf{q},\mathbf{q}',\mathbf{p}}$ are not continuous functions of the wave vectors. This is relevant in situations where one, or a few, modes are macroscopically populated, as it is the case in optical pumping by a coherent source. For example, this situation is encountered in parametric amplification and oscillation [24]. When the distribution of population is diluted over many modes, this discontinuity is irrelevant (see section 3.4) and can be removed by making $f_{\mathbf{q}'-\mathbf{q},\mathbf{p}}$ and $g_{\mathbf{q}'-\mathbf{q},\mathbf{p}}$ constant and equal to one. Coefficients $U_{\mathbf{q},\mathbf{q}',\mathbf{p}}$ and $G_{\mathbf{q},\mathbf{q}',\mathbf{p}}$ are then constant too.

Coupling to dark excitations

Hamiltonian H^{B} neglects all kinds of couplings between bright excitations and the electron-hole continuum (dark excitations). We give some examples of such couplings and show that our Hamiltonian is valid as long as the bright and dark excitations are not resonant and the population in dark modes remains negligeable.

First, as explained in section 3.1, such couplings can be due to electronic dispersion (see Eq. (3.15)) or the intrasubband Coulomb interaction (see Eq. (3.22)).

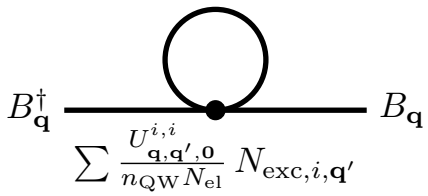

Figure 3.10: Graphical representation of the mean-field treatment of the interaction between bright and dark intersubband excitations given in Eq. (3.75). The loop corresponds to the sum over all modes.

They yield a one-body interaction, in the sense of bosonized excitations,

$$H^{\mathrm{B}}_{\mathrm{Dark},1} = \sum_{i\neq 0,\mathbf{q}} \gamma_{0,i}\, B^\dagger_{i,\mathbf{q}} B_{\mathbf{q}}, \tag{3.72}$$

mixing bright and dark excitations. This is a coupling between bright excitation and the electron-hole continuum. Second, generalizing calculations of section 3.2 to include dark excitations, we can see that bright excitations can interact with another excitation—photon or intersubband excitation—to create two dark excitations. These are two-body sources of decoherence of the form

$$H^{\mathrm{B}}_{\mathrm{Dark},2} = -\frac{1}{n_{\mathrm{QW}}N_{\mathrm{el}}} \sum U^{i,j,k}_{\mathbf{q},\mathbf{q}',\mathbf{p}}\, B^\dagger_{i,\mathbf{q}+\mathbf{p}} B^\dagger_{j,\mathbf{q}'-\mathbf{p}} B_{k,\mathbf{q}'} B_{\mathbf{q}}, \tag{3.73}$$

where indices i and j denote dark modes. A similar term can be written for the quartic ligth-matter part. However, because of the depolarization shift and the light matter coupling, intersubband polaritons are shifted away from dark excitations. Equations (3.72) and 3.73 describe non-resonant processes, so bright and dark excitations are decoupled. As long as bright intersubband excitations/polaritons are not resonant with the electron-hole continuum, contributions like (3.72) and (3.73) can be neglected. If they are resonant, these couplings cannot be neglected anymore and shorter lifetime of polaritons is expected. These processes are represented in figure 3.9

However, two-body interaction mixing bright and dark excitations can be resonant,

$$H^{\mathrm{B}}_{\mathrm{Dark},3} = -\frac{1}{n_{\mathrm{QW}}N_{\mathrm{el}}} \sum U^{i,j}_{\mathbf{q},\mathbf{q}',\mathbf{p}}\, B^\dagger_{\mathbf{q}+\mathbf{p}} B^\dagger_{i,\mathbf{q}'-\mathbf{p}} B_{j,\mathbf{q}'} B_{\mathbf{q}}, \tag{3.74}$$

and can, thus, affect the dynamics of polaritons. A mean-field treatment of Eq. (3.74)

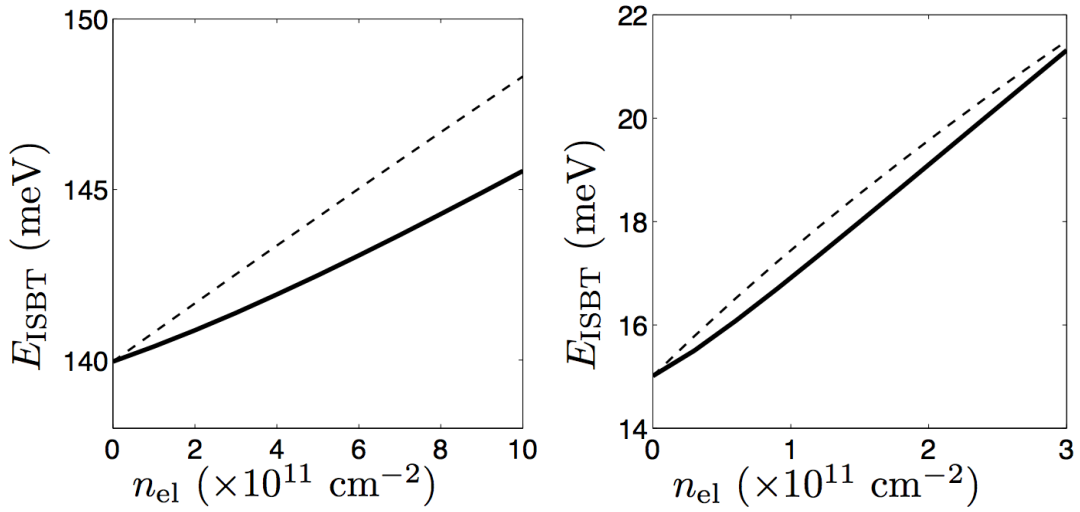

(a) (b)

Figure 3.11: Intersubband plasmon energy E_{ISBT} for a bare energy $\hbar\omega_{12} = 140$ meV (figure (a)) and 15 meV (figure (b)) as a function of the electron density in the wells. Solid line: result obtained from Eq. (3.76). Dashed line: result obtained while neglecting the intrasubband Coulomb interaction and ζ.

yields,

$$H^{\mathrm{B}}_{\mathrm{Dark,MF}} = -\frac{1}{n_{\mathrm{QW}} N_{\mathrm{el}}} \sum_{\mathbf{q}} \left(\sum_{i,\mathbf{q}'} U^{i,i}_{\mathbf{q},\mathbf{q}',\mathbf{0}}\, N_{\mathrm{exc},i,\mathbf{q}'} \right) B^{\dagger}_{\mathbf{q}} B_{\mathbf{q}}, \tag{3.75}$$

where $N_{\mathrm{exc},i,\mathbf{q}'}$ is the number of excitations in mode $(i,\mathbf{q}')$. This shows that the energy of bright excitations/polaritons depends on the population in all modes, including dark ones. However, as long as the population in the latter remains low, this effect is well described by Hamiltonian $H^{\mathrm{B}}_{\mathrm{ISB}}$ as given in Eq. (3.62) and terms like (3.74) can be neglected. Hamiltonian H^{B} is, thus, adapted to descibe optical injection of polaritons. In the case of electrical pumping, population in the dark modes can become significant and contributions like (3.74) should be added to the Hamiltonian.

3.3.2 Numerical results

We now provide the numerical values of the coefficients of the effective bosonic Hamiltonian H^{B}, highlighting the dependence over the main parameters.

Intersubband excitation energy

We start by evaluating the difference between Hamiltonian $\tilde{H}^{\mathrm{B}}$ of chapter 2 and the quadratic part of H^{B}. Remember that in Hamiltonian $\tilde{H}^{\mathrm{B}}$, the energy $\hbar\tilde{\omega}_{12}$ is not renormalized by the Coulomb correction $\gamma_{0,0}$ and that coefficient ζ is missing in the antiresonant terms. Since the quadratic light-matter coupling is the same in both Hamiltonians, we focus only on the matter part of the system. Performing a Bogoliubov transformation on the first line of Eq. (3.62), we obtain the renormalized energy of the intersubband excitation (plasmon),

$$E_{\mathrm{ISBT}} = \sqrt{\left(\hbar\tilde{\omega}_{12} + \frac{\hbar{\omega_{\mathrm{P}}}^2}{2\tilde{\omega}_{12}}\right)^2 - \left(\frac{\hbar{\omega_{\mathrm{P}}}^2}{2\tilde{\omega}_{12}}(1-\zeta)\right)^2}. \tag{3.76}$$

In Fig. (3.11) we plot the dispersion of the intersubband transition energy considering a GaAs quantum well of length $L_{\mathrm{QW}} = 11$ nm (left panel) and $L_{\mathrm{QW}} = 39$ nm (right panel), corresponding to bare transitions $\hbar\omega_{12}$ of 140 meV [14, 41] and 15 meV [51] respectively. The solid line depicts the intersubband transition energy calculated from Hamiltonian H^{B}. The dashed line represents the same quantity obtained from Hamiltonian $\tilde{H}^{\mathrm{B}}$, *i.e.*, with $\zeta = 0$ and no renormalization of the energy $\hbar\tilde{\omega}_{12}$ by $\gamma_{0,0}$. Notice that the renormalized intersubband energy E_{ISBT} converges to the bare transition energy $\hbar\omega_{12}$ for vanishing doping.

As expected, there is no significant difference between the two results. The behavior is qualitatively the same and the maximum relative difference between the two curves is of the order of 3%. Since Hamiltonian $\tilde{H}^{\mathrm{B}}$ is already known to give correct results in the linear regime, this confirms the validity of the quadratic part of Hamiltonian H^{B} and of our method, at least in the one-excitation subspace.

Interaction energy between intersubband excitations

We now consider the quartic part of Hamiltonian $H^{\mathrm{B}}_{\mathrm{ISB}}$. More precisely, we consider the interaction energy per particle $N_{\mathrm{exc}}/n_{\mathrm{QW}}N_{\mathrm{el}} \times U_{\mathbf{q},\mathbf{q}',\mathbf{p}}/n_{\mathrm{QW}}N_{\mathrm{el}}$ for the matter part or $N_{\mathrm{exc}}/n_{\mathrm{QW}}N_{\mathrm{el}} \times G_{\mathbf{q},\mathbf{q}',\mathbf{p}}/n_{\mathrm{QW}}N_{\mathrm{el}}$ for the light-matter part. We will show in the next section that this is, indeed, the relevant quantity when dealing with nonlinear processes.

In Fig. 3.12, we plot the energy $U_{\mathbf{q},\mathbf{q}',\mathbf{p}}$ (thick solid line) for a mid-infrared transition (left panel) and a THz transition (right panel). The other lines depict the individual contributions of the three terms in Eq. (3.68) (see caption for details). For the considered realistic parameters, the interaction energy grows with increasing

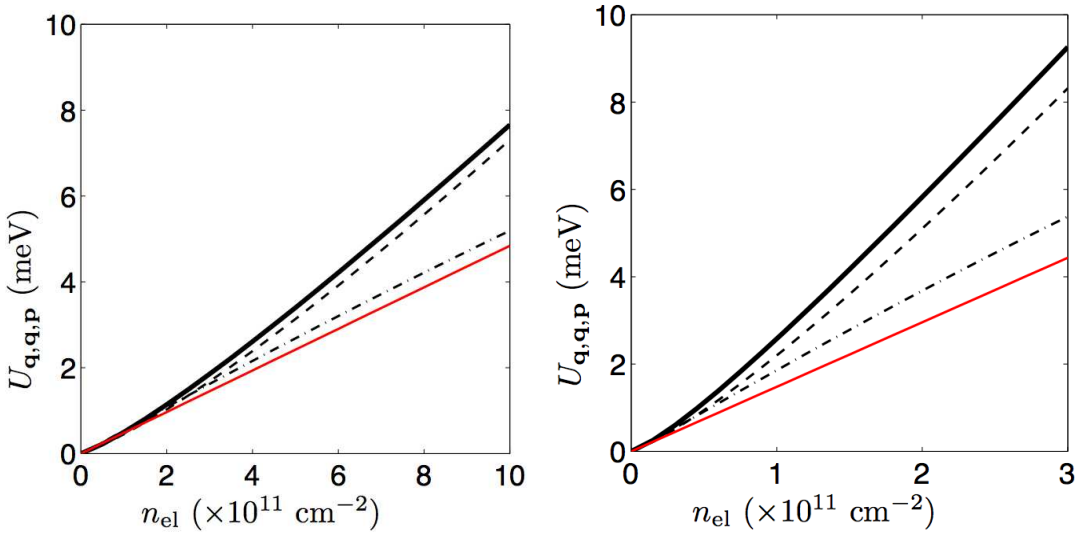

Figure 3.12: Thick solid line: Effective interaction energy $U_{\mathbf{q},\mathbf{q}',\mathbf{p}}$ between intersubband excitations including all the contributions in Eq. (3.68) for $\hbar\omega_{12} = 140$ meV (figure (a)) and $\hbar\omega_{12} = 15$ meV (figure (b)) as a function of the electron density in the wells. Dashed-line: First term in Eq. (3.68) corresponding to the intersubband Coulomb interaction. Thin red line: Absolute value of the second term in Eq. (3.68), namely the direct Coulomb interaction. Note that this term is negative, thus producing a red-shifted contribution. Dash-dotted line: Third term in Eq. (3.68), due to the exchange Coulomb interaction.

electron doping density almost linearly in both cases. Notice that, contrary to excitons [21, 92], the direct scattering contributes, so intersubband excitations are subject to dipole-dipole interactions. As explained in section 3.1, this is due to the fact that electron-electron and hole-hole interactions are screened differently by the Fermi sea [82].

For a doping density in the range of a few 10^{11} cm^{-2}, coefficient $U_{\mathbf{q},\mathbf{q}',\mathbf{p}}$ is of the order of few meV both for the cases of THz and mid-infrared transitions. Coefficient $G_{\mathbf{q},\mathbf{q}',\mathbf{p}}$, despite a different dependence over the electron density, is of the same order of magnitude. The interaction energy per particle can, thus, reach values close to the meV when the density of excitations in the system becomes significant. This is rather promising, since as shown in the case of exciton-polaritons [29, 98, 24], very interesting nonlinear polariton physics occurs when the interaction energy becomes comparable to the linewidth of the polariton modes. For THz polaritons, state-of-the-art samples [51] exhibits polariton linewidth as low as 1 meV.

3.4 Testing the quartic part of the Hamiltonian

We have seen that our method allows us to find the correct quadratic effective Hamiltonian. In this section, we now check on some examples that the quartic part is correct too. We also show that Hamiltonian H^{B} correctly describes the system when more than two excitations are present. Physical quantities can, indeed, be expressed as a perturbation series in the density of excitations $N_{\mathrm{exc}}/n_{\mathrm{QW}}N_{\mathrm{el}}$ whose leading terms come from the one- and two-body interactions. More precisely, the contribution of the two-body interactions is proportional to the interaction energy per particle defined in the previous section. As long as higher order terms in the perturbation series are not required, *i.e.*, if $N_{\mathrm{exc}}/n_{\mathrm{QW}}N_{\mathrm{el}}$ is small enough, we do not need to include n-body terms ($n > 2$). Therefore, we do not need to compute n-excitation matrix elements.

3.4.1 Saturation of the light-matter coupling

We focus here on the Rabi frequency, but similar calculation can be performed to study the saturation of the depolarization shift. We consider the absorption of a photon by the system while N_{exc} bright intersubband excitations are already present in a single mode, with $N_{\mathrm{exc}} > 2$. We make the calculation both with the fermionic and effective bosonic Hamiltonians.

In this particular case, the calculation in the fermionic framework yields an exact result. The unnormalized matrix element is

$$\langle F|\, b_{0,\mathbf{q}}^{N_{\rm exc}+1}\, H\, b_{0,\mathbf{q}}^{\dagger\, N_{\rm exc}} a_{\mathbf{q}}^{\dagger}\,|F\rangle = \hbar\Omega_q\,(N_{\rm exc}+1)!\,\mathcal{F}_{N_{\rm exc}+1}, \tag{3.77}$$

where $\mathcal{F}_{N_{\rm exc}+1}$ was defined in Eq. (3.36) and, thanks to the recursive relation (3.38), we finally obtain

$$\frac{\langle F|\, b_{0,\mathbf{q}}^{N_{\rm exc}+1}\, H\, b_{0,\mathbf{q}}^{\dagger\, N_{\rm exc}} a_{\mathbf{q}}^{\dagger}\,|F\rangle}{\sqrt{(N_{\rm exc}+1)!N_{\rm exc}!\mathcal{F}_{N_{\rm exc}+1}\mathcal{F}_{N_{\rm exc}}}} = \hbar\Omega_q\,\sqrt{N_{\rm exc}+1}\,\sqrt{1-\frac{N_{\rm exc}}{n_{\rm QW}N_{\rm el}}}. \tag{3.78}$$

With the bosonic Hamiltonian, the normalized matrix element is

$$\frac{\langle G|\, B_{\mathbf{q}}^{N_{\rm exc}+1}\, H^{\rm B}\, B_{\mathbf{q}}^{\dagger\, N_{\rm exc}} a_{\mathbf{q}}^{\dagger}\,|G\rangle}{\sqrt{(N_{\rm exc}+1)!N_{\rm exc}!}} = \hbar\Omega_q\,\sqrt{N_{\rm exc}+1}\left(1-\frac{N_{\rm exc}}{2n_{\rm QW}N_{\rm el}}\right). \tag{3.79}$$

Developing Eq. (3.78) to first order in density of excitations, we can check that results are identical. This shows that there is no need to include additional effective n-body interactions, with $n \in [3, N_{\rm exc}]$, in the bosonic Hamiltonian to correctly describe the system in the low density limit. In this limit, all the information we need is encoded in the effective one- and two-body interactions. Notice that two-body contribution is, as expected, proportional to the interaction energy per particle $N_{\rm exc}/n_{\rm QW}N_{\rm el} \times G_{\mathbf{q},\mathbf{q}',\mathbf{p}}$.

Equations (3.78) and (3.79) show a saturation of the light-matter coupling when the number of intersubband excitations increases. This is responsible for the polariton bleaching, which was observed recently [42]. In the bosonic picture, this saturation is due to the effective two-body light-matter interaction. In the fermionic picture, it is due to the depletion of the Fermi sea and Pauly blocking in the excited subband. When the number of intersubband excitations increases, the number of available electrons in the Fermi sea decreases. The collective effects, like the Rabi frequency and the depolarization shift, are then altered.

Notice, however, that the saturation does not behave as expected [42], *i.e.*, as the square root of the population difference between the two electronic subbands. Indeed, to first order in the density of excitations, the saturation should behave as $1 - N_{\rm exc}/n_{\rm QW}N_{\rm el}$ instead of $1 - N_{\rm exc}/2n_{\rm QW}N_{\rm el}$. As pointed out in section 3.3, this problem is due to discontinuity of the coefficient $G_{\mathbf{q},\mathbf{q}',\mathbf{p}}$ and disappears if we consider a situation where the $N_{\rm exc}$ excitations are spread over a large number n of

modes,

$$\frac{\langle G|\, B_{\mathbf{q}^{(n)}}^{N_n} \cdots B_{\mathbf{q}'}^{N_2} B_{\mathbf{q}}^{N_1+1}\; H^{\mathrm{B}}\; B_{\mathbf{q}}^{\dagger\, N_1} B_{\mathbf{q}'}^{\dagger\, N_2} \cdots B_{\mathbf{q}^{(n)}}^{\dagger\, N_n}\, a_{\mathbf{q}}^{\dagger}\, |G\rangle}{\sqrt{(N_1+1)}\, N_1! \cdots N_n!}$$
$$= \hbar\Omega_q \sqrt{N_1+1} \left(1 - \frac{N_1 + 2N_2 + \cdots + 2N_n}{2n_{\mathrm{QW}} N_{\mathrm{el}}}\right)$$
$$\approx \hbar\Omega_q \sqrt{N_1+1} \left(1 - \frac{N_{\mathrm{exc}}}{n_{\mathrm{QW}} N_{\mathrm{el}}}\right), \quad (3.80)$$

where $N_1 + N_2 + \cdots + N_n = N_{\mathrm{exc}}$. Of course, the same result is obtained with the fermionic Hamiltonian H using a generalization of Eq. (3.41).

3.4.2 Transition probabilities, Fermi Golden Rule

We now calculate the transition probabilities for processes involving pairs of inter-subband excitations using both the effective bosonic Hamiltonian approach and the fermionic formalism. We show, again, that the two approaches yield the same result to the lowest order in the density of excitations $N_{\mathrm{exc}}/n_{\mathrm{QW}}N_{\mathrm{el}}$. However, we do not obtain the same result for the Fermi Golden Rule, due to the overcompleteness of the many-excitation states. This discrepancy was pointed out [106] and can be effectively corrected by dividing the density of states in the bosonic framework by two.

Fermionic case

In this section, we use the commutator formalism and a first-order time-dependent perturbation theory to calculate the transition probability between an initial state $|\psi_i\rangle$ and a final state $|\psi_f\rangle$. The lifetime of the former is then calculated thanks to the Fermi golden rule as in Ref. [96]. Here, the two-body interactions are the perturbations. The calculations are detailed in appendix C.

The particular event we want to describe is the scattering of an initial pump beam of arbitrary intensity into a signal and an idler mode. We will, thus, consider initial and final states, respectively, to be

$$|\psi_i\rangle \;\propto\; b_{0,\mathbf{q}}^{\dagger\, N_{\mathrm{exc}}}\, |F\rangle\,, \quad (3.81)$$
$$|\psi_f\rangle \;\propto\; b_{0,\mathbf{q}+\mathbf{p}}^{\dagger}\, b_{0,\mathbf{q}-\mathbf{p}}^{\dagger}\, b_{0,\mathbf{q}}^{\dagger\, Nx-2}\, |F\rangle\,. \quad (3.82)$$

The transition probability is [96]

$$P_{\mathbf{p},\mathrm{fer}}(t) = \left|\langle\psi_f|\tilde{\psi}_t\rangle\right|^2, \tag{3.83}$$

where

$$\left|\tilde{\psi}_t\right\rangle = F_t(H - \langle\psi_i|\, H\,|\psi_i\rangle)\, P_\perp H\,|\psi_i\rangle\,. \tag{3.84}$$

As in section 3.2, $P_\perp$ is the projector over the subspace orthogonal to $|\psi_i\rangle$, and F_t verifies

$$|F_t(E)|^2 = \frac{2\pi t}{\hbar}\delta_t(E), \tag{3.85}$$

where δ_t converges to the Dirac delta function for long times. Taking into account the normalization, we obtain the transition probability from the initial to the final state

$$P_{\mathbf{p},\mathrm{fer}}(t) = \frac{2\pi t}{\hbar}\,\frac{N_{\mathrm{exc}}(N_{\mathrm{exc}}-1)}{n_{\mathrm{QW}}^2 N_{\mathrm{el}}^2}\,|U_{\mathbf{q},\mathbf{q},\mathbf{p}}|^2\,\delta_t(\Delta E_{\mathbf{p}}) + O\left(\left[\frac{N_{\mathrm{exc}}}{n_{\mathrm{QW}}N_{\mathrm{el}}}\right]^4\right), \tag{3.86}$$

where $\Delta E_{\mathbf{p}}$ is the energy difference between the initial and final states. In Eq. (3.86), it can be clearly seen that the strength of nonlinear processes is related to the interaction energy per particle $N_{\mathrm{exc}}/n_{\mathrm{QW}}N_{\mathrm{el}} \times U_{\mathbf{q},\mathbf{q},\mathbf{p}}$.

Because of the overcompleteness of the two-excitation states, we cannot directly use the matrix elements and the Fermi Golden Rule to obtain the lifetime of the initial state. With the same notations as in the previous paragraph, it is given by [96]

$$\frac{1}{T} \;=\; \frac{1}{2}\sum_{\mathbf{p}} \lim_{t\to+\infty} \frac{P_{\mathbf{p},\mathrm{fer}}(t)}{t}, \tag{3.87}$$

where it is implicitly assumed that the summation is restricted to small wavevectors. This result is very similar to the usual Fermi golden rule despite the presence of the counterintuitive 1/2 factor. This coefficient comes from the overcompleteness of the composite boson basis.

Bosonic case

In this paragraph we calculate the same quantities as in the previous one using Hamiltonian H^{B}. In this case we can use a traditional Fermi golden rule.

We start with the transition probability between two states. In this case the

initial and final states are

$$\begin{aligned} |\psi_i\rangle &\propto B_{\mathbf{q}}^{\dagger\, N_{\rm exc}} |G\rangle\,, \\ |\psi_f\rangle &\propto B_{\mathbf{q}+\mathbf{p}}^{\dagger} B_{\mathbf{q}-\mathbf{p}}^{\dagger} B_{\mathbf{q}}^{\dagger\, N_{\rm exc}-2} |G\rangle\,. \end{aligned} \tag{3.88}$$

The transition probability is, thus, given by

$$P_{\mathbf{p},\rm bos}(t) = \frac{2\pi t}{\hbar} \frac{N_{\rm exc}(N_{\rm exc}-1)}{n_{\rm QW}^2 N_{\rm el}^2} \left|U_{\mathbf{q},\mathbf{q},\mathbf{p}}\right|^2 \delta_t(\Delta E_{\mathbf{p}}). \tag{3.89}$$

A comparison with Eq. (3.86) shows that $P_{\mathbf{p},\rm fer}(t) = P_{\mathbf{p},\rm bos}(t)$ up to third order in $N_{\rm exc}/(n_{\rm QW}N_{\rm el})$. The two approaches are therefore equivalent as long as we calculate probabilities of transition in the first-order time-dependent perturbation theory.

We now compute the lifetime of the initial state using the Fermi golden rule

$$\frac{1}{T} = \sum_{\mathbf{p}} \lim_{t\to+\infty} \frac{P_{\mathbf{p},\rm bos}(t)}{t}, \tag{3.90}$$

where the summation is again restricted to small wavevectors. A comparison with Eq. (C.17) shows that this method underestimates the true lifetime by a factor two. This is coherent with the results in Ref. [96], which show how an effective Hamiltonian giving the correct transition probabilities needs to take into account an *ad hoc* factor 1/2 when calculating lifetimes, due to the overcompleteness of the composite boson basis. This is, of course, simply implies a renormalization of the composite boson density of states and can be corrected easily when one wants to use the bosonic approach.

3.4.3 General argument

We now give an argument to generalize the above observation: all many-excitation matrix elements can be developped as a perturbation series in the densities of excitations. The dominant terms of this development come from the one- and two-body interactions, giving contributions of zero-th and first order, respectively.

To see this, recall from section 3.2 that effective n-body interactions scale like $(n_{\rm QW}N_{\rm el})^{1-n}$. Moreover, there are $N_{\rm exc}(N_{\rm exc}-1)\dots(N_{\rm exc}-n+1)/n! \approx N_{\rm exc}^n/n!$ ways of associating $N_{\rm exc}$ excitations through a n-body interaction. The n-body interactions contribution to the $N_{\rm exc}$-excitation matrix elements, thus, scale like $N_{\rm exc}\,(N_{\rm exc}/n_{\rm QW}N_{\rm el})^{n-1}$. Dominant terms, indeed correspond to n equals to one and

two, *i.e.*, to one- and two-body interactions.

Matrix elements, and thus all relevant quantities, obtained from the bosonic Hamiltonian H^{B} are then first order approximations of the exact matrix elements.

3.5 Polariton Hamiltonian

In this section, we consider the interactions in the polariton basis. For simplicity, we neglect antiresonant terms. A Bogoliubov transformation of the quadratic parts of H and H^{B} gives the expression of the polaritonic operators (see Eq. (1.12)),

$$\begin{pmatrix} p_{\mathrm{U}\,\mathbf{q}} \\ p_{\mathrm{L}\,\mathbf{q}} \end{pmatrix} = \begin{pmatrix} w_{\mathrm{U},q} & x_{\mathrm{U},q} \\ w_{\mathrm{L},q} & x_{\mathrm{L},q} \end{pmatrix} \begin{pmatrix} a_{\mathbf{q}} \\ B_{\mathbf{q}} \end{pmatrix}, \tag{3.91}$$

where $p_{\mathrm{U}\,\mathbf{q}}$ and $p_{\mathrm{L}\,\mathbf{q}}$ are polaritonic operators of the upper and lower branch, respectively. Hopfield coefficients $w_{j,q}$ and $x_{j,q}$ are given in Eq. (1.13) where $\omega_{\mathrm{cav},q}$ and ω_{12} have to replaced by $\omega_{\mathrm{cav},q} + 2{\Omega_q}^2/\tilde{\omega}_{12}$ and $\tilde{\omega}_{12} + {\omega_{\mathrm{P}}}^2/2\tilde{\omega}_{12}$, respectively.

We can now use the reverse transformation to express the bosonic Hamiltonian in the polaritonic basis,

$$\begin{pmatrix} a_{\mathbf{q}} \\ B_{\mathbf{q}} \end{pmatrix} = \begin{pmatrix} w_{\mathrm{U},q} & w_{\mathrm{L},q} \\ x_{\mathrm{U},q} & x_{\mathrm{L},q} \end{pmatrix} \begin{pmatrix} p_{\mathrm{U}\,\mathbf{q}} \\ p_{\mathrm{L}\,\mathbf{q}} \end{pmatrix}. \tag{3.92}$$

Because of the quartic terms in Hamiltonian H_B, polaritons interact with each other through their matter part and can scatter. The polaritonic Hamiltonian, thus, has a quartic part too,

$$H^{\mathrm{B}} = \sum_{j,\mathbf{q}} \hbar\omega_{j,q}\, p^\dagger_{j\,\mathbf{q}} p_{j\,\mathbf{q}} + \frac{1}{2}\frac{1}{n_{\mathrm{QW}} N_{\mathrm{el}}} \sum_{\substack{i,j,k,\ell \\ \mathbf{q},\mathbf{q}',\mathbf{p}}} V^{ijk\ell}_{\mathbf{q},\mathbf{q}',\mathbf{p}}\, p^\dagger_{i\,\mathbf{q}+\mathbf{p}} p^\dagger_{j\,\mathbf{q}'-\mathbf{p}} p_{k\,\mathbf{q}'} p_{\ell\,\mathbf{q}}, \tag{3.93}$$

where indices i, j, k and ℓ belong to {L,P}. In the following, we will focus on the lower branch. The two-body interaction between lower polaritons is then

$$H_{\text{LP-LP}} = \frac{1}{2}\frac{1}{n_{\mathrm{QW}} N_{\mathrm{el}}} \sum_{\mathbf{q},\mathbf{q}',\mathbf{p}} V_{\mathbf{q},\mathbf{q}',\mathbf{p}}\, p^\dagger_{\mathrm{L}\,\mathbf{q}+\mathbf{p}} p^\dagger_{\mathrm{L}\,\mathbf{q}'-\mathbf{p}} p_{\mathrm{L}\,\mathbf{q}'} p_{\mathrm{L}\,\mathbf{q}}, \tag{3.94}$$

where we have omitted the superscripts for clarity. Using Eq. (3.92), the effective

interaction energy between lower polaritons is

$$V_{\mathbf{q},\mathbf{q}',\mathbf{p}} = x_{\mathrm{L},|\mathbf{q}'-\mathbf{p}|}x_{\mathrm{L},q'} \times \left(2\left(x_{\mathrm{L},|\mathbf{q}+\mathbf{p}|}|w_{\mathrm{L},q}| + |w_{\mathrm{L},|\mathbf{q}+\mathbf{p}|}|x_{\mathrm{L},q}\right) G_{\mathbf{q},\mathbf{q}',\mathbf{p}} - x_{\mathrm{L},|\mathbf{q}+\mathbf{p}|}x_{\mathrm{L},q}\, U_{\mathbf{q},\mathbf{q}',\mathbf{p}}\right). \quad (3.95)$$

Notice that, contrary to the case of exciton polaritons [29, 24], the different two-body interactions give opposite contributions. Moreover they are of the same order of magnitude. Therefore, by modifying the shape of the wells, the cavity and tuning the electron density, it is *a priori* possible to change the sign of polariton-polariton interaction energy, or even to turn it off.

As an example, we now consider the case where the lower branch is pumped at a wavevector $\mathbf{q}_\mathrm{p}$ so that the system is in the state $p^{\dagger\, N_\mathrm{exc}}_{\mathrm{L}\,\mathbf{q}_\mathrm{p}}|G\rangle/\sqrt{N_\mathrm{exc}!}$. This Hamiltonian allows us to describe single-mode (Kerr) and multimode (parametric) coherent nonlinearities [29, 24]. Notice that a detailed treatment of these effects requires to describe the coupling to the environment and to the external pump, for example through quantum Langevin equations. Here we just calculate the relevant matrix elements. For the parametric case, one has to consider the following interaction interaction channel

$$p^{\dagger\, N_\mathrm{exc}}_{\mathrm{L}\,\mathbf{q}_\mathrm{p}}|G\rangle \quad \rightarrow \quad p^\dagger_{\mathrm{L}\,\mathbf{q}_\mathrm{p}+\mathbf{p}}p^\dagger_{\mathrm{L}\,\mathbf{q}_\mathrm{p}-\mathbf{p}}p^{\dagger\, N_\mathrm{exc}-2}_{\mathrm{L}\,\mathbf{q}_\mathrm{p}}|G\rangle\,. \quad (3.96)$$

Pairs of polaritons scatter from the pumped mode into signal-idler pairs. As for the case of exciton-polaritons we expect that the maximum efficiency of this parametric processes is achieved when the energy conservation condition is fulfilled [107]. A mean-field approach of the problem[24, 29] shows that the matrix element between the initial and the final states is the relevant quantity to consider and has to be compared with the lifetime of the excitations. For high pump intensity, *i.e.*, $N_\mathrm{exc} \gg 1$ this matrix element is

$$M_{\mathbf{q}_\mathrm{p},\mathbf{p}} = \frac{N_\mathrm{exc}}{n_\mathrm{QW}N_\mathrm{el}}V_{\mathbf{q}_\mathrm{p},\mathbf{q}_\mathrm{p},\mathbf{p}}. \quad (3.97)$$

As discussed in section 3.3 and shown in figure 3.12, polaritons nonlinear interaction energies of the order of a the meV (thus comparable to THz polariton linewidths) can be achieved in the THz range. This results paves the way to a very interesting coherent nonlinear physics for this kind of composite excitations.

Conclusion

Intersubband polaritons are excitations in microcavity embedded doped quantum wells. They result from the strong coupling between a collective excitation of the Fermi sea (a linear superposition of electron-hole pairs) and the cavity field. In the diluted regime, *i.e.*, when the number of excitations is much lower than the number of electrons in the Fermi sea, they obey an approximate bosonic statistics. Therefore, it is possible to describe intersubband polaritons thanks to an effective bosonic Hamiltonian. Up to now, only quadratic Hamiltonians have been used, from which correct results and prediction were obtained. The reason for this success is that, so far, the number of excitations in experiments remained low (in the sense given above). In this limit, the physics of intersubband polaritons is dominated by one-body interactions, which can be reproduced by a bosonic quadratic Hamiltonian. However, when the number of excitations increases, two-body interactions become significant and polaritons are less and less bosonic. A quadratic Hamiltonian cannot reproduce these effects. Therefore, in this work, we presented a mathematically rigorous method to derive an effective bosonic Hamiltonian with quartic contributions. These terms correspond to an effective polariton-polariton interaction encoding both the screened Coulomb processes and the nonbosonicity.

In chapter 1, we gave an overview of the physics of intersubband polaritons in the low density regime. In chapter 2, we presented different Hamiltonian models describing intersubband polaritons. In particular, we explained why these excitations can be considered as bosons in this limit and we showed, based on simple physical arguments, how it is possible to derive an effective bosonic quadratic Hamiltonian. This Hamiltonian is capable of reproducing all experimental results obtained so far. However, it is limited to the low density regime where the physics is linear. In chapter 3, using a microscopic composite boson commutator approach, we derived the polariton-polariton interactions. We were then able to determine a new bosonic Hamiltonian encoding this two-body interaction in quartic terms. Relevant physical quantities can then be expressed as a perturbation series in the Coulomb interaction

and the non-bosonicity. In our case, this development is truncated to the first leading order, but it can be pushed further if necessary. To this end, we explained how our method can be extented to include higher order contributions in the effective Hamiltonian corresponding to effective n-body interactions ($n > 2$). Using realistic set of parameters, we determined the strength of the interactions between intersubband polaritons and we found that significant polariton-polariton interactions occur, especially for transitions in the THz range.

This work paves the way to promising future studies of nonlinear quantum optics in semiconductor intersubband systems such as quantum cascade devices. Using our quartic effective Hamiltonian and previous work on exciton polaritons, one should be able to predict and design new nonlinear devices operating in the mid infrared to THz range. Moreover, our approach is not limited to intersubband polaritons and can extended to any system whose excitations result from the strong coupling between pairs of fermions and a bosonic field. For example, it could be applied to the recently discovered magnetopolaritons, obtained by strongly coupling a cavity mode to the cyclotron transition of a two-dimensional electron gas under magnetic field [108, 109, 110]. Like intersubband polaritons, these excitations were modeled by a quadratic effective bosonic Hamiltonian and only the low density regime has been explored so far. By applying our method to magnetopolaritons, it should be possible to take into account the polariton-polariton interaction, so that the nonlinear regime could be explored too.

Moreover, in the case of graphene, it has been shown that the system should undergo a quantum phase transition similar to the one occuring in the Dicke model when varying the electron density [110, 111]. It is then legitimate to ask how this phase transition is modified in presence of polariton-polariton interactions.

Appendix A

Details about the formalism

In this appendix, we give the explicit notations for Hamiltonian H and intersubband excitation operators with quantum well and spin indexes. Electronic wavefunctions are localized in quantum wells and we neglect electronic tunneling from one well to another. We thus neglect Coulomb interaction between electrons in different wells, which are sufficiently apart. Hamiltonian H and bright intersubband excitations can then be written with all indexes,

$$\begin{aligned} H_{\text{Elec}} &= \sum_{j=1}^{n_{\text{QW}}} \sum_{\mathbf{k},\sigma,\mu} \hbar\omega_{\mu,k}\, c^{(j)\,\dagger}_{\mu,\mathbf{k},\sigma}\, c^{(j)}_{\mu,\mathbf{k},\sigma} \\ H_{\text{I1}} &= \sum_{j=1}^{n_{\text{QW}}} \sum_{\mathbf{k},\mathbf{q},\sigma} \hbar\chi_q \left(c^{(j)\,\dagger}_{2,\mathbf{k}+\mathbf{q},\sigma}\, c^{(j)}_{1,\mathbf{k},\sigma} + c^{(j)\,\dagger}_{1,\mathbf{k}+\mathbf{q},\sigma}\, c^{(j)}_{2,\mathbf{k},\sigma}\right)\left(a_{\mathbf{q}} + a^{\dagger}_{-\mathbf{q}}\right) \\ H_{\text{Coul}} &= \frac{1}{2}\sum_{j=1}^{n_{\text{QW}}} \sum_{\substack{\mathbf{k},\mathbf{k}',\mathbf{q},\sigma,\sigma' \\ \mu,\mu',\nu,\nu'}} V_q^{\mu\nu\nu'\mu'}\, c^{(j)\,\dagger}_{\mu,\mathbf{k}+\mathbf{q},\sigma}\, c^{(j)\,\dagger}_{\nu,\mathbf{k}'-\mathbf{q},\sigma'}\, c^{(j)}_{\nu',\mathbf{k}',\sigma'}\, c^{(j)}_{\mu',\mathbf{k},\sigma}, \end{aligned} \tag{A.1}$$

and,

$$b^{\dagger}_{0,\mathbf{q}} = \frac{1}{\sqrt{n_{\text{QW}} N_{\text{el}}}} \sum_{j=1}^{n_{\text{QW}}} \sum_{\mathbf{k},\sigma} \nu^{*}_{0,j,\mathbf{k}}\, c^{(j)\,\dagger}_{2,\mathbf{k}+\mathbf{q},\sigma}\, c^{(j)}_{1,\mathbf{k},\sigma}, \tag{A.2}$$

where $\nu_{0,j,\mathbf{k}} = \Theta(k_F - k)$ for all j, $\mathbf{k}$ is a wavevector such that $k < k_F$, $\sigma, \sigma' \in \{\downarrow, \uparrow\}$ and $\mu, \mu', \nu, \nu' \in \{1, 2\}$. Bright intersubband excitations are, thus, linear superposition of pairs of fermions with the same spin. We could generalize Eq. (A.2) by allowing the two fermions to have different spins but the resulting collective excitation would be dark and thus not relevant if we consider only polariton.

Appendix B

Second-quantized Hamiltonian

In this appendix, we show details concerning the derivation of the second-quantized Hamiltonian of the system. We focus, here, only on the matter and light-matter part, considering that the free photonic part is already second-quantized.

The Hamiltonian, in Coulomb gauge, describing an ensemble of electrons trapped in the heterostructure potential, interacting with each other and with the electromagnetic field is given by [79]

$$H = H_{\mathrm{Cav}} + \sum_{j=1}^{n_{\mathrm{QW}}N_{\mathrm{el}}} \frac{1}{2m^*}\left(\mathbf{p}_j + e\mathbf{A}(\mathbf{r}_j, z_j)\right)^2 + V_{\mathrm{QW}}(z_j) + H_{\mathrm{Coul}}, \tag{B.1}$$

where the spins indexes have been omitted and e is the absolute value of the electron charge. In this expression, $\mathbf{p}_j$, $(\mathbf{r}_j, z_j)$ and $\mathbf{A}$ are respectively the momentum and position of the j^{th} electron and the transverse vector potential of the electromagnetic field. The first term is the Hamiltonian of the electromagnetic field in the cavity without the electron gas.

$$H_{\mathrm{Cav}} = \sum_{\mathbf{q}} \hbar\omega_{\mathrm{cav},q}\left(a^\dagger_{\mathbf{q}}a_{\mathbf{q}} + \frac{1}{2}\right), \tag{B.2}$$

where $a_{\mathbf{q}}$ is annihilation operator for photons satisfying

$$\left[a_{\mathbf{q}}, a^\dagger_{\mathbf{q}'}\right] = \delta_{\mathbf{q},\mathbf{q}'}. \tag{B.3}$$

The second term describes the dynamics of free electrons interacting with the electromagnetic field of the cavity. The third term is the heterostructure potential, confining the electrons in the quantum wells. The fourth term is the Coulomb inter-

action containing not only electron-electron pair interaction terms but also electron-ion and ion-ion terms. Contrary to the electromagnetic field, ions of the lattice are treated as an external potential and there is no degree of freedom associated to them. We consider here the three-dimensional Coulomb potential, decreasing as $1/r$. The reason is that, even if the quantum well is a quasi two-dimensional structure, the electric field lines are present in both the wells and the barriers. The Coulomb Hamiltonian thus describes the dynamics of a quasi two-dimensional electron gas subject to three-dimensional Coulomb interactions. Notice that Eq. (B.1) is already a simplification of a more general Hamiltonian. Indeed, electromagnetic field has been truncated to its lowest TM mode as explained in the first chapter and spin interactions have been omitted [79].

Terms of the Hamiltonian can be grouped in a different way

$$H = H_{\mathrm{Cav}} + H_{\mathrm{Elec}} + H_{\mathrm{I1}} + H_{\mathrm{I2}} + H_{\mathrm{coul}}, \tag{B.4}$$

where H_{Cav} was given above and

$$\begin{aligned} H_{\mathrm{Elec}} &= \sum_j \frac{{\mathbf{p}_j}^2}{2m^*} + V_{\mathrm{QW}}(z_j), \\ H_{\mathrm{I1}} &= \sum_j \frac{e}{m^*}\mathbf{p}_j.\mathbf{A}(\mathbf{r}_j, z_j), \\ H_{\mathrm{I2}} &= \sum_j \frac{e^2}{2m^*}\mathbf{A}(\mathbf{r}_j, z_j)^2, \\ H_{\mathrm{Coul}} &= \sum_{i\neq j} \frac{q_i q_j}{8\pi\epsilon_0\epsilon_r} \frac{1}{\sqrt{(\mathbf{r}_i - \mathbf{r}_j)^2 + (z_i - z_j)^2}}. \end{aligned} \tag{B.5}$$

In the Coulomb Hamiltonian, $q_{i,j}$ are particle charges, $-e$ for electrons and e for ions. For electrons, $\mathbf{r}$ and z are variables whereas for ions they are external parameters. Also, self-interaction terms have been omitted. We will now give the second-quantized versions of these terms.

B.1 Quasi two-dimensional gas of independent electrons

The second term in Eq. (B.4) is the Hamiltonian for the electrons trapped in the potential created by the semiconductor heterostructure without electromagnetic field

and not subject to the Coulomb interaction. Since it is a one-body interaction, its second quantized version is given by [112]

$$H_{\text{Elec}} = \int \mathrm{d}\mathbf{r}\,\mathrm{d}z\,\Psi^{\dagger}(\mathbf{r},z)\left(\frac{\mathbf{p}^2}{2m^*}+V_{\text{QW}}(z)\right)\Psi(\mathbf{r},z). \tag{B.6}$$

Operators Ψ and $\Psi^{\dagger}$ are fermionic field operators

$$\Psi(\mathbf{r},z) = \sum_{n,\mathbf{k}} \psi_{n,\mathbf{k}}(\mathbf{r},z)\,c_{n,\mathbf{k}}, \tag{B.7}$$

where $\psi_{n,\mathbf{k}}(\mathbf{r},z)$ is the one-electron wavefunction given in Eq. (1.1) and $c_{n,\mathbf{k}}$ is the fermionic annihilation operator for mode $(n,\mathbf{k})$. These operators satisfy the fermionic anti-commutation rules,

$$\left\{c_{n,\mathbf{k}}, c^{\dagger}_{n',\mathbf{k}'}\right\} = \delta_{\mathbf{k},\mathbf{k}'}\,\delta_{n,n'}. \tag{B.8}$$

The creation field $\Psi^{\dagger}$ is the Hermitian conjugate. In this basis the Hamiltonian is diagonal, so it takes the simple form

$$H_{\text{Elec}} = \sum_{n,\mathbf{k}}\left(\hbar\omega_n + \frac{\hbar^2k^2}{2m^*}\right)c^{\dagger}_{n,\mathbf{k}}c_{n,\mathbf{k}}, \tag{B.9}$$

which is the kinetic energy operator of quasi two-dimensional electron gas. As mentioned in the first chapter, the sum over n is restricted to the first two subbands for our purpose. In our model, electrons in different wells are not coupled, so operators in Eq. (B.9) create and annihilate electrons in the same well. Here, the index for the well and the sum over this index are implicit.

B.2 Light-matter coupling

In this section we will treat terms coming from the light-matter coupling H_{I1} and H_{I2}. The first one describes absorption or emission of photons by the electron gas. The second one describes scattering of photons on the electron gas, which yields the A^2-term.

B.2.1 Absorption and emission of photons

Here, we will present the calculation in the case of a perfect cavity. Such a cavity supports a TM_0 mode which we will not treat for the reason given in the first chapter. Despite this fact, the physics is the same for more realistic cavities.

The second-quantized expression of the transverse vector potential in the TM mode (other than the TM_0) is [78]

$$\mathbf{A}(\mathbf{r}, z) = \sum_{\mathbf{q}} \sqrt{\frac{\hbar}{\epsilon_0 \epsilon_r S L_{\text{cav}} \omega_{\text{cav},q}}} \left(a_{\mathbf{q}} \mathbf{u}_{\mathbf{q}} + a_{\mathbf{q}}^\dagger \mathbf{u}_{\mathbf{q}}^* \right), \tag{B.10}$$

where the polarization vector $\mathbf{u}_{\mathbf{q}}$ is

$$\mathbf{u}_{\mathbf{q}} = \mathrm{e}^{\mathrm{i}\mathbf{q}\cdot\mathbf{r}} \left(\mathrm{i} \sin(q_z z) \cos(\theta)\, \mathbf{e}_1 + \cos(q_z z) \sin(\theta)\, \mathbf{e}_z \right). \tag{B.11}$$

Vectors $\mathbf{e}_1$ and $\mathbf{e}_z$ are normalized and respectively in the plane of the cavity and parallel to the z axis, q_z is the quantized z component of the photonic wave vector, L_{cav} is the width of the cavity and and ϵ_r is the dielectric constant of the cavity (without the electron gas). The angle θ between the total photonic wave vector and $\mathbf{e}_z$ (figure 1.3a) is related to the in-plane wave vector by the following relation

$$\sin(\theta) = \frac{q}{\sqrt{q^2 + {q_z}^2}}. \tag{B.12}$$

Because the wells are much thinner than the cavity and the potential vector varies smoothly on a scale L_{cav}, it can be considered constant in the wells. To simplify the problem even further, we assume that all the wells are close to the mirrors of the cavity, at $z = 0$ and $z = L_{\text{cav}}$. The dependence over z can then be removed and, in this configuration, the vector potential is parallel to the z axis.

Since the photonic part is already second-quantized, only the electronic part needs to be transformed. Because H_{I1} is also a one-body operator for the electrons, an expression similar to Eq. (B.6) can be used. If we denote p_z and A_z the z components of the impulsion and the vector potential, we obtain

$$H_{\text{I1}} = \int \mathrm{d}\mathbf{r}\, \mathrm{d}z\, \Psi^\dagger(\mathbf{r}, z) \left(\frac{e}{m^*} p_z A_z(\mathbf{r}) \right) \Psi(\mathbf{r}, z), \tag{B.13}$$

which gives

$$H_{\mathrm{I1}} = \sum_{\mathbf{q}} \sqrt{\frac{\hbar e^2 \sin(\theta)^2}{\epsilon_0 \epsilon_r m^{*2} S L_{\mathrm{cav}} \omega_{\mathrm{cav},q}}} \times \sum_{n,n',\mathbf{k},\mathbf{k}'} \frac{1}{S} \int \mathrm{d}\mathbf{r}\, \mathrm{e}^{\mathrm{i}(\mathbf{k}+\mathbf{q}-\mathbf{k}').\mathbf{r}} \int \mathrm{d}z\, \chi_{n'}(z)\, p_z\, \chi_n(z)\; c^\dagger_{n',\mathbf{k}'} c_{n,\mathbf{k}}\, a_{\mathbf{q}} + h.c. \quad \text{(B.14)}$$

The integral over $\mathbf{r}$ yields a delta function $\delta_{\mathbf{k}',\mathbf{k}+\mathbf{q}}$ resulting from the momentum conservation: the photonic wave vector is transfered to a pair of fermions. The integral over z determines the selection rules and the strength of the coupling between the electromagnetic field and the electrons. For symmetric quantum wells, it is non zero only if m and n have a different parity—in this case $(m,n) = (1,2)$ or $(2,1)$—so, the electric field couples electrons from the lowest subband to the first excited one, thus creating or destroying electron-hole pairs.

We said in the first chapter that only the z component of the electric field (vector potential) couples to the intersubband excitations. Previous calculation is, thus, still valid if the vector potential has non-zero components in the plane. Without loss of generality, assume that it has an x component. We obtain a term similar to Eq. (B.14) where p_z is replaced by p_x, which acts on the integral over $\mathbf{r}$. The integral over z reduces to a scalar product between χ_n and χ_m and is non-zero only for $m = n$. This justifies that the in-plane vector potential couples only to intrasubband excitations. Also, when $\theta = 0$, the coupling vanishes. In this configuration the photonic mode "propagates" along the normal to the cavity and the electric field is in the plane of the cavity. Accordingly, it cannot couple to intersubband excitations.

We finally obtain

$$H_{\mathrm{I1}} = \sum_{\mathbf{k},\mathbf{q}} \mathrm{i}\hbar\chi_q \left(a_{\mathbf{q}} + a^\dagger_{-\mathbf{q}}\right)\left(c^\dagger_{2,\mathbf{k}+\mathbf{q}} c_{1,\mathbf{k}} - c^\dagger_{1,\mathbf{k}} c_{2,\mathbf{k}-\mathbf{q}}\right), \quad \text{(B.15)}$$

where

$$\hbar\chi_q = \sqrt{\frac{\hbar e^2 \sin(\theta)^2}{\epsilon_0 \epsilon_r m^{*2} S L_{\mathrm{cav}} \omega_{\mathrm{cav},q}}}\, p_{12}, \quad p_{12} = \int_0^L \mathrm{d}z\, \chi_2(z)\, p_z\, \chi_1(z). \quad \text{(B.16)}$$

For sake of simplicity, we will consider a real light-matter coupling. This is obtained by a simple redefinition of the photonic operators.

B.2.2 Photon scattering and A^2-term

The fourth term in Eq. (B.4) also results from the light-matter coupling. We use the same expression and hypotheses for the vector potential than in the previous section and the derivation is very similar. We obtain

$$H_{\mathrm{I2}} = \sum_{\mathbf{k},\mathbf{q},\mathbf{q}'} \frac{\hbar e^2 \sin(\theta)\sin(\theta')}{2\epsilon_0\epsilon_r m^* S L_{\mathrm{cav}}\sqrt{\omega_{\mathrm{cav},q}\omega_{\mathrm{cav},q'}}} \left(c^\dagger_{1,\mathbf{k}+\mathbf{q}-\mathbf{q}'}c_{1,\mathbf{k}} + c^\dagger_{2,\mathbf{k}+\mathbf{q}-\mathbf{q}'}c_{2,\mathbf{k}}\right) \times \left(a_{-\mathbf{q}'} + a^\dagger_{\mathbf{q}'}\right)\left(a_{\mathbf{q}} + a^\dagger_{-\mathbf{q}}\right). \quad \text{(B.17)}$$

This expression can be simplified by using the light-matter constant $\hbar\chi_q$ previously defined, the energy of the intersubband transition $\hbar\omega_{12}$ and the oscillator strength of the quantum wells intersubband transitions f_{1j}

$$H_{\mathrm{I2}} = \sum_{\mathbf{k},\mathbf{q},\mathbf{q}'} \frac{\sum_j f_{1j}}{f_{12}} \frac{\hbar\chi_q \hbar\chi^*_{q'}}{\hbar\omega_{12}} \left(c^\dagger_{1,\mathbf{k}+\mathbf{q}-\mathbf{q}'}c_{1,\mathbf{k}} + c^\dagger_{2,\mathbf{k}+\mathbf{q}-\mathbf{q}'}c_{2,\mathbf{k}}\right) \times \left(a_{-\mathbf{q}'} + a^\dagger_{\mathbf{q}'}\right)\left(a_{\mathbf{q}} + a^\dagger_{-\mathbf{q}}\right). \quad \text{(B.18)}$$

The oscillator strengths satisfy

$$f_{1j} = \frac{2|p_{1j}|^2}{m_0\hbar\omega_{12}}, \quad \text{and} \quad \sum_j f_{1j} = \frac{m_0}{m^*}, \quad \text{(B.19)}$$

where m_0 is free electron's mass. For an infinite quantum well, $f_{12} = 256/27\pi^2 \times m_0/m^* \approx 0.96\, m_0/m^*$ and for a parabolic quantum well, it is equal to one.

It is now advantageous to perform the electron-hole transformation described in Eq. (2.23),

$$H_{\mathrm{I2}} = \sum_{\mathbf{q}} \frac{\sum_j f_{1j}}{f_{12}} \frac{n_{\mathrm{QW}} N_{\mathrm{el}} |\hbar\chi_q|^2}{\hbar\omega_{12}} \left(a_{-\mathbf{q}} + a^\dagger_{\mathbf{q}}\right)\left(a_{\mathbf{q}} + a^\dagger_{-\mathbf{q}}\right) + \sum_{\mathbf{k},\mathbf{q},\mathbf{q}'} \frac{\sum_j f_{1j}}{f_{12}} \frac{\hbar\chi_q \hbar\chi^*_{q'}}{\hbar\omega_{12}} \left(c^\dagger_{2,\mathbf{k}+\mathbf{q}-\mathbf{q}'}c_{2,\mathbf{k}} - h^\dagger_{-\mathbf{k}-\mathbf{q}-\mathbf{q}'}h_{-\mathbf{k}}\right)\left(a_{-\mathbf{q}'} + a^\dagger_{\mathbf{q}'}\right)\left(a_{\mathbf{q}} + a^\dagger_{-\mathbf{q}}\right). \quad \text{(B.20)}$$

The first term is the A^2-term. The second term is the scattering part of the term H_{I2}. It describes the scattering of photons on the electron gas. Because it involves only electron pairs in the same subband, it cannot induce intersubband transitions.

Electrons scatter in the same subband and absorb the energy and wave vector differences between initial and final photonic states.

B.3 Coulomb interaction

As explained at the beginning of the appendix, the Coulomb interaction has three different contributions: electrons interacting with each other, with the ions of the lattice and ions interacting with each other. Moreover, the lattice is treated as a static distribution of positive charges, which then induces an external potential acting on the electrons. Because we consider a homogeneous medium, it is a homogeneous distribution (jellium model) over the whole volume of each quantum wells.

The second-quantized Hamiltonian for the three dimensional Coulomb interaction is derived in Refs. [81] and [80]. The main point of this calculation is that, to ensure the neutrality of the system, the ion-ion and electron-ion interactions compensate the electron-electron one for $\mathbf{q}_{3D} = 0$. Our starting point is, thus, this three dimensional Coulomb interaction in the jellium model,

$$H_{\text{Coul}} = \frac{1}{2} \sum_{\mathbf{k},\mathbf{k}',\mathbf{q}_{3D}\neq 0} V^{3D}_{q_{3D}}\, c^{\dagger}_{\mathbf{k}+\mathbf{q}_{3D}} c^{\dagger}_{\mathbf{k}'-\mathbf{q}_{3D}} c_{\mathbf{k}'} c_{\mathbf{k}}, \tag{B.21}$$

$$V^{3D}_{q} = \frac{4\pi e^2}{\epsilon_0 \epsilon_r S L q^2}. \tag{B.22}$$

Though correct, these expressions are not convenient because they are expressed in the wrong basis. To express the previous result in the proper basis, we need to calculate the Coulomb interaction between confined electrons. We first perform a one-dimensional Fourier transform along the z direction,

$$\begin{aligned} V_q(z) &= \sum_{\mathbf{q}_z} V^{3D}_{q_3 D}\, \mathrm{e}^{\mathrm{i}q_z z} \\ &= \frac{2e^2}{\epsilon_0 \epsilon_r S} \int \mathrm{d}q_z \frac{\mathrm{e}^{\mathrm{i}q_z z}}{q^2 + {q_z}^2} \\ &= \frac{2\pi e^2}{\epsilon_0 \epsilon_r S q}\, \mathrm{e}^{-qz}, \end{aligned} \tag{B.23}$$

where $\mathbf{q}$ and q_z are the in-plane and z component of the wave vector $\mathbf{q}_{3D}$ and $2\pi e^2/\epsilon_0\epsilon_r S q$ is the Coulomb potential for a true two-dimensional electron gas. We can now compute the matrix elements of the Coulomb interaction in the proper

basis,

$$H_{\text{Coul}} = \frac{1}{2} \sum_{\substack{\mathbf{k},\mathbf{k}',\mathbf{q}\neq 0 \\ \mu,\mu',\nu,\nu'}} V_q^{\mu\nu\nu'\mu'} \, c^\dagger_{\mu,\mathbf{k}+\mathbf{q}} c^\dagger_{\nu,\mathbf{k}'-\mathbf{q}} c_{\nu',\mathbf{k}'} c_{\mu',\mathbf{k}}, \tag{B.24}$$

$$V_q^{\mu\nu\nu'\mu'} = \frac{2\pi e^2}{\epsilon_0 \epsilon_r S q} \, I_q^{\mu\nu\nu'\mu'}, \tag{B.25}$$

where the geometrical factor is

$$I_q^{\mu\nu\nu'\mu'} = \iint \mathrm{d}z_1 \mathrm{d}z_2 \, \chi_\mu(z_2)\chi_\nu(z_1) \, \mathrm{e}^{-q|z_2-z_1|} \, \chi_{\nu'}(z_1)\chi_{\mu'}(z_2). \tag{B.26}$$

We now give the expression of this geometrical factor for an infinite square quantum well. As explained in section 2.1, there are only four relevant coefficients to compute divided into two categories—intrasubband and intersubband—depending on whether electrons are scattered into the same subband or not.

Coefficients for the intrasubband processes are

$$I_p^{\mu\nu\nu\mu} = \frac{32\mu^2\nu^2\pi^4(\mathrm{e}^{-pL} - 1 + pL) + 2(pL)^5 + 8\pi^2(\mu^2+\nu^2)(pL)^3}{(pL^2)\left[(pL)^2 + 4\pi^2\mu^2\right]\left[(pL)^2 + 4\pi^2\nu^2\right]} + \delta_{\mu,\nu} \frac{(pL)^5 + 4\pi^2\mu^2(pL)^3}{(pL^2)\left[(pL)^2 + 4\pi^2\mu^2\right]^2} \, . \tag{B.27}$$

These coefficients tend to one as q tends to zero. Intrasubband Coulomb processes are, thus, divergent in 0 and tend to a true two-dimensional Coulomb interactions. Remember, however, that the divergence is removed by the absence of the term $\mathbf{q} = 0$ in Eq. (B.24).

Coefficient for intersubband processes is

$$I_q^{1212} = 2qL \frac{45\pi^6 - 64\pi^4 qL\left(\mathrm{e}^{-qL}+1\right) + 59\pi^4(qL)^2 + 15\pi^2(qL)^4 + (qL)^6}{\left(9\pi^4 + 10\pi^2(qL)^2 + (qL)^4\right)^2}, \tag{B.28}$$

and the divergence in zero is removed in the long wavelength limit,

$$I_q^{1212} \approx qL \frac{10}{9\pi^2}. \tag{B.29}$$

Appendix C

Calculation with the Fermionic Hamiltonian

In this appendix, we show the details of the calculation of section 3.4. We will need the following relation

$$H\, b_{0,\mathbf{q}}^{\dagger\, N_{\rm exc}} |F\rangle = N_{\rm exc}\, b_{0,\mathbf{q}}^{\dagger\, N_{\rm exc}-1} \left[H, b_{0,\mathbf{q}}^\dagger\right] |F\rangle + \frac{N_{\rm exc}(N_{\rm exc}-1)}{2}\, b_{0,\mathbf{q}}^{\dagger\, N_{\rm exc}-2} \left[\left[H, b_{0,\mathbf{q}}^\dagger\right], b_{0,\mathbf{q}}^\dagger\right] |F\rangle\,. \quad \text{(C.1)}$$

C.1 Transition probabilities

The transition probability between two (properly normalized) states

$$|\psi_i\rangle \propto b_{0,\mathbf{q}}^{\dagger\, N_{\rm exc}} |F\rangle\,, \quad \text{(C.2)}$$

$$|\psi_f\rangle \propto b_{0,\mathbf{q}+\mathbf{p}}^\dagger b_{0,\mathbf{q}-\mathbf{p}}^\dagger b_{0,\mathbf{q}}^{\dagger\, N_{\rm exc}-2} |F\rangle\,, \quad \text{(C.3)}$$

is given by the scalar product between the final state and the time evolved initial state [96, 106]. Because of the overcompleteness of the two-excitations states, we need to use the orthonormalization trick described in section 3.2,

$$P_{\mathbf{p},\rm fer}(t) = \left|\langle\psi_f|\tilde{\psi}_t\rangle\right|^2, \quad \text{(C.4)}$$

where

$$\left|\tilde{\psi}_t\right\rangle = F_t(H - \langle\psi_i|\, H\, |\psi_i\rangle)\, P_\perp H\, |\psi_i\rangle\,. \quad \text{(C.5)}$$

The operator $P_\perp$ is the projector over the subspace orthogonal to $|\psi_i\rangle$, and F_t verifies

$$|F_t(E)|^2 \;=\; \frac{2\pi t}{\hbar}\delta_t(E), \tag{C.6}$$

where δ_t converges to the Dirac delta function for long times. In the following, we will develop Eq. (C.4) to first order in the density of excitations $N_{\rm exc}/n_{\rm QW}N_{\rm el}$.

Using Eqs. (C.1), (3.3) to (3.9), (3.13) and (3.22) to (3.24), we make the fermionic Hamiltonian act on the initial state,

$$\begin{aligned} H\, b_{0,\mathbf{q}}^{\dagger\, N_{\rm exc}}\,|F\rangle = N_{\rm exc}\left(\left(\hbar\tilde{\omega}_{12}+\frac{\hbar{\omega_{\rm P}}^2}{2\tilde{\omega}_{12}}\right) b_{0,\mathbf{q}}^{\dagger\, N_{\rm exc}}\,|F\rangle - \sum_{i\neq 0}\gamma_{0,i}\, b_{i,\mathbf{q}}^\dagger b_{0,\mathbf{q}}^{\dagger\, N_{\rm exc}-1}\,|F\rangle\right) \\ + \frac{N_{\rm exc}(N_{\rm exc}-1)}{2n_{\rm QW}N_{\rm el}}\,\frac{e^2 n_{\rm el}}{2\epsilon_0\epsilon_r}\sum_{m,n,\mathbf{Q}}\frac{\xi_{n,0}^{m,0}(\mathbf{Q})}{Q\epsilon(\mathbf{Q})}\, b_{m,\mathbf{q}+\mathbf{Q}}^\dagger b_{n,\mathbf{q}-\mathbf{Q}}^\dagger b_{0,\mathbf{q}}^{\dagger\, N_{\rm exc}-2}\,|F\rangle \\ - \frac{N_{\rm exc}(N_{\rm exc}-1)}{n_{\rm QW}N_{\rm el}}\sum_{m,\mathbf{Q}} N_{\rm el}V_Q^{1212}\,\lambda_{0,0}^{m,0}(\mathbf{Q}-\mathbf{q})\, b_{0,\mathbf{Q}}^\dagger b_{m,2\mathbf{q}-\mathbf{Q}}^\dagger b_{0,\mathbf{q}}^{\dagger\, N_{\rm exc}-2}\,|F\rangle\,. \end{aligned} \tag{C.7}$$

To project the resulting state on the subspace orthogonal to the initial state, we need the following matrix element,

$$\langle\psi_i|\, H\,|\psi_i\rangle = N_{\rm exc}\left(\hbar\tilde{\omega}_{12}+\frac{\hbar{\omega_{\rm P}}^2}{2\tilde{\omega}_{12}}\right) - \frac{N_{\rm exc}(N_{\rm exc}-1)}{2n_{\rm QW}N_{\rm el}}U_{\mathbf{q},\mathbf{q},\mathbf{0}}, \tag{C.8}$$

where $U_{\mathbf{q},\mathbf{q},\mathbf{0}}$ is given in Eq. (3.57). The projection is then

$$\begin{aligned} P_\perp\, H\, b_{0,\mathbf{q}}^{\dagger\, N_{\rm exc}}\,|F\rangle = -N_{\rm exc}\sum_{i\neq 0}\gamma_{0,i}\, b_{i,\mathbf{q}}^\dagger b_{0,\mathbf{q}}^{\dagger\, N_{\rm exc}-1}\,|F\rangle + \frac{N_{\rm exc}(N_{\rm exc}-1)}{2n_{\rm QW}N_{\rm el}}U_{\mathbf{q},\mathbf{q},\mathbf{0}}\, b_{0,\mathbf{q}}^{\dagger\, N_{\rm exc}}\,|F\rangle \\ + \frac{N_{\rm exc}(N_{\rm exc}-1)}{2n_{\rm QW}N_{\rm el}}\,\frac{e^2 n_{\rm el}}{2\epsilon_0\epsilon_r}\sum_{m,n,\mathbf{Q}}\frac{\xi_{n,0}^{m,0}(\mathbf{Q})}{Q\epsilon(\mathbf{Q})}\, b_{m,\mathbf{q}+\mathbf{Q}}^\dagger b_{n,\mathbf{q}-\mathbf{Q}}^\dagger b_{0,\mathbf{q}}^{\dagger\, N_{\rm exc}-2}\,|F\rangle \\ - \frac{N_{\rm exc}(N_{\rm exc}-1)}{n_{\rm QW}N_{\rm el}}\sum_{m,\mathbf{Q}} N_{\rm el}V_Q^{1212}\,\lambda_{0,0}^{m,0}(\mathbf{Q}-\mathbf{q})\, b_{0,\mathbf{Q}}^\dagger b_{m,2\mathbf{q}-\mathbf{Q}}^\dagger b_{0,\mathbf{q}}^{\dagger\, N_{\rm exc}-2}\,|F\rangle\,. \end{aligned} \tag{C.9}$$

The first term in the first line comes from the coupling to the dark intersubband excitations. Because this process is non resonant, we neglect it as explained in section 3.3. The second term will give a second order contribution in $N_{\rm exc}/n_{\rm QW}N_{\rm el}$ so we neglect it too. Remaining terms are all of first order in the density of excitations.

We now apply F_t to the final state. Because the previous projection is already of first-order in the perturbation parameter, we can consider only its zero-th order

contribution, *i.e*, we do as if intersubband excitations were exact eigenstates of H. We obtain

$$\langle F|\, b_{0,\mathbf{q}}^{N_{\rm exc}-2} b_{0,\mathbf{q}-\mathbf{p}} b_{0,\mathbf{q}+\mathbf{p}}\, F_t(H - \langle\psi_i|\, H\, |\psi_i\rangle) \approx F_t(\Delta E_{\mathbf{p}})\ \langle F|\, b_{0,\mathbf{q}}^{N_{\rm exc}-2} b_{0,\mathbf{q}-\mathbf{p}} b_{0,\mathbf{q}+\mathbf{p}}, \tag{C.10}$$

where $\Delta E_{\mathbf{p}}$ is the energy difference between the initial and final states. Taking into account the normalization, which brings an additional factor $N_{\rm exc}(N_{\rm exc}-1)$ ot the denominator, we finally obtain the transition probability from the initial to the final state,

$$P_{\mathbf{p},\rm fer}(t) = \frac{2\pi t}{\hbar}\, \frac{N_{\rm exc}(N_{\rm exc}-1)}{n_{\rm QW}^2 N_{\rm el}^2}\ |U_{\mathbf{q},\mathbf{q},\mathbf{p}}|^2\ \delta_t(\Delta E_{\mathbf{p}}) + O\left(\left[\frac{N_{\rm exc}}{n_{\rm QW}N_{\rm el}}\right]^4\right). \tag{C.11}$$

C.2 Fermi Golden Rule

With the same notations, the contribution of the many-body physics to the lifetime of the initial state is [96, 106]

$$\frac{t}{T} \;=\; \left\langle \tilde{\psi}_t \middle| \tilde{\psi}_t \right\rangle - \left| \langle \psi_i | \tilde{\psi}_t \rangle \right|^2. \tag{C.12}$$

The second term can be calculated using the same method as for the transition rate and is found to contribute only to higher orders in the perturbation. We, thus, neglect it.

The first term is

$$\left\langle \tilde{\psi}_t \middle| \tilde{\psi}_t \right\rangle \propto \langle F|\, b_{0,\mathbf{q}}^{N_{\rm exc}}\, H\, P_\perp\, |F(H - \langle\psi_i|\, H\, |\psi_i\rangle)|^2\, P_\perp\, H\, b_{0,\mathbf{q}}^{\dagger\, N_{\rm exc}}\, |F\rangle\,. \tag{C.13}$$

We use Eq. (C.9) to replace the ket by its expression. To avoid useless complication, we remove the coupling between bright and dark excitation because we already know that they yield non resonant contributions. We also notice that the second term of the first line is orthogonal to $\langle F|\, b_{0,\mathbf{q}}^{N_{\rm exc}}\, H\, P_\perp$, so it does not contribute at all. We,

thus, obtain

$$\begin{aligned}\frac{1}{T} \propto \frac{N_{\rm exc}(N_{\rm exc}-1)}{2n_{\rm QW}N_{\rm el}}\,\frac{e^2 n_{\rm el}}{2\epsilon_0\epsilon_r}\sum_{m,n,\mathbf{Q}\neq 0}\delta_t(\Delta E_{\mathbf{Q}})\,\frac{\xi^{n,0}_{m,0}(\mathbf{Q})}{Q\epsilon(\mathbf{Q})}\\ \times\langle F|\, b^{N_{\rm exc}}_{0,\mathbf{q}} H P_\perp\, b^\dagger_{m,\mathbf{q}+\mathbf{Q}} b^\dagger_{n,\mathbf{q}-\mathbf{Q}} b^{\dagger\,N_{\rm exc}-2}_{0,\mathbf{q}}\,|F\rangle\\ -\frac{N_{\rm exc}(N_{\rm exc}-1)}{n_{\rm QW}N_{\rm el}}\sum_{n,\mathbf{Q}\neq 0}\delta_t(\Delta E_{\mathbf{q}-\mathbf{Q}})\,N_{\rm el}V_Q^{1212}\,\lambda^{n,0}_{0,0}(\mathbf{Q}-\mathbf{q})\\ \times\langle F|\, b^{N_{\rm exc}}_{0,\mathbf{q}} H P_\perp\, b^\dagger_{0,\mathbf{Q}} b^\dagger_{n,\mathbf{2q}-\mathbf{Q}} b^{\dagger\,N_{\rm exc}-2}_{0,\mathbf{q}}\,|F\rangle\,, \quad \text{(C.14)}\end{aligned}$$

where indices m and n and the wave vector $\mathbf{Q}$ are all non zero. We also made F_t act at zero-th order. We now replace state $\langle F|\, b^{N_{\rm exc}}_{0,\mathbf{q}}\, H\, P_\perp$ by its expression from which we, again, remove the first line,

$$\begin{aligned}\frac{1}{T} \propto \frac{N_{\rm exc}(N_{\rm exc}-1)}{2n_{\rm QW}N_{\rm el}}\,\frac{e^2 n_{\rm el}}{2\epsilon_0\epsilon_r}\sum_{\mathbf{Q}}\delta_t(\Delta E_{\mathbf{Q}})\,\frac{\xi^{0,0}_{0,0}(\mathbf{Q})}{Q\epsilon(\mathbf{Q})}\,U_{\mathbf{q},\mathbf{q},\mathbf{Q}}\\ -\frac{N_{\rm exc}(N_{\rm exc}-1)}{n_{\rm QW}N_{\rm el}}\sum_{\mathbf{Q}}\delta_t(\Delta E_{\mathbf{q}-\mathbf{Q}})\,N_{\rm el}V_Q^{1212}\,\lambda^{0,0}_{0,0}(\mathbf{Q}-\mathbf{q})\,U_{\mathbf{q},\mathbf{q},\mathbf{Q}}\,. \quad \text{(C.15)}\end{aligned}$$

Here, the sum over the wave vector $\mathbf{Q}$ has been implicitely truncated to small wave vectors. We conserved only resonant terms, so we do not consider processes where bright excitations are scattered to dark states. These processes are, indeed, non resonant (see section 3.3).

The previous expression, despite correct, does not look like traditional Fermi Golden Rule. It is, however, possible to simplify it by using the overcompleteness of the two-excitation states. We use Eq. (3.34) to express $b^\dagger_{m,\mathbf{q}+\mathbf{Q}}b^\dagger_{n,\mathbf{q}-\mathbf{Q}}$ and $b^\dagger_{0,\mathbf{Q}}b^\dagger_{n,\mathbf{2q}-\mathbf{Q}}$ in a different way and do the calculation again,

$$\begin{aligned}\frac{1}{T} \propto -\frac{N_{\rm exc}(N_{\rm exc}-1)}{2n_{\rm QW}N_{\rm el}}\,\frac{e^2 n_{\rm el}}{2\epsilon_0\epsilon_r}\sum_{\mathbf{Q},\mathbf{Q}'}\delta_t(\Delta E_{\mathbf{Q}})\,\frac{\lambda^{0,n}_{0,m}(\mathbf{Q}')\xi^{n,0}_{m,0}(\mathbf{Q})}{n_{\rm QW}N_{\rm el}\,Q\epsilon(\mathbf{Q})}\,U_{\mathbf{q},\mathbf{q},\mathbf{Q}+\mathbf{Q}'}\\ +\frac{N_{\rm exc}(N_{\rm exc}-1)}{n_{\rm QW}N_{\rm el}}\sum_{\mathbf{Q},\mathbf{Q}'}\delta_t(\Delta E_{\mathbf{q}-\mathbf{Q}})\,N_{\rm el}V_Q^{1212}\,\frac{\lambda^{0,n}_{0,0}(\mathbf{Q}')\lambda^{n,0}_{0,0}(\mathbf{Q}-\mathbf{q})}{n_{\rm QW}N_{\rm el}}\,U_{\mathbf{q},\mathbf{q},\mathbf{Q}+\mathbf{Q}'}\,. \quad \text{(C.16)}\end{aligned}$$

We now take the mean of these two expression and normalize our result,

$$\frac{1}{T} \;=\; \frac{1}{2}\sum_{\mathbf{p}}\lim_{t\to+\infty}\frac{P_{\mathbf{p},\rm fer}(t)}{t}, \quad \text{(C.17)}$$

where it is implicitly assumed that the summation is restricted to small wavevectors. This result is now very similar to the usual Fermi golden rule despite the presence of the counterintuitive 1/2 factor. This coefficient comes from the overcompleteness of the composite boson basis.

Bibliography

[1] L. Nguyen-thê, S. De Liberato, M. Bamba, and C. Ciuti, "Effective polariton-polariton interactions of cavity-embedded two-dimensional electron gases," *Phys. Rev. B*, vol. 87, p. 235322, Jun 2013.

[2] E. M. Purcell, H. C. Torrey, and R. V. Pound, "Resonance absorption by nuclear magnetic moments in a solid," *Phys. Rev.*, vol. 69, pp. 37–38, Jan 1946.

[3] S. Haroche and J. M. Raimond, *Exploring the Quantum: Atoms, Cavities and Photons*. Oxford University Press, 2006.

[4] P. Goy, J. M. Raimond, M. Gross, and S. Haroche, "Observation of cavity-enhanced single-atom spontaneous emission," *Phys. Rev. Lett.*, vol. 50, pp. 1903–1906, Jun 1983.

[5] G. Gabrielse and H. Dehmelt, "Observation of inhibited spontaneous emission," *Phys. Rev. Lett.*, vol. 55, pp. 67–70, Jul 1985.

[6] R. G. Hulet, E. S. Hilfer, and D. Kleppner, "Inhibited spontaneous emission by a rydberg atom," *Phys. Rev. Lett.*, vol. 55, pp. 2137–2140, Nov 1985.

[7] W. Jhe, A. Anderson, E. A. Hinds, D. Meschede, L. Moi, and S. Haroche, "Suppression of spontaneous decay at optical frequencies: Test of vacuum-field anisotropy in confined space," *Phys. Rev. Lett.*, vol. 58, pp. 666–669, Feb 1987.

[8] S. Peil and G. Gabrielse, "Observing the quantum limit of an electron cyclotron: Qnd measurements of quantum jumps between fock states," *Phys. Rev. Lett.*, vol. 83, pp. 1287–1290, Aug 1999.

[9] D. Meschede, H. Walther, and G. Müller, "One-atom maser," *Phys. Rev. Lett.*, vol. 54, pp. 551–554, Feb 1985.

[10] G. Rempe, H. Walther, and N. Klein, "Observation of quantum collapse and revival in a one-atom maser," *Phys. Rev. Lett.*, vol. 58, pp. 353–356, Jan 1987.

[11] R. J. Thompson, G. Rempe, and H. J. Kimble, "Observation of normal-mode splitting for an atom in an optical cavity," *Phys. Rev. Lett.*, vol. 68, pp. 1132–1135, Feb 1992.

[12] J. M. Raimond, M. Brune, and S. Haroche, "Manipulating quantum entanglement with atoms and photons in a cavity," *Rev. Mod. Phys.*, vol. 73, pp. 565–582, Aug 2001.

[13] C. Weisbuch, M. Nishioka, A. Ishikawa, and Y. Arakawa, "Observation of the coupled exciton-photon mode splitting in a semiconductor quantum microcavity," *Phys. Rev. Lett.*, vol. 69, pp. 3314–3317, Dec 1992.

[14] D. Dini, R. Köhler, A. Tredicucci, G. Biasiol, and L. Sorba, "Microcavity polariton splitting of intersubband transitions," *Phys. Rev. Lett.*, vol. 90, p. 116401, Mar 2003.

[15] J. P. Reithmaier, G. Sek, A. Löffler, C. Hofmann, S. Kuhn, S. Reitzenstein, L. V. Keldysh, V. D. Kulakovskii, T. L. Reinecke, and A. Forchel, "Strong coupling in a single quantum dot-semiconductor microcavity system," *Nature*, vol. 432, pp. 197–200, Nov 2004.

[16] T. Yoshie, A. Scherer, J. Hendrickson, G. Khitrova, H. M. Gibbs, G. Rupper, C. Ell, O. B. Shchekin, and D. G. Deppe, "Vacuum rabi spliting with a single quantum dot in a photonic crystal nanocavity," *Nature*, vol. 432, pp. 200–203, Nov 2004.

[17] E. Peter, P. Senellart, D. Martrou, A. Lemaître, J. Hours, J. M. Gérard, and J. Bloch, "Exciton-photon strong-coupling regime for a single quantum dot embedded in a microcavity," *Phys. Rev. Lett.*, vol. 95, p. 067401, Aug 2005.

[18] A. Wallraff, D. I. Schuster, A. Blais, L. Frunzio, R.-S. Huang, J. Majer, S. Kumar, S. M. Girvin, and R. J. Schoelkopf, "Strong coupling of a single photon to a superconducting qubit circuit quantum electrodynamics," *Nature*, vol. 431, pp. 162–167, Sep 2004.

[19] A. Blais, R.-S. Huang, A. Wallraff, S. M. Girvin, and R. J. Schoelkopf, "Cavity quantum electrodynamics for superconducting electrical circuits: An architecture for quantum computation," *Phys. Rev. A*, vol. 69, p. 062320, Jun 2004.

[20] V. Savona, Z. Hradil, A. Quattropani, and P. Schwendimann, "Quantum theory of quantum-well polaritons in semiconductor microcavities," *Phys. Rev. B*, vol. 49, pp. 8774–8779, Apr 1994.

[21] C. Ciuti, V. Savona, C. Piermarocchi, A. Quattropani, and P. Schwendimann, "Role of the exchange of carriers in elastic exciton-exciton scattering in quantum wells," *Phys. Rev. B*, vol. 58, pp. 7926–7933, Sep 1998.

[22] G. Rochat, C. Ciuti, V. Savona, C. Piermarocchi, A. Quattropani, and P. Schwendimann, "Excitonic bloch equations for a two-dimensional system of interacting excitons," *Phys. Rev. B*, vol. 61, pp. 13856–13862, May 2000.

[23] C. Ciuti, P. Schwendimann, B. Deveaud, and A. Quattropani, "Theory of the angle-resonant polariton amplifier," *Phys. Rev. B*, vol. 62, pp. R4825–R4828, Aug 2000.

[24] C. Ciuti, P. Schwendimann, and A. Quattropani, "Theory of polariton parametric interactions in semiconductor microcavities," *Semiconductor Science and Technology*, vol. 18, no. 10, p. S279, 2003.

[25] I. Carusotto and C. Ciuti, "Probing microcavity polariton superfluidity through resonant rayleigh scattering," *Phys. Rev. Lett.*, vol. 93, p. 166401, Oct 2004.

[26] C. Ciuti and I. Carusotto, "Quantum fluid effects and parametric instabilities in microcavities," *Phys. Stat. Sol. (b)*, vol. 242, pp. 2224–2245, Jul 2005.

[27] A. Amo, J. Lefrère, S. Pigeon, C. Adrados, C. Ciuti, I. Carusotto, R. Houdré, E. Giacobino, and A. Bramati, "Superfluidity of polaritons in semiconductor microcavities," *Nature Physics*, vol. 5, pp. 805–810, Sep 2009.

[28] A. Amo, S. Pigeon, D. Sanvitto, V. G. Sala, R. Hivet, I. Carusotto, F. Pisanello, G. Leménager, R. Houdré, E. Giacobino, C. Ciuti, and A. Bramati, "Polariton superfluids reveal quantum hydrodynamic solitons," *Science*, vol. 332, no. 6034, pp. 1167–1170, 2011.

[29] I. Carusotto and C. Ciuti, "Quantum fluids of light," *Rev. Mod. Phys.*, vol. 85, pp. 299–366, Feb 2013.

[30] S. I. Tsintzos, N. T. Pelekanos, G. Konstantinidis, Z. Hatzopoulos, and P. G. Savvidis, "A gaas polariton light-emitting diode operating near room temperature," *Nature*, vol. 453, p. 372, 2008.

[31] G. Malpuech, A. Di Carlo, A. V. Kavokin, J. J. Baumberg, M. Zamfirescu, and P. Lugli, "Room-temperature polariton lasers based on gan microcavities," *Appl. Phys. Lett*, vol. 81, p. 412, 2002.

[32] S. Christopoulos, G. B. H. von Högersthal, A. J. D. Grundy, P. G. Lagoudakis, A. V. Kavokin, J. J. Baumberg, G. Christmann, R. Butté, E. Feltin, J.-F. Carlin, and N. Grandjean, "Room-temperature polariton lasing in semiconductor microcavities," *Phys. Rev. Lett.*, vol. 98, p. 126405, Mar 2007.

[33] A. Verger, C. Ciuti, and I. Carusotto, "Polariton quantum blockade in a photonic dot," *Phys. Rev. B*, vol. 73, p. 193306, May 2006.

[34] I. Carusotto, D. Gerace, H. E. Tureci, S. De Liberato, C. Ciuti, and A. Imamoglu, "Fermionized photons in an array of driven dissipative nonlinear cavities," *Phys. Rev. Lett.*, vol. 103, p. 033601, Jul 2009.

[35] T. C. H. Liew and V. Savona, "Single photons from coupled quantum modes," *Phys. Rev. Lett.*, vol. 104, p. 183601, May 2010.

[36] M. Bamba, A. Imamoğlu, I. Carusotto, and C. Ciuti, "Origin of strong photon antibunching in weakly nonlinear photonic molecules," *Phys. Rev. A*, vol. 83, p. 021802, Feb 2011.

[37] A. Le Boité, G. Orso, and C. Ciuti, "Steady-state phases and tunneling-induced instabilities in the driven dissipative bose-hubbard model," *Phys. Rev. Lett.*, vol. 110, p. 233601, Jun 2013.

[38] C. Ciuti, G. Bastard, and I. Carusotto, "Quantum vacuum properties of the intersubband cavity polariton field," *Phys. Rev. B*, vol. 72, p. 115303, Sep 2005.

[39] S. De Liberato, C. Ciuti, and I. Carusotto, "Quantum vacuum radiation spectra from a semiconductor microcavity with a time-modulated vacuum rabi frequency," *Phys. Rev. Lett.*, vol. 98, p. 103602, Mar 2007.

[40] M. Kardar and R. Golestanian, "The "friction of vacuum", and other fluctuation-induced forces," *Rev. Mod. Phys.*, vol. 71, p. 1233, 1999.

[41] G. Günter, A. A. Anappara, J. Hees, A. Sell, G. Biasiol, L. Sorba, S. De Liberato, C. Ciuti, A. Tredicucci, A. Leitenstorfer, and R. Huber, "Sub-cycle switch-on of ultrastrong light-matter interaction," *Nature*, vol. 458, pp. 178 –181, Mar 2009.

[42] S. Zanotto, R. Degl'Innocenti, J.-H. Xu, L. Sorba, A. Tredicucci, and G. Biasiol, "Ultrafast optical bleaching of intersubband cavity polaritons," *Phys. Rev. B*, vol. 86, p. 201302, Nov 2012.

[43] J. Faist, F. Capasso, D. L. Sivco, C. Sirtori, A. L. Hutchinson, and A. Y. Cho, "Quantum cascade laser," *Science*, vol. 264, pp. 553–556, Apr 1994.

[44] L. Sapienza, A. Vasanelli, C. Ciuti, C. Manquest, C. Sirtori, R. Colombelli, and U. Gennser, "Photovoltaic probe of cavity polaritons in a quantum cascade structure," *Appl. Phys. Lett*, vol. 90, p. 201101, May 2007.

[45] R. Colombelli, C. Ciuti, Y. Chassagneux, and C. Sirtori, "Quantum cascade intersubband polariton light emitters," *Semiconductor Science and Technology*, vol. 20, p. 985, Oct 2005.

[46] L. Sapienza, A. Vasanelli, R. Colombelli, C. Ciuti, Y. Chassagneux, C. Manquest, U. Gennser, and C. Sirtori, "Electrically injected cavity polaritons," *Phys. Rev. Lett.*, vol. 100, p. 136806, Apr 2008.

[47] Y. Todorov, P. Jouy, A. Vasanelli, L. Sapienza, R. Colombelli, U. Gennser, and C. Sirtori, "Stark-tunable electroluminescence from cavity polariton states," *Appl. Phys. Lett*, vol. 93, p. 171105, Oct 2008.

[48] S. De Liberato and C. Ciuti, "Stimulated scattering and lasing of intersubband cavity polaritons," *Phys. Rev. Lett.*, vol. 102, p. 136403, Mar 2009.

[49] S. De Liberato and C. Ciuti, "Quantum theory of intersubband polarons," *Phys. Rev. B*, vol. 85, p. 125302, Mar 2012.

[50] A. Delteil, A. Vasanelli, P. Jouy, D. Barate, J. C. Moreno, R. Teissier, A. N. Baranov, and C. Sirtori, "Optical phonon scattering of cavity polaritons in an electroluminescent device," *Phys. Rev. B*, vol. 83, p. 081404, Feb 2011.

[51] Y. Todorov, A. M. Andrews, R. Colombelli, S. De Liberato, C. Ciuti, P. Klang, G. Strasser, and C. Sirtori, "Ultrastrong light-matter coupling regime with polariton dots," *Phys. Rev. Lett.*, vol. 105, p. 196402, Nov 2010.

[52] A. Delteil, A. Vasanelli, Y. Todorov, C. Feuillet Palma, M. Renaudat St-Jean, G. Beaudoin, I. Sagnes, and C. Sirtori, "Charge-induced coherence between intersubband plasmons in a quantum structure," *Phys. Rev. Lett.*, vol. 109, p. 246808, Dec 2012.

[53] S. De Liberato, C. Ciuti, and C. C. Phillips, "Terahertz lasing from intersubband polariton-polariton scattering in asymmetric quantum wells," *Phys. Rev. B*, vol. 87, p. 241304, Jun 2013.

[54] M. F. Pereira and H. Wenzel, "Interplay of coulomb and nonparabolicity effects in the intersubband absorption of electrons and holes in quantum wells," *Phys. Rev. B*, vol. 70, p. 205331, Nov 2004.

[55] O. Kyriienko and I. A. Shelykh, "Intersubband polaritonics revisited," *J. Nanophoton.*, vol. 6, p. 061804, Nov 2012.

[56] I. I. Rabi, "Space quantization in a gyrating magnetic field," *Phys. Rev.*, vol. 51, pp. 652–654, Apr 1937.

[57] C. Cohen-Tannoudji, J. Dupont-Roc, and G. Grynberg, *Processus d'interaction entre photons et atomes*. CNRS Editions, 2001.

[58] A. A. Anappara, A. Tredicucci, G. Biasiol, and L. Sorba, "Electrical control of polariton coupling in intersubband microcavities," *Appl. Phys. Lett*, vol. 87, p. 051105, Jul 2005.

[59] A. Auer and G. Burkard, "Entangled photons from the polariton vacuum in a switchable optical cavity," *Phys. Rev. B*, vol. 85, p. 235140, Jun 2012.

[60] M. H. Devoret, S. M. Girvin, and R. J. Schoelkopf, "How strong can the coupling between a josephson junction atom and a transmission line resonator be?," *Ann. Phys.*, vol. 16, pp. 767–779, Oct 2007.

[61] R. H. Dicke, "Coherence in spontaneous radiation processes," *Phys. Rev.*, vol. 93, pp. 99–110, Jan 1954.

[62] R. Bonifacio and G. Preparata, "Coherent spontaneous emission," *Phys. Rev. A*, vol. 2, pp. 336–347, Aug 1970.

[63] R. Bonifacio, P. Schwendimann, and F. Haake, "Quantum statistical theory of superradiance. i," *Phys. Rev. A*, vol. 4, pp. 302–313, Jul 1971.

[64] R. Bonifacio, P. Schwendimann, and F. Haake, "Quantum statistical theory of superradiance. ii," *Phys. Rev. A*, vol. 4, pp. 854–864, Sep 1971.

[65] J. J. Hopfield, "Theory of the contribution of excitons to the complex dielectric constant of crystals," *Phys. Rev.*, vol. 112, pp. 1555–1567, Dec 1958.

[66] A. A. Anappara, A. Tredicucci, F. Beltram, G. Biasiol, and L. Sorba, "Tunnel-assisted manipulation of intersubband polaritons in asymmetric coupled quantum wells," *Appl. Phys. Lett*, vol. 89, p. 171109, Oct 2006.

[67] A. A. Anappara, A. Tredicucci, F. Beltram, G. Biasiol, L. Sorba, S. De Liberato, and C. Ciuti, "Cavity polaritons from excited-subband transitions," *Appl. Phys. Lett*, vol. 91, p. 231118, Dec 2007.

[68] J. Plumridge, E. Clarke, R. Murray, and C. Phillips, "Ultra-strong coupling effects with quantum metamaterials," *Solid State Communications*, vol. 146, p. 406, Jun 2008.

[69] M. Porer, J.-M. Ménard, A. Leitenstorfer, R. Huber, R. Degl'Innocenti, S. Zanotto, G. Biasiol, L. Sorba, and A. Tredicucci, "Nonadiabatic switching of a photonic band structure: Ultrastrong light-matter coupling and slow-down of light," *Phys. Rev. B*, vol. 85, p. 081302, Feb 2012.

[70] P. Jouy, A. Vasanelli, Y. Todorov, L. Sapienza, R. Colombelli, U. Gennser, and C. Sirtori, "Intersubband electroluminescent devices operating in the strong-coupling regime," *Phys. Rev. B*, vol. 82, p. 045322, Jul 2010.

[71] E. Dupont, J. A. Gupta, and H. C. Liu, "Giant vacuum-field rabi splitting of intersubband transitions in multiple quantum wells," *Phys. Rev. B*, vol. 75, p. 205325, May 2007.

[72] M. Załużny and W. Zietkowski, "Intersubband cavity polaritons: The role of higher photonic modes," *Phys. Rev. B*, vol. 80, p. 245301, Dec 2009.

[73] M. Geiser, C. Walther, G. Scalari, M. Beck, M. Fisher, L. Nevou, and J. Faist, "Strong light-matter coupling at terahertz frequencies at room temperature in electronic lc resonators," *Appl. Phys. Lett*, vol. 97, p. 191107, Nov 2010.

[74] M. Geiser, F. Castellano, G. Scalari, M. Beck, L. Nevou, and J. Faist, "Ultrastrong coupling regime and plasmon polaritons in parabolic semiconductor quantum wells," *Phys. Rev. Lett.*, vol. 108, p. 106402, Mar 2012.

[75] Y. Todorov, A. M. Andrews, I. Sagnes, R. Colombelli, P. Klang, G. Strasser, and C. Sirtori, "Strong light-matter coupling in subwavelength metal-dielectric microcavities at terahertz frequencies," *Phys. Rev. Lett.*, vol. 102, p. 186402, May 2009.

[76] W. Kohn, "Cyclotron resonance and de haas-van alphen oscillations of an interacting electron gas," *Phys. Rev.*, vol. 123, pp. 1242–1244, Aug 1961.

[77] P. Jouy, *Optoelectronic quantum devices for ultra-strong light-matter interaction at mid-infrared wavelengths.* PhD thesis, Université Paris Diderot, Feb 2012.

[78] K. Kakazu and Y. S. Kim, "Quantization of electromagnetic fields in cavities and spontaneous emission," *Phys. Rev. A*, vol. 50, pp. 1830–1839, Aug 1994.

[79] C. Cohen-Tannoudji, J. Dupont-Roc, and G. Grynberg, *Photons et atomes : Introduction à l'électrodynamique quantique.* CNRS Editions, 2001.

[80] G. F. Giuliani and G. Vignale, *Quantum Theory of the Electron Liquid.* Cambridge University Press, 2008.

[81] H. Haug and S. W. Koch, *Quantum Theory of the Optical and Electronic Properties of Semiconductors.* World Scientific, 5 ed., 2009.

[82] S.-C. Lee and I. Galbraith, "Intersubband and intrasubband electronic scattering rates in semiconductor quantum wells," *Phys. Rev. B*, vol. 59, pp. 15796–15805, Jun 1999.

[83] S.-C. Lee and I. Galbraith, "Influence of exchange scattering and dynamic screening on electron-electron scattering rates in semiconductor quantum wells," *Phys. Rev. B*, vol. 62, pp. 15327–15330, Dec 2000.

[84] D. F. Walls and G. J. Milburn, *Quantum Optics.* Springer, 2008.

[85] T. Usui, "Excitations in a high density electron gas. i," *Progress of Theoretical Physics*, vol. 23, pp. 787–798, May 1960.

[86] F. Tassone and Y. Yamamoto, "Exciton-exciton scattering dynamics in a semiconductor microcavity and stimulated scattering into polaritons," *Phys. Rev. B*, vol. 59, pp. 10830–10842, Apr 1999.

[87] Y. Todorov and C. Sirtori, "Intersubband polaritons in the electrical dipole gauge," *Phys. Rev. B*, vol. 85, p. 045304, Jan 2012.

[88] E. Hanamura and H. Haug, "Condensation effects of excitons," *Physics Reports*, vol. 33, no. 4, pp. 209 – 284, 1977.

[89] A. A. Anappara, S. De Liberato, A. Tredicucci, C. Ciuti, G. Biasiol, L. Sorba, and F. Beltram, "Signatures of the ultrastrong light-matter coupling regime," *Phys. Rev. B*, vol. 79, p. 201303, May 2009.

[90] O. Betbeder-Matibet and M. Combescot, "Commutation technique for interacting close-to-boson excitons," *The European Physical Journal B - Condensed Matter and Complex Systems*, vol. 27, pp. 505–516, Jun 2002.

[91] M. Combescot, O. Betbeder-Matibet, and F. Dubin, "The exciton many-body theory extended to any kind of composite bosons," *The European Physical Journal B - Condensed Matter and Complex Systems*, vol. 52, pp. 181–189, 2006. 10.1140/epjb/e2006-00277-7.

[92] M. Combescot, O. Betbeder-Matibet, and F. Dubin, "The many-body physics of composite bosons," *Physics Reports*, vol. 463, no. 5-6, pp. 215 – 320, 2008.

[93] M. Combescot, X. Leyronas, and C. Tanguy, "On the n-exciton normalization factor," *The European Physical Journal B - Condensed Matter and Complex Systems*, vol. 31, pp. 17–24, Jan 2003.

[94] M. Hawton and D. Nelson, "Quasibosonic exciton dynamics near the semiconductor band edge," *Phys. Rev. B*, vol. 57, pp. 4000–4008, Feb 1998.

[95] M. Combescot, M. G. Moore, and C. Piermarocchi, "Optical traps for electrons produced by pauli blocking," *Europhysics Letter*, vol. 47, p. 47012, Feb 2011.

[96] M. Combescot and O. Betbeder-Matibet, "Shiva diagrams for composite-boson many-body effects: how they work," *The European Physical Journal B - Condensed Matter and Complex Systems*, vol. 55, pp. 63–76, 2007.

[97] D. E. Nikonov, A. Imamoğlu, L. V. Butov, and H. Schmidt, "Collective intersubband excitations in quantum wells: Coulomb interaction versus subband dispersion," *Phys. Rev. Lett.*, vol. 79, pp. 4633–4636, Dec 1997.

[98] D. Porras, C. Ciuti, J. J. Baumberg, and C. Tejedor, "Polariton dynamics and bose-einstein condensation in semiconductor microcavities," *Phys. Rev. B*, vol. 66, p. 085304, Aug 2002.

[99] C. Ciuti, "Branch-entangled polariton pairs in planar microcavities and photonic wires," *Phys. Rev. B*, vol. 69, p. 245304, Jun 2004.

[100] M. F. Pereira, "Intersubband antipolaritons: Microscopic approach," *Phys. Rev. B*, vol. 75, p. 195301, May 2007.

[101] M. Combescot and O. Betbeder-Matibet, "The effective bosonic hamiltonian for excitons reconsidered," *Europhysics Letter*, vol. 52, p. 87, Jan 2002.

[102] M. M. Glazov, H. Ouerdane, L. Pilozzi, G. Malpuech, A. V. Kavokin, and A. D'Andrea, "Polariton-polariton scattering in microcavities: A microscopic theory," *Phys. Rev. B*, vol. 80, p. 155306, Oct 2009.

[103] M. Vladimirova, S. Cronenberger, D. Scalbert, K. V. Kavokin, A. Miard, A. Lemaître, J. Bloch, D. Solnyshkov, G. Malpuech, and A. V. Kavokin, "Polariton-polariton interaction constants in microcavities," *Phys. Rev. B*, vol. 82, p. 075301, Aug 2010.

[104] M. Combescot, M. G. Moore, and C. Piermarocchi, "Optical traps for dark excitons," *Phys. Rev. Lett.*, vol. 106, p. 206404, May 2011.

[105] M. Combescot, M. G. Moore, and C. Piermarocchi, "Erratum: Optical traps for dark excitons [phys. rev. lett. 106, 206404 (2011)]," *Phys. Rev. Lett.*, vol. 108, p. 189905, May 2012.

[106] M. Combescot, O. Betbeder-Matibet, and R. Combescot, "Exciton-exciton scattering: Composite boson versus elementary boson," *Phys. Rev. B*, vol. 75, p. 174305, May 2007.

[107] P. G. Savvidis, J. J. Baumberg, R. M. Stevenson, M. S. Skolnick, D. M. Whittaker, and J. S. Roberts, "Angle-resonant stimulated polariton amplifier," *Phys. Rev. Lett.*, vol. 84, pp. 1547–1550, Feb 2000.

[108] D. Hagenmüller, S. De Liberato, and C. Ciuti, "Ultrastrong coupling between a cavity resonator and the cyclotron transition of a two-dimensional electron gas in the case of an integer filling factor," *Phys. Rev. B*, vol. 81, p. 235303, Jun 2010.

[109] G. Scalari, C. Maissen, C. Turčinková, D. Hagenmüller, S. De Liberato, C. Ciuti, C. Reichl, D. Schuh, W. Wegscheider, M. Beck, and J. Faist, "Ultrastrong coupling of the cyclotron transition in a 2d electron gaz to a thz metamaterial," *Science*, vol. 335, pp. 1323–1326, Mar 2012.

[110] D. Hagenmüller and C. Ciuti, "Cavity qed of the graphene cyclotron transition," *Phys. Rev. Lett.*, vol. 109, p. 267403, Dec 2012.

[111] C. Emary and T. Brandes, "Chaos and the quantum phase transition in the dicke model," *Phys. Rev. E*, vol. 67, p. 066203, Jun 2003.

[112] A. L. Fetter and J. D. Walecka, *Quantum Theory of Many-Particle Systems*. Dover, 2003.